STUDY ON HUMAN 5-AMINOLAEVULINATE SYNTHASE AND THE MOLECULAR BASIS FOR PYRIDOXINE RESPONSIVE X-LINKED SIDEROBLASTIC ANAEMIA

A THESIS SUBMITTED FOR THE DEGREE OF

DOCTOR OF PHILOSOPHY

By Sooad K. Al-Daihan

Supervised by Peter Shoolingin Jordan

University of Southampton

Department of Biochemistry

August
2001

UNIVERSITY OF SOUTHAMPTON

ABSTRACT

FACULTY OF SCIENCE

DIVISION OF BIOCHEMISTRY AND MOLECULAR BIOLOGY

Doctor of Philosophy

Study on human 5-aminolaevulinate synthase and the molecular basis for pyridoxine responsive X-linked sideroblastic anaemia

By: Sooad Al-Daihan

Abstract

5-Aminolaevulinic acid is the first precursor of haem biosynthesis and is formed by the condensation between glycine and succinyl-CoA in a reaction catalysed by 5-aminolaevulinic acid synthase (ALAS). Pyridoxal 5'-phosphate (PLP) is required as a coenzyme. The enzyme is confined to animals, fungi and some bacteria.

The results reported in this thesis show that recombinant human erythrocyte 5-aminolaevulinic acid synthase (ALAS2), expressed as a His-tagged protein in *Escherichia coli,* is active *in vitro* with a final specific activity of 18μmole/mg/hr. Steady state kinetics analysis of ALAS2 revealed a K_m for glycine of 13.9mM and a K_m value for the second substrate, succinyl CoA, of 0.8μM. The reaction catalysed by ALAS2 was followed by UV/visible spectroscopy. The results showed that the enzyme binds to the coenzyme pyridoxal 5'-phosphate *via* an aldimine linkage. Two mutant forms of human ALAS2, Thr388Ser and Arg452His, both of which lead to pyridoxine responsive X-linked sideroblastic anaemias, were isolated and characterised by kinetic and spectroscopic techniques. Another mutation, Arg517Cys, that causes a refractory form of sideroblastic anaemia was also isolated and characterised by kinetic and spectroscopic analysis. Arginine 517 is implicated in binding the carboxyl group of the substrate glycine. In addition, the arginine 517 residue was mutated to leucine and lysine. Only the Arg517Lys mutant showed activity (5%), the other two mutants being completely inactive.

The similarity in the main-chain folds between ALAS2 and 2-amino-3-oxononanoate synthase (AONS), a closely related PLP-dependent enzyme, permitted the construction of a model structure for human ALAS2, using the sequence alignment of AONS as a template. The location of human mutations in the model structure of ALAS2 provides a rational explanation for many of the physiological effects of pyridoxine therapy.

CONTENTS

List of figures: **Page no.**

List of schemes:

List of tables:

Acknowledgements

I wish to express my sincere gratitude to Professor Peter Shoolingin-Jordan, my supervisor, who giving me the opportunity to work in his laboratory, for his vast academic knowledge, valuable comments he gave me throughout my works, and for his advise and generous support.

Many thanks must go to my parents without whom this work would not have been possible.

Many thanks to Professor Sylvia Bottomley for her kind gift of T388S and R452H mutants.

I am very grateful to Dr. Sarwar, for his valuable assistance in the molecular biology field and for his constructive criticism of my work.

I am deeply grateful to my friend Dr. Roy, for her support, guidance and assistance in protein purification and also for the coffee that she made every morning.

I particularly would like to thank Dr. Wang, for kindly sharing her experience in protein modelling.

I would like to thank my friend Abeer, for the nice and hard time we spent together, and of course to all my colleagues in the lab there whom I have worked along side over the past few years.

Many thanks must go to my husband. His moral support and tolerance have been very important to me.

I never forget my brothers, and my sisters, for their endless help and support.

Finally, many thanks must go to my little son "Faisal".

Abbreviations used in the thesis

5-ALAS	5-Aminolaevulinic acid synthase
ALAS-H	Hepatic aminolaevulinic acid synthase
ALAS-E	Erythroid Aminolaevulinic acid synthase
5-ALA	5-Aminolaevulinic acid
PLP	Pyridoxal 5'-phosphate
ALAD	Aminolaevulinic acid dehydratase
PBGD	Porphobilinogen deaminase
UROS	Uroporphyrinogen synthase
UROD	Uroporphyrinogen decarboxylase
CPO	Coproporphyrinogen oxidase
PPO	Protoporphyrinogen oxidase
FC	Ferrochelatase
PBG	Porphobilinogen
PRE	Preuroporphyrinogen
URO	Uroporphyrinogen III
COP	Coproporphyrinogen III
PPO	Protoporphyrinogen III
DNA	Deoxyribonucleic acid
cDNA	Complementary DNA
ATP	Adenosial triphosphate
PCR	Polymerase chain reaction
TCA	Trichloroacetic acid
Kb	Kilobase pair
M_r	Relative molecular weight
SDS	Sodium dodecyl sulphate
TEMED	N,N,N',N'-tetramethylenediamine
6xHis	6 Histidine tag protein
CoA	Coenzyme A
AONS	8-Amino-7-oxononanoate synthas
SPT	Serine palmitoyltransferase
AKB	2-Amino-3-oxobutyrate-CoA ligase

PMSF	Phenylmethylsulfonyl fluoride
IPTG	Isopropyl-beta-D-thiogalactopyranoside, dioxane free
XLSA	X-Linked sideroblastic anamia
A and Abs	Absorbance
TOF	Time of flight

Amino acid Abbreviations

Amino Acid Name	3 Letter Abbreviation	1 Letter Abbreviation
Alanine	Ala	A
Arginine	Arg	R
Asparagine	Asn	N
Aspartate	Asp	D
Cysteine	Cys	C
Glutamate	Glu	E
Glutamine	Gln	Q
Glycine	Gly	G
Histidine	His	H
Isoleucine	Iso	I
Leucine	Leu	L
Lysine	Lys	K
Methionine	Met	M
Phenyalanine	Phe	F
Proline	Pro	P
Serine	Ser	S
Threonine	Thr	T
Tryptophan	Trp	W
Tyrosine	Tyr	Y
Valine	Val	V

Chapter 1

Introduction

1.1 Porphyrins

Porphyrins are present in the vast majority of living organisms as prosthetic groups for a wide number of proteins. They are macrocyclic compounds that contain four pyrrole rings (building blocks) linked together by methene bridges. Porphyrins vary in the nature of side chains attached to each of the four pyrrole rings. Porphyrins can bind with a range of different metal ions to modulate the properties of the macrocyclic ring for the purposes of catalysing a variety of novel bioinorganic reactions, such as electron transport reactions and other redox process. Haem is one of the most widely used tetrapyrroles in biological systems, although factor F_{430}, sirohaem and vitamin B_{12} as well as chlorophylls, all arise from the common haem pathway intermediate, uroporphyrinogen III (scheme 1.1).

1.1.1 Factor F_{430}

Coenzyme F_{430} is the most recently discovered cyclic tetrapyrrole, which is the prosthetic group of methyl coenzyme M reductase, the enzyme that catalyses the final step in methane production. Coenzyme F_{430} has been found only in methanogenic bacteria. These bacteria require nickel for growth, which is the metal ion found in F_{430}.

1.1.2 Chlorophyll

Chlorophylls are very effective photoreceptors because they contain a conjugated network of alternating single and double bonds. Another distinctive feature of chlorophyll is the presence of the additional fused ring system, ring E, and

the long phytol chain esterified to the ring D propionic acid. Magnesium is the metal ion found in chlorophylls.

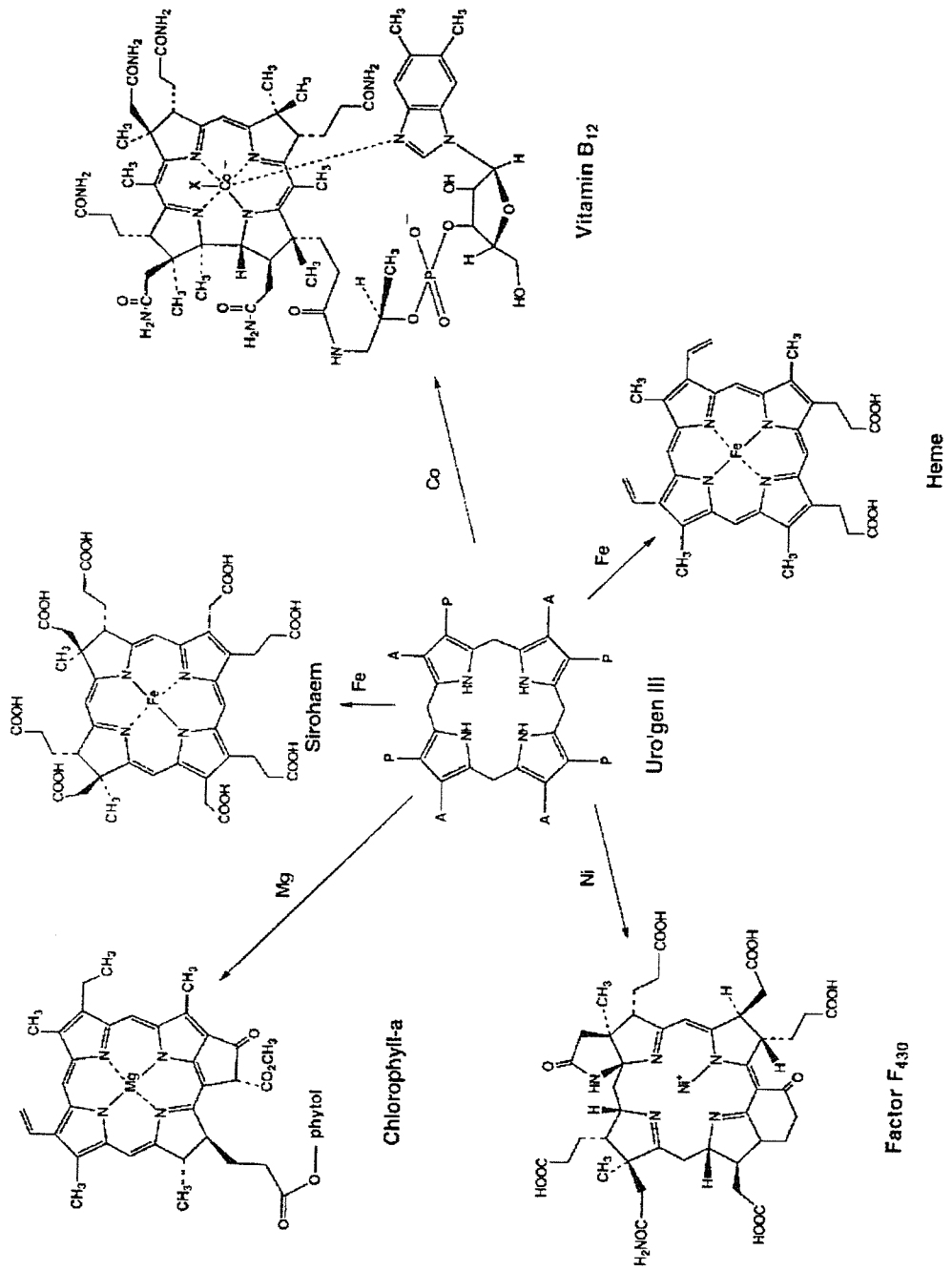

Scheme 1.1 Uroporphyrinogen III is the precursor of all tetrapyrrole prosthetic groups

1.1.3 Cobalamin

Cobalamin (vitamin B_{12}) in the form of coenzyme B_{12}, is important for the action of enzymes that catalyse three main types of reaction; intramolecular rearrangements, methylations and reduction of ribonucleotides to deoxyribonucleotides. Cobalt is the ion bound in the centre of the cobalamin molecule. Commercially available vitamin B_{12}, called cyanocobalamin, has cyanide as a ligand to cobalt. This must be substituted to generate the two biochemically active coenzymes forms, methylcobalamin and adenosylcobalamin. Methylmalonyl coenzyme-A mutase, which is involved in propionic acid, isoleucine and valine catabolism, requires adenosylcobalamin as its coenzyme. Homocysteine methyltransferase, which catalyses the methylation of homocysteine to methionine, also requires methylcoblamin as a coenzyme.

1.1.4 Haem

Haem is one of the most important prosthetic groups, being a constituent of haemoglobin, myoglobin, cytochromes, catalase, and tryptophan pyrrolase. Haem consists of an organic part (protoporphyrin) and an iron atom that can exist in the ferrous (Fe^{2+}) or the ferric (Fe^{3+}) oxidation state. Haemoglobin is the most abundant haem-containing protein in animals. The name haemoglobin arises from *haima*, a Greek word for blood and the word globin, a colourless protein. It is the oxygen transport protein in the red blood cells, carries oxygen from the lungs to the tissues and also transports carbon dioxide away from the tissues back to the lungs. Vertebrate haemoglobin consists of two pairs of subunits, each subunit containing a haem group that can bind one molecule of molecular oxygen. When dioxygen binds, displacing water, ferrous iron is reversibly oxidised to ferric iron (Fe^{3+}). Myoglobin, in contrast to haemoglobin is a compactly folded, single polypeptide chain containing a single haem molecule. Myoglobin is found in muscle cells, where it stores oxygen and transports oxygen to the mitochondria. Haemoglobin and

myoglobin both consist of eight α-helical segments making up 75% of the protein structure.

1.1.4.1 Biosynthesis of haem

The major sites of haem production are the liver and the developing erythrocyte or erythroblast. The first step and the last three steps in the pathway occur in mitochondria, while the other steps occur in the cytosol (Bottomley *et al.*, 1995) (figure 1.1).

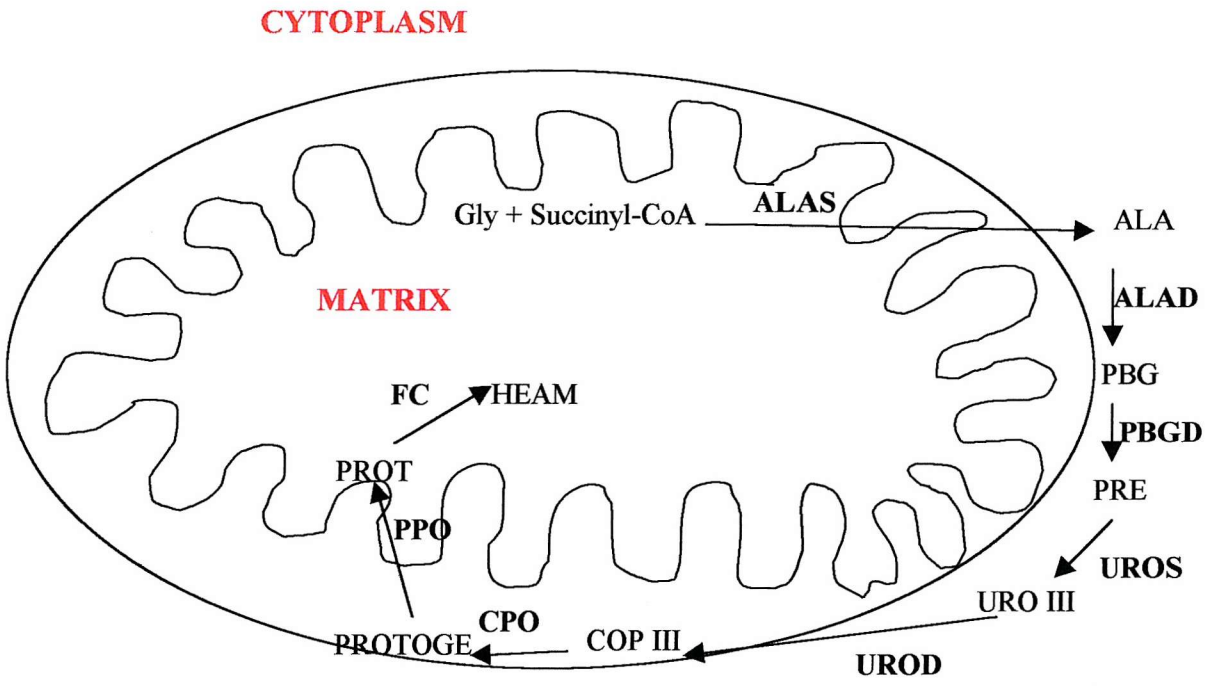

Figure 1.1 Location of the enzymes involved in haem biosynthesis

Abbreviations: 5-Aminolaevulinic acid synthase (ALAS), Aminolaevulinic acid dehydratase (ALAD), porphobilinogen deaminase (PBGD), uroporphyrinogen synthase (UROS), uroporphyrinogen decarboxylase (UROD), coproporphyrinogen oxidase (CPO), protoporphyrinogen oxidase (PPO) and ferrochelatase (FC).

To biosynthesise one molecule of haem, eight molecules of glycine, eight molecules of succinyl-CoA and one ferrous iron atom are required. In a reaction that involves decarboxylation, glycine condenses with succinyl-CoA to form 5-aminolaevulinic acid and two molecules of 5-aminolaevulinic acid condense to produce porphobilinogen (PBG). Four molecules of PBG then polymerise to form the linear tetrapyrrole preuroporphyrinogen (PRE) which is isomerised and cyclised to form the first macrocyclic precursor uroporphyrinogen III (URO). The acetic acid side chains of this porphyrinogen are decarboxylated to form coproporphyrinogen III (COP) and two of the propionic acid side chains are oxidised to vinyl groups to generate protoporphyrinogen IX (PPO). The protoporphyrinogen IX ring is oxidised to produce protoporphyrin IX and ferrous iron is finally inserted yielding haem. Scheme 1.2 shows the haem biosynthesis pathway.

5-Aminolaevulinic acid synthase, that catalyses the first step of haem synthesis, is located in mitochondria where the main synthesis of succinyl-CoA occurs. Although succinyl-CoA is generated by other enzyme systems such as methylmalonyl-CoA mutase, succinate thiokinase and acetoacetyl-CoA:succinate transferase, the major source of succinyl-CoA for haem biosynthesis is from the action of α-ketoglutarate dehydrogenase in the mitochondrial tricarboxylic acid cycle. By passive diffusion, 5-aminolaevulinic acid leaves the mitochondria for the cytosol where 5-aminolaevulinic acid dehydratase (ALAD), porphobilinogen deaminase (PBGD), uroporphyrinogen synthase (UROS) and uroporphyrinogen decarboxylase (UROD) are located. The last three enzymes of the pathway, coproporphyrinogen oxidase (CPO), protoporphyrinogen oxidase (PPO) and ferrochelatase (FC), are present in the mitochondria. In an active step, requiring ATP, coproporphyrinogen III is transported into the mitochondria through specific channels in the outer mitochondrial membrane (Shoolingin-Jordan and Cheung, 1999).

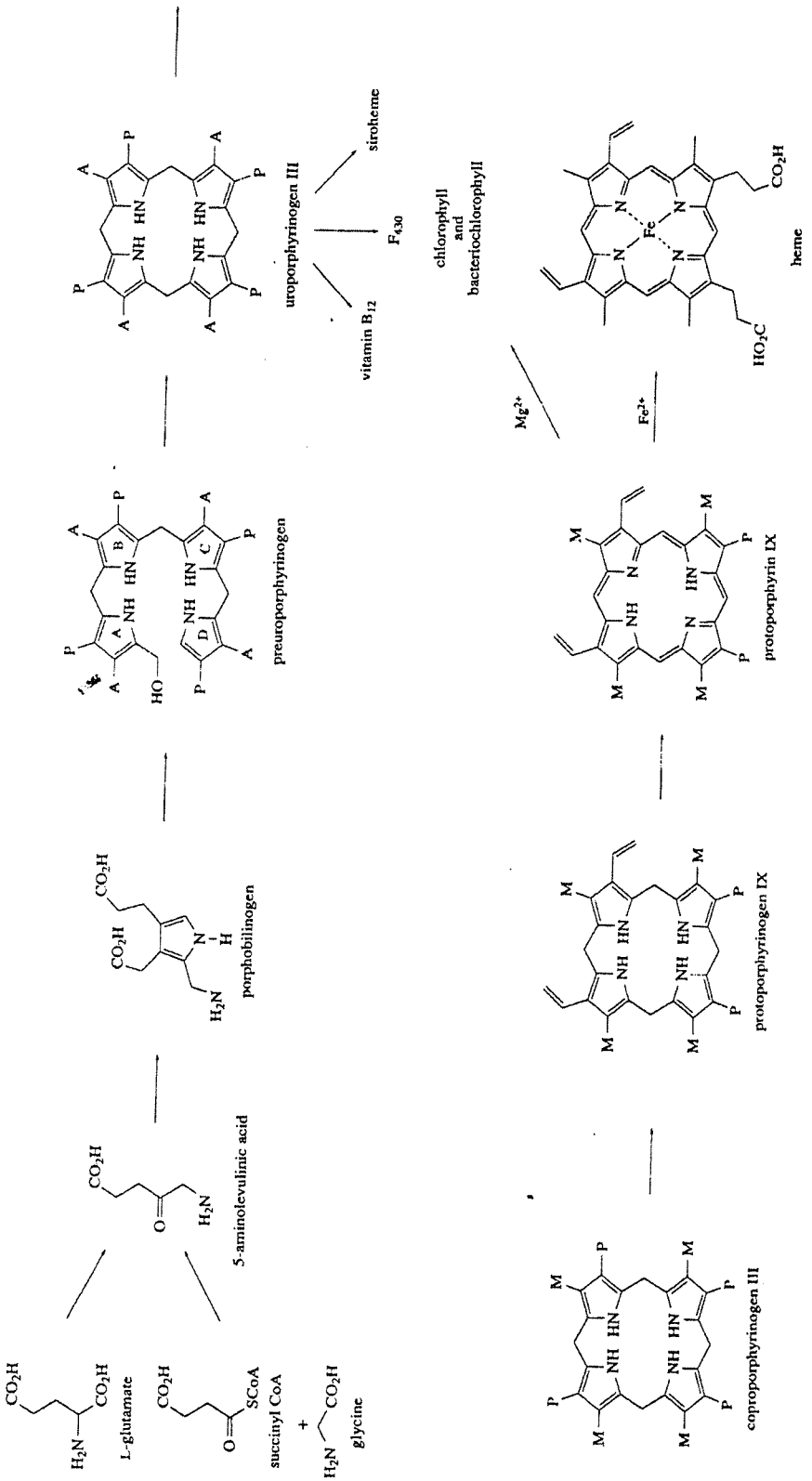

Scheme 1.2 Haem pathway

1.2 The biosynthesis of 5-aminolaevulinic acid

According to the organism, there are two different routes to generate 5-aminolaevulinic acid. Higher plants, anaerobic bacteria and algae produce 5-aminolaevulinic acid through the C_5 pathway, by utilising the intact carbon skeleton of glutamate. Animals, fungi, aerobic and photosynthetic bacteria follow a C_4 pathway (Shemin pathway) to synthesis 5-aminolaevulinic acid by a condensation reaction between glycine and succinyl-CoA, catalysed by ALAS (Ferreira and Gong, 1995).

1.2.1 Glutamate Pathway

The glutamate pathway (C_5 pathway) was discovered in the 1970s by Beale and Castelfranco. In this pathway, three enzymes are involved in the conversion of glutamate into 5-aminolaevulinic acid utilising tRNA as a coenzyme. Glutamyl-$tRNA^{Glu}$ synthetase plays a dual role in biological systems in that it provides glutamyl-$tRNA^{Glu}$ for both protein and haem biosynthesis, catalysing the ligation of glutamate to $tRNA^{Glu}$ in the presence of ATP and magnesium ions. The α-carboxyl-activated glutamate is reduced to glutamate 1-semialdehyde by the enzyme glutamyl tRNA reductase in an NADPH dependent reaction. Finally, glutamate 1-semialdehyde aminotransferase, a pyridoxal 5'-phosphate-dependent enzyme, converts glutamate 1-semialdehyde into 5-aminolaevulinic acid (scheme 1.3).

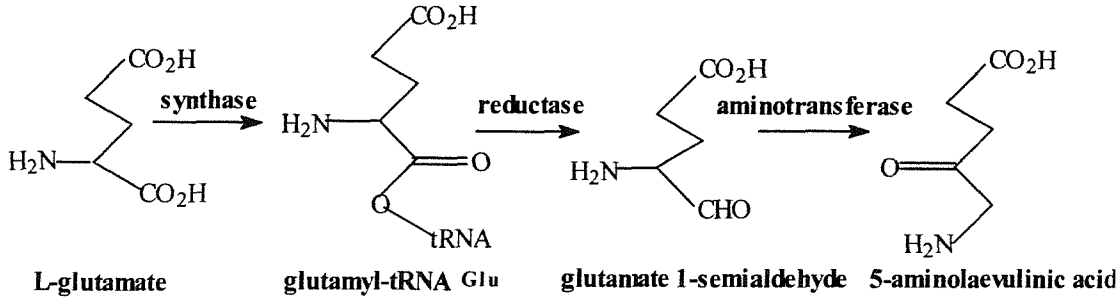

Scheme 1.3 Glutamate pathway

1.2.2 Shemin pathway

Using labelling experiments, Shemin and his co-workers (For a review see Jordan, 1991), found that glycine and succinyl-CoA are condensed to produce 5-aminolaevulinic acid in the presence of ALAS, with PLP acting as a coenzyme (scheme 1.4). PLP has been shown to form a Schiff base linkage with a conserved lysine, lysine 391 in human ALAS2 and lysine 313 in mouse (Hunter and Ferreira 1999a).

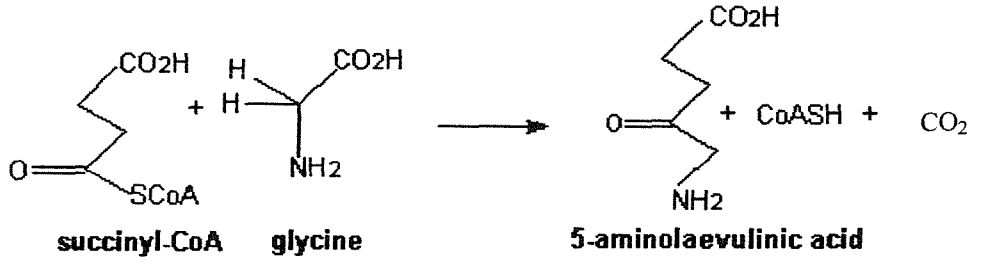

Scheme 1.4 Shemin pathway.

1.3 Historical aspects and occurrence of the 5-aminolaevulinate synthase

ALAS was firstly described in the *Rhodobacter sphaeroides* (*Rhodopseudomonas sphaeroides*) and since that time the enzyme has been isolated from several eukaryotic sources including human, mouse and avian erythrocytes and from yeast. The primary sequences of the ALAS proteins have been derived from gene/cDNA sequences from several sources. Comparison of the sequences suggests that the enzyme consists of a *C*-terminal catalytic core, which is common to all organisms, with a variable *N*-terminal region that is involved in mitochondrial import and regulatory mechanisms (Shoolingin-Jordan and Cheung, 1999). The chick embryo liver enzyme appears to have an amphipathic *N*-terminal region, whereas in yeast it is basic with several threonine and serine residues, representing a

good recognition sequence for mitochondrial targetting (Jordan, 1991) (Ferreira and Gong, 1995). However, the prokaryote enzymes are smaller and consist of the catalytic core component only.

1.4 Properties ALAS

The condensation of succinyl-CoA and glycine to produce 5-aminolaevulinic acid requires PLP as a coenzyme and is the rate-controlling step in haem biosynthesis. Although the enzyme is initially synthesised as a pre-enzyme on cytoplasmic free ribosomes, mature ALAS is located in the mitochondrial matrix and is bound to the inner membrane. The pre-enzyme contains an *N*-terminal sequence that is thought to direct the protein to the mitochondrial matrix before it is converted into the mature enzyme (Srivastava *et al.*, 1983). ALAS has a half-life of 1-3 hrs and exists as homodimers in all species.

Two separate ALAS enzymes have been identified in animals:

1- The hepatic or housekeeping ALAS1 (ALAS-H) that is encoded by a gene located on chromosome 3 (Sutherland *et al.*, 1988). ALAS-H is strongly induced in animals by a wide range of drugs e.g. 2-allyl-2-isopropylacetamide and 3,5-dicarbethoxy-1,4-dihydrocollidine.

2- The erythroid enzyme ALAS2 (ALAS-E) that is encoded by a gene located at Xp11.21 on the X-chromosome. Defects in the ALAS2 gene cause X-linked sideroblastic anaemias (Cox *et al.*, 1990).

The housekeeping ALAS precursor protein has a M_r of 70.6 k in contrast to 64.6 k for the erythroid precursor. The mature mitochondrial forms of the housekeeping and erythroid ALAS isozymes have M_rs of 64.6 k and 59.5 k, respectively. The two isozymes show low amino acid identity in their *N*-terminal sequences whereas there is 66% sequence identity in the *C*-terminal.

1.5 Substrate specificity

ALAS accepts no other amino acid substrate except glycine, but is less specific for succinyl-CoA and can accept other acyl-CoA derivatives such as acetoacetyl-CoA, acetyl-CoA and valeryl-CoA. Acetoacetyl-CoA is transformed into product at a rate of 10% when compared with the rate of succinyl-CoA, whereas, acetyl-CoA and valeryl-CoA are very poor substrates. Despite this specificity, ALAS has a K_m value in the millimolar range for glycine and in the micromolar range for succinyl-CoA.

1.5.1 Glycine

One of the first amino acids discovered, and the first amino acid isolated from proteins in pure form, was glycine (Arnstein, 1954). Glycine is the simplest amino acid with no centre of asymmetry at the α-carbon atom and can be synthesised from carbon dioxide and ammonia by the action of the reversible PLP-dependent enzyme, glycine synthase. Glycine can also be synthesised from serine or threonine in a reaction catalysed by serine hydroxymethyltransferase (figure 1.2). This enzyme catalyses the transfer of the β-carbon atom of serine to tetrahydrofolate to form glycine and N^5,N^{10}-methylenetetrahydrofolate. Glycine can also be synthesised from threonine in a reaction catalysed by threonine aldolase.

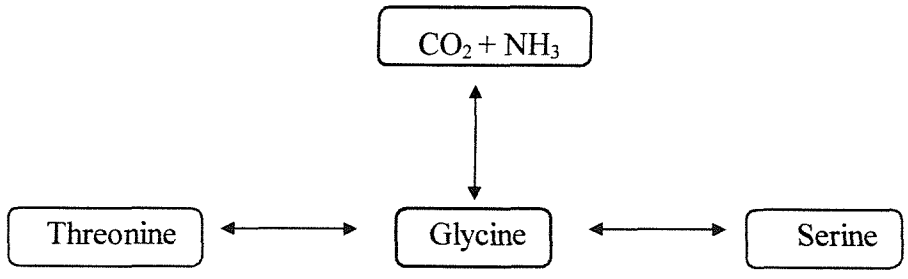

Figure 1.2 Biosynthesis of glycine from different sources.

1.5.1.1 Roles of glycine in human metabolism

Many of the complex molecules found in living organisms are synthesised from simple substances and glycine, as a precursor of nitrogen compounds, is no exception occupying a central position in human metabolism. In addition to its importance for haem biosynthesis, glycine plays a role in the biosynthesis of serine, nucleic acids (purine), creatine, glutathione and protein. As mentioned before, serine is one of the most important substrates involved in the formation of glycine through the action of serine hydroxymethyltransferase but since this is a reversible reaction, glycine is also the precursor of serine by condensation with N^5,N^{10}-methylenetetrahydrofolate.

In pyrimidine biosynthesis, glycine participates in the formation of the methyl group of thymine and is also an essential precursor in purine ring biosynthesis. The purine ring is assembled *de novo* from several simple precursors and glycine provides C-4, C-5, and N-7 (scheme 1.5). Glycine also plays a key role in creatine biosynthesis that requires 196 mg N, as glycine, per day. Creatine is synthesised by the transfer of the guanidino group of arginine to the glycine nitrogen atom, with a methyl group coming from *S*-adenosylmethionine. In most animals this reaction only takes place in the kidney. The subsequent methylation of guanidinoacetate occurs in the liver (Matthews *et al.*, 1997).

Glutathione (GSH), is the main sulphydryl compound in mammalian cells. It is present in millimolar quantities and predominantly found in the reduced form (GSH) as a tripeptide of cysteine, glycine and glutamate. The oxidised form of glutathione (GSSG) consists of two GSH molecules linked by a disulphide bridge. GSH helps to maintain the thiol groups of proteins in the reduced state and the iron of haem in the ferrous (Fe^{2+}) state (Meister and Anderson, 1983). The first step in GSH synthesis is the condensation of the γ-carboxyl group of glutamate with the α-amino group of cysteine to form γ-glutamylcysteine catalysed by the γ-glutamylcysteine synthase enzyme. The α-carboxyl group of cysteine in γ-glutamylcysteine is then activated to form an acyl phosphate to permit condensation with glycine to form GSH in a reaction catalysed by GSH synthase. If glycine is

present in insufficient amounts for the formation of GSH, 5-oxoproline is formed in substantial amounts and excreted in the urine (Jackson *et al.* 1987). Therefore, 5-oxoprolinuria can be used as an index of glycine insufficiency (Jackson, 1990). Scheme 1.5 shows the involvement of glycine in glutathione biosynthesis.

Finally, as mentioned above, glycine is the amino acid used by the first enzyme of haem biosynthesis pathway, 5-aminolevulinate synthase (ALAS) (Jordan, 1991). Shemin established, by isotopic labelling, that glycine was the most efficient precursor of the haem nitrogen atoms. Other experiments using [^{14}C] labelled glycine proved that the C-2 carbon atom, but not the carboxyl carbon atom, of glycine was incorporated into 8 of the positions in the haem macrocyclic ring (reviewed in Jordan, 1991). Haem formation consumes approximately 38 mg N, as glycine, per day (Reed , 1988).

Carbon skeleton of purine shows the atom derived from glycine

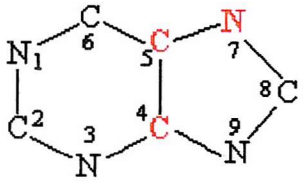

C-4, C-5 and N-7 derived from glycine

Creatine formation

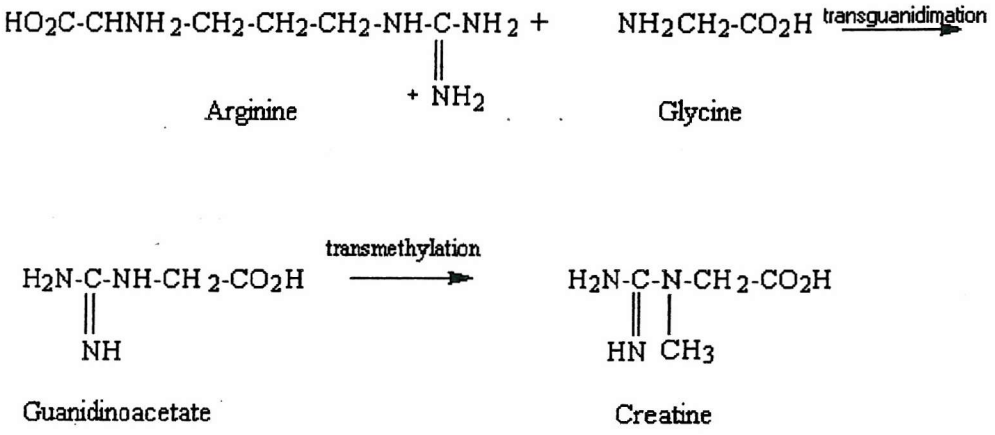

Glutathione formation

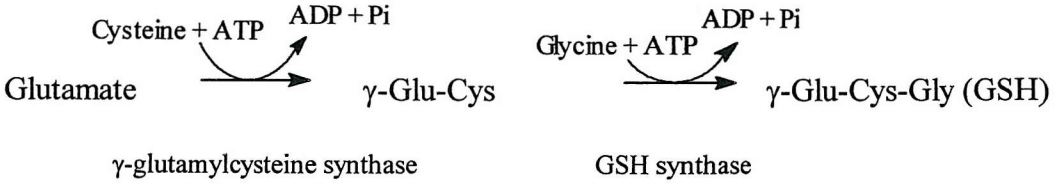

Abbreviations: Glu:glutamate, Cys:cysteine, Gly: glycine, GSH:glutathione

Scheme 1.5 Some additional roles of glycine.

1.6 5-Aminolaevulinate synthase mechanism

In common with other pyridoxal 5'-phosphate-dependent enzymes, the initial stage in the condensation reaction between glycine and succinyl-CoA, is the formation of a Schiff base between pyridoxal 5'-phosphate and an invariant lysine residue (K391) which is in a strongly conserved region of the protein (Scheme 1.6). The amino group of glycine then forms a Schiff base linkage with carbonyl group of pyridoxal 5'-phosphate by transaldimination. To react with succinyl-CoA, the enzyme-bound glycine-pyridoxal 5'-phosphate complex must form a stabilised carbanion at the glycine α-carbon atom. The two major mechanistic possibilities have been investigated by following the pathway of the two glycine hydrogen atoms at the C-2 position when converted to 5-aminolaevulinic acid. Initial decarboxylation would leave the two hydrogen atoms of $2RS[^3H_2]$ glycine undisturbed but initial deprotonation would lead to a loss of half the tritium label. It was observed that to generate a stabilised carbanion, half of the tritium is lost in the enzymic conversion to 5-aminolaevulinic acid. This indicates that deprotonation is the initial mechanism, rather than decarboxylation (Akhtar and Jordan, 1968). The condensation of succinyl-CoA with the enzyme pyridoxal 5'-phosphate-glycine carbanion intermediate, yields an enzyme-pyridoxal 5'-phosphate-2-amino-3-ketoadipic acid complex. Transformation into 5-aminolaevulinic acid could theoretically occur by two ways, either by Schiff base hydrolysis of the intermediate to produce free 2-amino-3-ketoadipic acid, which would then decarboxylate non-enzymically to 5-aminolaevulinic acid or, alternatively, by an enzyme catalysed decarboxylation (Jordan, 1991). Further experiments concluded that ALAS also catalysed the decarboxylation of the bound 2-amino-3-ketoadipic acid (Abboud *et al.*, 1974).

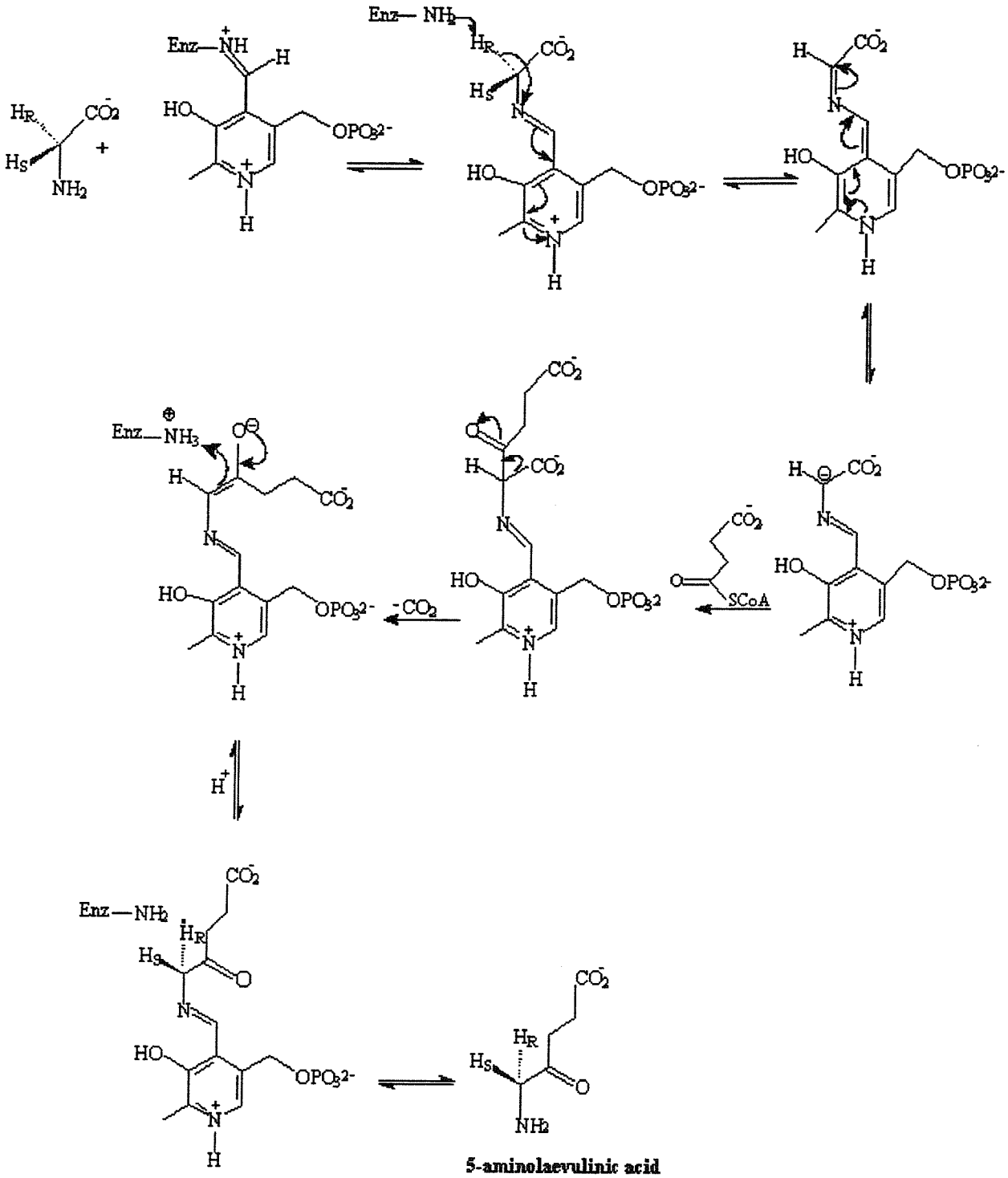

Scheme 1.6 The mechanism of ALAS.

1.7 Other enzymes involved in haem formation

1.7.1 5-Aminolaevulinic acid dehydratase

The second enzyme in the haem pathway is called 5-aminolaevulinic acid dehydratase (ALAD) (also called porphobilinogen synthase). Human ALAD is encoded by a gene localised on chromosome 9q34 and has two alleles. Hereditary deficiency of ALAD is associated with the genetic disease Doss or 5-aminolaevulinic acid dehydratase porphyria. ALAD catalyses the asymmetric condensation of two 5-aminolaevulinic acid molecules to form the monopyrrole porphobilinogen (PBG). The mammalian enzyme is a homooctamer containing about 350 amino acids per subunit. The human enzyme has a native M_r of ~290 k with a subunit M_r of approximately 36 k. Each enzyme subunit contains two 5-aminolaevulinic acid binding sites that function in a specific order. The X-ray structure of human ALAD is described as a "tetramer of dimers", the dimer has extensive interactions between the TIM barrels so that the active sites are perpendicular to one another (Nicola Mills-Davies, PhD thesis, 2000). Similar to human ALAD, ALAD from *E.coli* is shown to form a homo-octameric structure and each subunit adopts a TIM barrel fold with a 30 residue long *N*-terminal arm. Pairs of monomers associate with their arms wrapped around each other and four dimers interact *via* arm regions to form octamers in which each active site is located on the surface (Erskine *et al.*, 1999). There are differences between the ALAD enzymes in term of their metal requirement e.g. human ALAD is Zn^{2+} dependent and plant ALAD is Mg^{2+} dependent. Also the differences arise in the kinetic parameters and susceptibility of the enzymes to oxidation and inactivation by inhibitors. Lead is a potent inhibitor of human ALAD and is one of the main features of lead poisoning (Warren *et al.*, 1998). Anaemia and excretion of high amounts of 5-aminolaevulinic acid in the urine are the main symptoms of lead poisoning.

1.7.2 Porphobilinogen deaminase

Porphobilinogen deaminase (PBG) catalyses the polymerisation of four PBG units to form an unstable 1-hydroxymethylbilane intermediate called preuroporphyrinogen (PRE). PBG deaminase has been isolated from many sources such as human erythrocytes, *R.sphaeroides*, spinach and recombinant *E. coli*. All PBG deaminases exist as monomeric proteins of M_r ranging from 34 to 44 k, and all contain the prosthetic group, the dipyrromethane coenzyme, which is bound to the catalytic site. The coenzyme consists of two molecules of PBG linked together and acts as a primer for preuroporphyrinogen formation. There are two isoforms of PBGD in humans, the erythroid and the ubiquitous enzyme, both of which originate from a single gene on chromosome 11. The human erythroid PBGD contains 344 amino acids, whereas there are additional 17 amino acids at the *N*-terminal of the ubiquitous enzyme (Elder, 1998). From most sources, PBGD enzymes exhibit high thermal stability, similar pH optima from 8.0 – 8.5 and isoelectric points in the range of 4.0 – 4.5. Genetic lesions cause acute intermittent porphyria (AIP), which is one of the most common hereditary porphyrias, transmitted as an autosomal dominant disorder with incomplete penetrance (Grandchamp, 1998). In most developed countries, acute attacks of AIP are thought to affect about 1 to 2 per 100,000 individuals. The symptoms include abdominal pain associated with gastrointestinal dysfunction including nausea, vomiting and constipation. Hypertension and tachycardia may also occur. Muscle weakness can extend to paralysis of leg and arm muscles. AIP is more common in women than men and recurring attacks may be associated with pre-menstrual periods or pregnancy. Patients with AIP have decreased PBGD level in all tissues with 50% of the enzyme on average. Measurement of PBGD in erythrocytes in addition to elevated urinary excretion of 5-aminolaevulinic acid and porphobilinogen is a diagnostic test for the disease. Treatment includes haem arginate and selected analgesics, antiemetics, rehydration and parenteral nutrition. A high carbohydrate diet may also be beneficial. To prevent acute attacks of AIP in patients and latent carrier avoidance of certain drugs and chemicals, which are known to induce AIP, is essential.

The structure of human PBGD has been solved to a resolution of 2.65 Å (Fiyaz, PhD thesis, 2001). The three-dimensional structure of human R167-ubiquitous PBGD consists of three domains. Domain 1 and 2 possess a similar topology consisting of a doubly wounded, five stranded mainly parallel β-sheet, whereas domain three is an open faced three-stranded anti-parallel β-sheet with three α-helical segments and a large loop.

1.7.3 Uroporphyrinogen III synthase

Uroporphyrinogen III synthase is a monomeric enzyme with M_r in the range of 29-33 k, and isolelectric points around pH 5. The enzyme catalyses the cyclization of preuroporphyrinogen by joining the A and D rings, with inversion of the terminal pyrrole ring, ring D, to form uroporphyrinogen III. This rearrangement interrupts the linear repeating order of acetic acid and propionic acid side chains at the β-positions of the pyrrole rings. Uroporphyrinogen III synthases from all sources are highly unstable enzymes. Since, all other tetrapyrroles originate from uroporphyrinogen III, it is considered an extremely important intermediate. Haem is produced from uroporphyrinogen III by decarboxylation of the acetic acid side chains to coproporphrinogen III, whereas in the case of sirohaem, or factor F_{430}, methylation of uroporphyrinogen III at C-2 and C-7 occurs to yield dihydrosirohydrochlorin (precorrin-2), which is also the precursor of vitamin B_{12} (Shoolingin-Jordan and Cheung, 1999). In the absence of uroporphyrinogen III synthase the deaminase product, preuroporphyrinogen, cyclises spontaneously to give uroporphyrinogen I. Congenital erythropoietic porphyria (CEP) is caused by a homozygous defect of uroporphyrinogen synthase and is the rarest autosomal-recessive disorder of porphyrin metabolism. As a result of this deficiency, high amounts of uroporphyrin I and coproporphyrin I accumulate in all cells and tissues, leading to severe photosensitivity.

1.7.4 Uroporphyrinogen III decarboxylase

Uroporphyrinogen III decarboxylase exists as a homodimer with M_r of 42 k. The enzyme catalyses the decarboxylation of the four acetate side chains of uroporphyrinogen III to form coproporphyrinogen III. The enzyme also catalyses the decarboxylation of uroporphyrinogen I to coproporphyrinogen I. Coproporphyrinogen I is unable to act as a substrate for the next pathway enzyme coproporphyrinogen oxidase. In addition to uroporphyrinogens I and III, the enzyme can also act on uroporphyrinogens II and IV. Properties of the enzyme indicate that no coenzyme or metal ion is required. Unlike other enzymes involved in the haem biosynthesis pathway, uroporphyrinogen III decarboxylase appears to exist in a single form with no tissue-specific isozymes (Shoolingin-Jordan and Cheung, 1999). Porphyria cutanea tarda (PCT) and hepatoerythropoietic porphyria (HEP) are due to heterozygous and homozygous uroporphyrinogen III decarboxylase deficiency, respectively (Sassa and Kappas, 2000). Symptoms of PCT are characterised by chronic blistering lesions of sun-exposed skin, marked accumulation of porphyrins in the liver and the appearance of excess porphyrins in plasma and urine. The homozygous disease, HEP is very rare and causes haemolysis, anaemia and severe photosensitive dermatitis. The photosensitivity is mediated by the presence of uroporphyrin and partially decarboxylated intermediate porphyrins in the skin and plasma (Thadani *et al.*, 2000).

The three dimensional X-ray structure of recombinant human uroporphyrinogen decarboxylase has been determined at 1.6 Å (Whitby *et al.*, 1998). The 3D structure of UROD consist of a single domain containing an $(\alpha/\beta)_8$ barrel.

1.7.5 Coproporphyrinogen III oxidase

Coproporphyrinogen III oxidase (CPO) has a M_r of 36k. CPO converts coproporphyrinogen III to protoporphyrinogen IX by the oxidative decarboxylation of the A and B ring propionate side chains to give vinyl groups. There are two classes of the enzyme, one found in aerobic organisms and the other class found in

anaerobic cells. All enzymes isolated from aerobic organisms require molecular oxygen as an electron acceptor, whereas other electron acceptors are used in anaerobic organisms. Unlike uroporphyrinogen III decarboxylase, coproporphyrinogen III oxidase is specific only for coproporphyrinogen III, which explains why coproporphyrinogen I accumulates in congenital erythropoietic porphria. The deficiency of CPO causes hereditary coproporphyria (HCP), which is an autosomal dominant hepatic porphyria. The disease may be less severe compared to AIP, but the neurological features are generally identical. The factors that influence clinical expression of AIP such as drugs, hormones and nutritional changes also influence HCP. In most cases, the activity of the enzyme is reduced to 50% of normal enzyme levels and there is a dramatic increase in the excretion of coproporphyrinogen III (Sassa and Kappas, 2000).

1.7.6 Protoporphyrinogen IX oxidase

Protoporphyrinogen IX is converted, in a six-electron oxidation, to protoporpyrin IX, the first conjugated (and therefore coloured) macrocyclic ring intermediate in the pathway. The mechanism involves loss of hydrogen atoms attached to the carbon bridges between the pyrrole rings (*meso*-positions). Protoporphyrinogen IX oxidase (PPO) is a mitochondrial enzyme with a M_r 50.8 k and has an absolute requirement for oxygen. Deficiency in PPO activity causes variegate porpyhria (VP), which is also an autosomal dominant hepatic porphyria. Some of the clinical features of VP are closely similar to AIP, but it is less common than AIP (Elder *et al.*, 1997).

1.7.7 Ferrochelatase

Ferrochelatase catalyses the insertion of ferrous iron into the centre of the macrocycle to yield haem. Ferrochelatase is a membrane-associated protein, occurring inside the mitochondria and can use Fe^{2+}, Co^{2+} and Zn^{2+} as a substrate metal. Ferrochelatase is a monomeric protein with a M_r in the region of 40-48 k.

The metal ion chelatases of tetrapyrrole biosynthesis are classified either as ATP-independent enzymes, such as protoporphyrin IX ferrochelatase, or as ATP-dependent enzymes, such as Mg chelatase involved in chlorophyll biosynthesis. Partial deficiency of ferrochelatase leads to erythropoietic protoporphyria (EPP), which is inherited in an autosomal dominant fashion. The disease usually presents in childhood (Thadani *et al.*, 2000) and EPP causes mild to moderate photosensitivity and high levels of protoporphyrin accumulate in erythrocytes, plasma and bone marrow (Cox, 1997). Rarely, severe and fatal hepatic complications are associated with accumulation of protoporphyrin in the liver (Sassa and Kappas, 2000). Table 1.1and figure 1.3 summarised the porphyrias resulting from deficiencies of haem-synthesising enzymes.

Table 1.1 The porphyrias resulting from deficiencies of haem-synthesising enzymes.

Disease	Enzyme	Inheritance	Organ affected
Doss porphyria	5-Aminolaevulinic acid dehydratase	Recessive	Nervous system
Acute intermittent porohyria	Porphobilinogen deaminase	Dominant	Nervous system
Congenital erythropoietic porphyria	Uroporphyrinogen III synthase	Recessive	Skin and appendages, tissue macrophage system
Porphyria cutanea tarda	Uroporphyrinogen decarboxylase	Dominant	Skin
Hereditary coproporphyria	Coproporphyrinogen oxidase	Dominant	Nervous system
Variegate porphyria	Protoporphyrinogen oxidase	Dominant	Nervous system
Protoporphyria	Ferrochelatase	Dominant	Gallstones, liver disease and skin

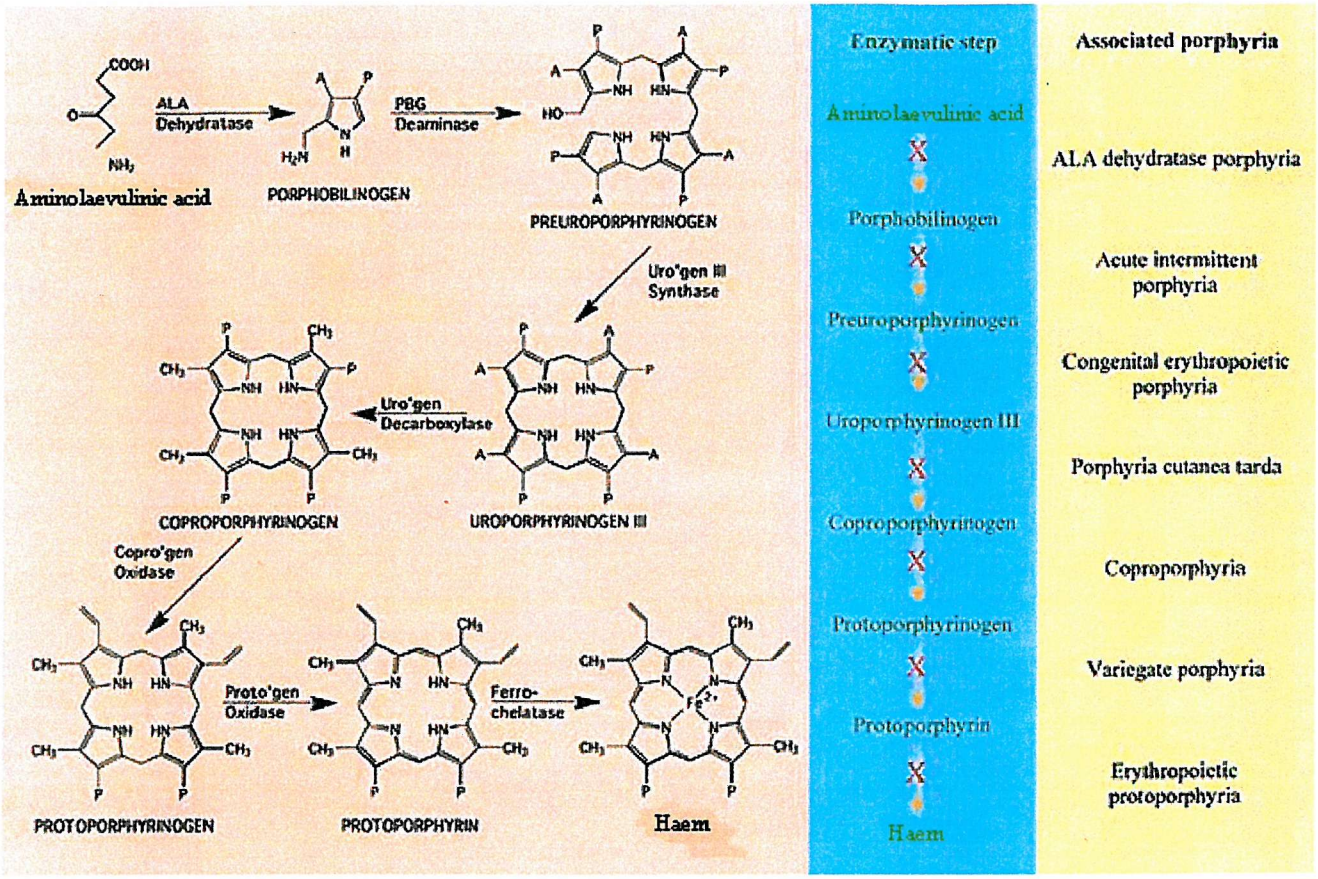

Figure 1.3 The defect or deficiency of the haem pathway enzymes that causes porphyria.

1.8 Erythroid 5-aminolaevulinic acid synthase defects and X-linked sideroblastic anaemia

The sideroblastic anaemias are a heterogeneous group of disorders characterised by anaemia of varying severity, the presence of ring sideroblasts in the

bone marrow with the erythrocytes derived from these bone marrow cells being typically hypochromic and microcytic. These characteristics reflect the lack of a normal complement of haemoglobin and progressive accumulation of iron (Bottomley *et al.*, 1995). There are two types of sideroblastic anaemias, either idiopathic acquired sideroblastic anaemia, presenting as a clonal disorder in later life, and hereditary sideroblastic anaemia, resulting from mutations in the erythroid-specific isozyme of 5-aminolevulinate synthase. Mutation detection can be achieved by studying either cDNA derived from the RNA of reticulocytes or genomic DNA. Patients with the acquired disorder respond rarely to pyridoxine treatment (vitamin B_6), the dietary precursor of the coenzyme pyridoxal 5'-phosphate, whereas, one third of patients with sex-linked inherited sideroblastic anaemia respond to pyridoxine treatment (Cox *et al.*, 1994), indicating that the most probable cause of the anaemia is either a low level of ALAS activity or a reduced availability of pyridoxal 5'-phosphate within developing erythroid cells. On this basis, addition of pyridoxal 5'-phosphate, the coenzyme, *in vitro* or supplementation of pyridoxine *in vivo* should enhance or restore the enzyme activity to near normal. The defective activity of ALAS2 in bone marrow erythroblasts of patients with X-linked sideroblastic anaemia diminishes haem biosynthesis, leading to insufficient protoporphyrin IX to use all of the available iron, and therefore to reduced concentration of Hb and increased iron concentration in the tissues. Accumulation of iron is particularly damaging to the heart, pancreas, liver and pituitary, which can lead to arthritic signs, cirrhosis of the liver, heart failure and endocrine disorders (Cotter *et al.*, 1999).

The human ALAS2 gene is composed of 11 exons of varying sizes (figure 1.4) covering 22kb of the X-chromosome. Exon 1 encodes a short 5'-untranslated region of the ALAS2 mRNA. Translation of ALAS2 commences at nucleotide 16 in exon 2 and terminates within exon 11 to give a precursor protein of 587 amino acids. This is cleaved at residue 78 to form the mature enzyme after import into mitochondria, therefore exon 2 encodes the mitochondrial targetting presequence of the enzyme (region 1). Only exons 5-11 are thought to form the catalytic core of the

enzyme (region 3) since the bacterial ALAS lacks the sequence specified by exons 1-4. Exons 3 and 4 encode the remaining *N*-terminal region of the mature human protein (region 2).

As a result of extensive studies, over 22 mutations have been described in ALAS2 in over 30 kindreds. Most of the mutations are found in exons 5-11 and usually involve a single base substitution. There is one case of a mutation leading to a stop codon (R204X). Table 1.2 summarises some of these mutations. XLSAs are classified into three categories:

Mutations refractory to dietary pyridoxine supplement.

Mutations partially responsive to dietary pyridoxine supplement.

Mutations completely responsive to dietary pyridoxine supplement.

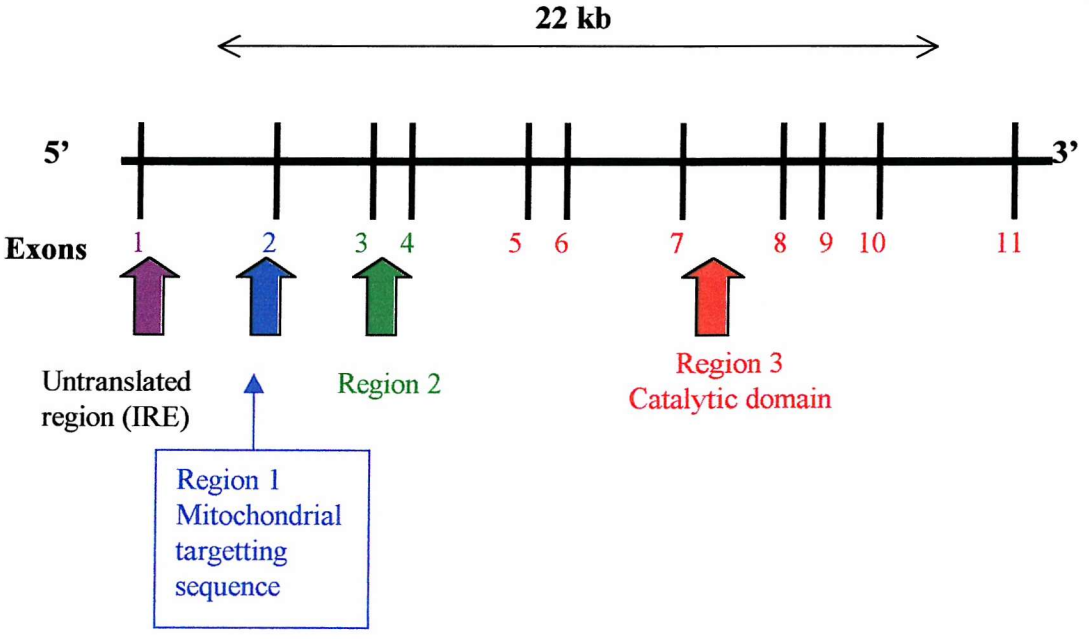

Figure 1.4 Structure of human ALAS2 gene (Bishop *et al.*, 1995).

Table 1.2 Defects of the human erythroid ALAS2 gene in patients with X-linked sideroblastic anaemia (Cotter *et al.*, 1999).

Exon	Mutation	Amino acid substitution	Sex	Response to pyridoxine	Reference
5	TTC-TTA	F165L	M	+	Cotter et al (1994)
5	GCT-ACT	A172T	F	++++	Cotter et al (1995)
5	CGC-CTC	R170L	M	++	Edgar et al (1998)
5	GAT-GTT	D190V	M	Refractory	Furuyama et al (1997)
5	TAC-CAC	Y199H	M	++	Cotter et al (1999)
7	GGT-AGT	G291S	M	+++	Prades et al (1995)
7	AAG-GAG	K299Q	M	++++	Cotter et al (1995)
8	ACT-AGT	T388S	M	++	Cox et al (1994)
9	CGC-TGC	R411C	M	+++	Cotter et al (1999)
9	CGA-CAA	R448Q	M	++	Cotter et al (1999)
9	CGC-TGC	R452C	M	+	Cotter et al (1999)
9	CGC-CAC	R452H	M	+	Edgar et al (1997)
9	ATC-AAC	I476N	M	+++	Cotter et al (1992)
9	ATG-GTG	M426V	M	+++	Furuyama et al (1997)
10	CGC-TGC	R517C	F	Refractory	May and Bishop (1998)

Abbreviations: M, male; F, female; + - ++++, response to B_6.

1.9 ALAS and other pyridoxal 5'-phosphate (PLP)-dependent enzymes

Pyridoxal 5'-phosphate-dependent enzymes catalyse a wider range of metabolic reactions than those containing any other coenzyme (John, 1995). Almost all PLP-dependent enzymes act upon amino acids. In PLP enzymes, PLP exists as a Schiff base with its aldehyde group forming an imine linkage with the ε-amino group of an enzyme lysine residue. This is called an "internal" aldimine. On addition of the substrate a transaldimination process occurs, by where the substrate amino group displaces the lysine to form an "external" aldimine complex. This complex is held in the active site by non-covalent interactions. In addition to being able to form imines to bind amino groups of the substrates though its aldehyde group, PLP also provides an electron sink to withdraw electrons from the substrates to facilitate a range of reactions. The PLP-dependent enzymes can be classified into α-, β- and γ-families.

The α-family is the largest family. Containing the enzymes that catalyse transformations of amino acids in which manipulations of the external aldimine are limited to the α-carbon atom that carries the amino group forming the linkage to the conzyme (scheme 1.7). The other two families, the β- and γ-families, catalyse reaction that involve the β- or γ- carbon atoms. The α- and γ-families are thought to be distantly related with one another, but are not homologous with the β-family (Alexander *et al.*, 1993). Table 1.3 shows examples of enzymes belonging to each family. The 3D structure of nine PLP-dependent enzymes, out of a 13 determined, shows similarities in the main-chain folds (Alexeev *et al.*, 1998). Three of these enzymes utilise the same mechanistically intriguing strategy that ALAS follows. The related enzymes are 8-amino-7-oxononanoate synthase (AONS), serine palmitoyltransferase (SPT) and 2-amino-3-oxobutyrate-CoA ligase (AKB).

Table 1.3 The α-, β- and γ-families of PLP-dependent enzymes.

α Family	β Family	γ Family
Serine hydroxymethyl-transferase	L-Serine dehydratase	*O*-Succinylhomoserine(thio)-lyase
Glycine *C*-acetyltransferase	D-Serine dehydratase	*O*-Acetylhomoserine(thio)-lyase
5-Aminolaevulinate synthase	Threonine dehydratase	Cystathionine γ-lyase
8-Amino-7-oxononanoate synthase	Tryptophan synthase	Cystathionine β-lyase
Serine-pyruvate Aminotransferase	Threonine synthase	
	Cysteine synthase	

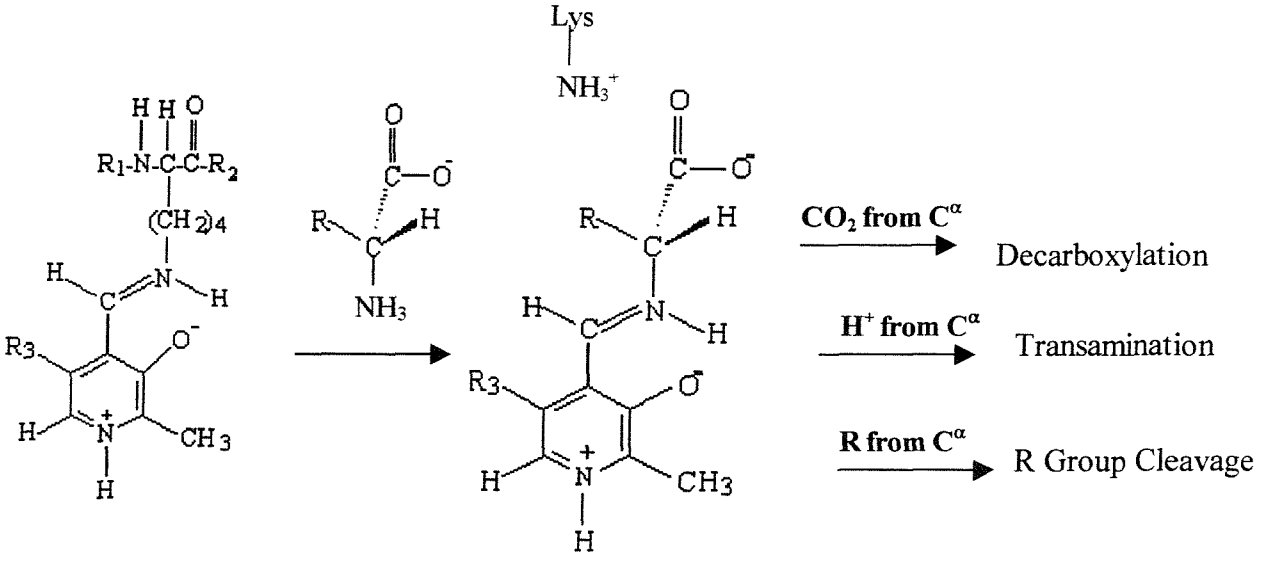

Internal aldimine External aldimine

R_1, R_2 = Protein chain, $R_3 = CH_2OPO_3^{2-}$

Scheme 1.7 Different reaction types in the α subfamily result from different C^{α} bond cleavage after conversion to external aldimine (Tan *et al.*, 1998).

Aim of the study

In this study, three mutations in human erythroid ALAS have been investigated. These are T388S, R452H and R517C. The first mutant is from patients who responded well to dietary pyridoxine treatment, while R452H from patients who responded partially. The third mutation is from a patient where the anaemia was refractory to pyridoxine treatment. Additional mutations, R517K and R517L, were also constructed to investigate further.

The wild type and mutant proteins were expressed and kinetic characterisation of the purified enzymes will be carried out to provide information about their ability to interact with the two substrates and pyridoxal 5'-phosphate. The interaction of the mutant enzymes with pyridoxal 5'-phosphate were also investigated by spectroscopic analysis and circular dichroism. Attempts were made either to crystallise the enzyme or to carry out molecular modelling to generate a 3-dimensional structure that could be used to explain the molecular basis of some of the X-linked sideroblastic anaemias. One question that will be addressed, in particular, is why some patients respond well to pyridoxine treatment while the disease is refractory in others.

Chapter 2

MATERIALS AND METHODS

2.1 Materials

Growth media, tryptone and yeast extract were obtained from Difco Laboratories, Detroit, USA. Bacto agar was purchased from Lab M, Bury, UK. Talon resin was supplied by the Clotchen Company. Tris base was supplied by ICN Biomedical Inc, USA. Sodium hydroxide, sodium chloride, potassium phosphate, trichloroacetic acid were supplied by Fisher Scientific, Loughborough, UK. *p*-Dimethylaminobenzaldehyde was from BDH, Poole, UK. All other chemicals were purchased from Sigma Chemical Company, Poole, UK. Membrane filters (0.2μm) were purchased from Whatman International, Kent, UK. Syringe filters (0.2μm) were from Sartorious, Göttingen, Germany and gel electrophoresis equipment was supplied by Genetic Research Instrumentation Ltd., Braintree, UK.

2.2 Media

2.2.1 Luria Broth (LB) media

Bacto tryptone	10 g
Bacto yeast extract	5 g
NaCl	5 g

This was made up to 1L with distilled water and autoclaved immediately.

2.2.2 LB plates

15g Bacto agar was added to a litre of LB media before autoclaving. Plates were then stored at 4°C.

2.3 Molecular biology methods

2.3.1 Bacterial strains and vectors

The bacterial strains and vectors used are shown in tables 2.1 and 2.2 respectively.

Table 2.1 Bacterial strains used in this study.

Strain	Genotype
JM101	F' *tra*D36 *lac*lqΔ(*lac*Z)M15 *pro*AB+/*sup*E *thi* Δ(*lac-pro*AB)
JM109	e14$^-$(McrA$^-$) *rec*A1 *end*A1 *gyr*A96 *thi* *hsd*R17(r_k-m_k+) *sup*E44 *rel*A1 Δ(*lac-pro*AB) [F' *tra*D36 *pro*AB+ *lac*lqΔ(*lac*Z)M15]
BL21	F$^-$ *omp*T *[lon]* *hsd*S_B(r_B-m_B- an *E.coli* B strain) with DE3 a λ prophage carrying the T7 RNA polymerase gene
DH5α	F$^-$ ϕ80d*lac*ZΔM15 *rec*A1 *end*A1 *gyr*A96 *thi*-1 *hsd*R17(r_k- m_k+) *sup*E44 *deo*R *rel*A1 Δ(*lac* ZYA-*arg*F)U169 λ-

Table 2.2 Vectors used in this study

Plasmid	Properties	Plasmid size (kb)	Source
pT7-7	Expression vector	2.47	Tabor, 1990
pTrc-His	Expression vector	4.4	Invitrogen

2.3.2 Solutions

2.3.2.1 Ampicillin stock solution

Ampicillin sodium salt was dissolved in AnalaR water to a concentration of 100mg/ml, and filtered through a 0.2μm filter. It was used in media at a final concentration of 100μg/ml. This solution was stored at –20° C

2.3.2.2 IPTG (1M)

$C_9H_{18}O_5S$ 2.38 g

Made up to 10ml with sterile water and sterilised by filtration.

2.3.2.3 50x TAE buffer

Tris/HCl	242 g
EDTA	37.2 g
Acetic acid	57.1ml

Made up to 1L with distilled water.

2.3.2.4 Ethidium bromide solution

A stock solution of 10mg/ml was made and used at a final concentration of 0.5μg/ml.

2.3.2.5 DNA loading buffer

0.25% Bromophenol blue

0.25% Xylene cyanol

30% Glycerol

This mixture was made in distilled water and autoclaved.

2.3.2.6 Calcium chloride solution (50mM)

$CaCl_2.2H_2O$ 7.4 g

Made up to 1L, autoclaved and stored at 4°C.

2.3.2.7 Wizard miniprep solutions

All these solutions were purchased from Promega in kit form.

Cell resuspension solution

50 mM Tris/HCl, pH 7.5

10 mM EDTA

100 μg/ml RNase A

Cell lysis solution

0.2 N NaOH

1% SDS

Cell neutralisation solution

1.32 M Potassium acetate, pH 4.8.

Wash solution

20 ml of 200 mM NaCl

20 mM Tris/HCl, pH 7.5

5 mM EDTA

The aqueous solution is diluted with 95% ethanol to a final concentration of 55%.

2.3.3 Methods used

2.3.3.1 Small-scale isolation of plasmids

An overnight culture of cells (10ml) was harvested. The supernatant was discarded and the bacterial pellet was resuspended in cell resuspension solution (250 μl). Cell lysis solution (250μl) was added and the solution was mixed by inverting the tube. The mixture was then incubated at room temperature for 5 min. Alkaline protease solution (10μl) was added to the lysed cells and the solution was gently mixed. This was allowed to stand for 5min and the neutralisation solution (350μl) was then added. The solution was mixed immediately by inverting the tube. The mixture was then centrifuged at room temperature for 10min. at 12,000 x g. The clear lysate was transferred to a Wizard *Plus* SV minipreps spin column and centrifuged at 12,000 x g for 1min. at room temperature. The flow-through was

discarded from the collection tube and 750µl of wash solution was added to the spin column. After centrifugation at 12,000 x g for 1 min. at room temperature, the flow-through was discarded, as before, and 250µl of the column wash solution was added, followed by centrifugation for 2 min. at room temperature. The spin column was transferred to a sterile microfuge tube and Nuclease-Free Water (obtained from Promega) (100µl) was added, followed by centrifugation at 12,000 x g for 1min. at room temperature. Finally, the DNA product was kept at -20 °C.

2.3.3.2 Large-scale preparation of plasmid DNA

A starter culture of 30ml of the required bacterial strain was grown overnight in LB media supplement with ampicillin. This was used to inoculate 500 ml of LB media containing ampicillin, which was then incubated for 2.5 hours at 37°C with vigorous shaking. Chloramphenicol, (34mg/ml) (2.5ml) in absolute ethanol, was then added and the flask was incubated for a further 12-16 hours overnight at 37°C. The cells were harvested by centrifugation at 4000 rpm for 15 min. at 4°C. The supernatant was discarded and the pellet was resuspended in 100 ml ice-cold STE buffer before centrifugation as above.

The pellet was then resuspended in 10ml solution I and 1ml of a freshly prepared solution of lysozyme (10mg/ml in 10mM Tris/HCl, pH 8.0) was added, followed by 20ml of freshly prepared solution II. The mixture was inverted several times and left for 10 min at room temperature. Solution III (15ml) was added and the bottle was shaken until only one liquid phase could be distinguished. The flask was left for 10 min at 4°C when a white flocculent precipitate formed (cell debris), which was removed by centrifugation at 4000 rpm for 15 min at 4°C, the rotor being allowed to stop without braking. The supernatant was filtered through four layers of Miracloth (Calbiochem, USA). Isopropanol (0.6 volume) was added and the solution was stored at room temperature for 10 min to precipitate nucleic acids. The precipitate was collected by centrifugation at room temperature and the supernatant was discarded. The pellet was washed with 70% ethanol that was drained off and the pellet was dried in air. The pellet was then dissolved in TE buffer (3ml) and transferred to a 50ml centrifuge tube. The dissolved pellet was mixed with ice-cold

5M LiCl (3ml) and the resulting precipitate was collected by centrifugation for 15 min at 4 °C. After centrifugation, the pellet was washed with 70% ethanol and then fully dried before the next stage. The pellet was dissolved in TE containing DNAase-free pancreatic RNAase, then transferred to a microfuge tube and kept for 30 min at room temperature. The plasmid DNA was precipitated by the addition of 1.6M NaCl (500µl) containing 13% (w/v) PEG 8000 and recovered by centrifugation at 4 °C. The supernatant was removed by aspiration and the pellet was redissolved in TE buffer (400µl). The solution was extracted once with phenol:chloroform and once with chloroform. The aqueous phases from the extractions were transferred to a fresh microfuge tube and 10M ammonium acetate (100µl) was added, followed by two volumes of absolute ethanol. The tube was stored for 10 min at room temperature. The precipitated plasmid DNA was removed by centrifugation at 4 °C and the pellet was then washed with 70% ethanol and the tube left open to allow the ethanol to evaporate. The pellet was finally dissolved in TE buffer (500µl). The quantity and the quality of the DNA obtained was determined by measuring the absorbance of a 1:100 dilution of this solution at 260nm and by calculating the ratio of the absorbance at 260nm and 280nm.

2.3.3.3 DNA sequencing

OSWEL DNA Sequencing Service (University of Southampton) carried out DNA sequencing of human ALAS. By using appropriate oligonucleotide primers, the whole coding region of the protein could be sequenced in three parts. Primers were designed to have a high T_m and a low number of possible hairpin turns.

2.3.3.4 Quantifying DNA

The amount of DNA present in solution was determined by taking an absorbance measurement at 260nm. An O.D of 1 corresponds to 50µg/ml for double stranded DNA and 40µg/ml for single stranded DNA. The absorbance was also measured at 280nm. The ratio between the two readings gives an estimate of the purity of the DNA. Pure, double stranded DNA has an OD_{260}/OD_{280} between 1.8 and 2.0.

2.3.3.5 Site-directed mutagenesis by PCR

The R452H and T388S cDNA samples were gifts from Professor Sylvia Bottomley (Oklahoma). The mutant cDNA of these clones should have been ligated between the *Bam*HI-*Eco*RI sites of pTrcHisB. However, sequencing of the mutant clones did not reveal a *Bam*HI site. Therefore, to carry out any further cloning it was necessary to introduce a *Bam*HI site at the 5'-end of the cDNA using the following primers:

*Bam*HI 5' GCGCGGATTCCGAAGAGCAAGTTGTGCAGAAGGC 3'

*Eco*RI 5' ACGAATTCAGTCGACTCAGGCATAGGTGGTGACATAC 3'

To generate native human ALAS2, T388S was subjected to PCR mutagensis using site specific primers, the sequence of the primers are given below:

Primer 1 5' CATCTCTGGAACTCTTGGCAAGG 3'

Primer 2 5' CCTTGCCAAGAGTTCCAGAGATG 3'

T388S has the AGT codon for serine, which was converted to the ACT codon for threonine to generate the wild-type DNA. To carry out the PCR reaction, the template DNA was diluted to a concentration of 60ng/μl, whereas the concentration of the primers was calculated on the bases of the length of the primer (i.e. an 18 mer=100ng was used). PCR was carried out in two stages; the first stage involved two half reactions, each using one of the mutant primers and a primer on either end of the cDNA, having a restriction site *Bam*HI or *Eco*RI. In the second stage, PCR was carried out by using the product of two half reactions and the two primers at the end of the gene. Each stage of PCR relies on the use of different temperatures for the three steps of the reaction- denaturation, annealling and extension (figure 2.1). A high temperature, usually 94-95 ^{o}C, is used to separate the strands of the DNA template. The temperature is then lowered to allow the primers to base pair to their complementary sequences on the template strands and this temperature varies depending on the primers. Finally, for efficient DNA synthesis, the temperature is adjusted to optimal for the DNA ploymerase activity. To amplify the target DNA it is necessary to cycle through these temperatures several times (25-40 cycles depending on the application).

A) 1st PCR reaction

In two sterile 0.5ml Eppendorfs, the DNA template (50ng) was mixed with the 10mM dNTPs and reaction buffer containing 2mM $MgSO_4$. In one tube the 5'-primer with the *Bam*HI site and the mutagenic primer on the coding strand (non-sense strand) were added; in the second tube the 5'-primer having *Eco*RI site and the mutagenic primer on the non-coding strand (sense strand) were added. The volumes were adjusted to 39.5µl with sterile water before heating to 95°C for 5 min in a heated PCR block. Volume of 0.5µl of Vent polymerase enzyme (1U) was then added to each tube and the contents mixed gently. The conditions for the PCR of long fragments was as follows:

Stage	Temp ^{0}C	Time
Strand separation	94^{0}C	1 min
Annealing	58^{0}C	1 min
Extension	72^{0}C	1 min 40 sec

NB. The annealing temperature based upon the T_m of the primers and the extension time was calculated for a gene sequence of 1kb = 1 min so, for the short fragment, the extension time was 20 seconds, whereas it was 1 min 40 sec for the long fragment.

The DNA products, after the PCR reaction, were visualised on a 2% agarose gel, for the short fragment, and 1% for the long fragment. The bands corresponding to the expected size of each fragment were excised from the gel and the DNA was extracted using a Geneclean II kit (see section 2.3.3.10). The solution was evaporated to dryness and the DNA (~50ng/µl) was dissolved in 20µl of sterile water.

B) 2nd PCR reaction

Using a sterile Eppendorf tube, 1.5µl of each 1st PCR reaction product (~50ng) were mixed with 1.5µl dNTP's (10mM) and the two primers at either end (i.e. having *BamHI* and *Eco*RI respectively) in reaction buffer containing 2mM $MgSO_4$.

Using sterile water, the volume was made up to 39.5µl before heating to 95°C for 5 min. The addition of 0.5µl Vent polymerase (1U) was followed by 5 cycles of:

Stage	Temp °C	Time
Strand separation	94°C	1 min
Annealing	48°C	1 min
Extension	65°C	1 min 40 sec

After 5 cycles another 25 cycles were performed consisting of:

Stage	Temp °C	Time
Strand separation	94°C	1 min
Annealing	62°C	1 min
Extension	72°C	1 min 40 sec

After the PCR reaction, the mutated DNA was run on an agarose gel and the DNA was isolated using the Geneclean II kit, as before. The same process was used to generate R517C/K/L mutants, using native DNA as a template. The sequences of the R517C primers are as follows:

Primer 1 5' GAAGAGCTCCTGTGC TTGGCACCCTCC 3'
Primer 2 5' GGAGGGTGCCAAGCACAGGAGCTCTTC 3'

In the native arginine uses the CGC codon, which was changed to TGC in the R517C mutant coding for cysteine. The arginine codon CGC was changed to AAA and CTG codon coding for lysine and leucine, respectively.

The R517K primers are given below:

Primer 1 5' GAAGAGCTCCTGAAATTGGCACCCTCC 3'

Primer 2 5' GGAGGGTGCCAATTTCAGGAGCTCTTC 3'

Finally, the primers of R517L were follows:

Primer 1 5' GAAGAGCTCCTGCTGTTGGCACCCTCC 3'

Primer 2 5' GGAGGGTGCCAAGACCAGGAGCTCTTC 3'

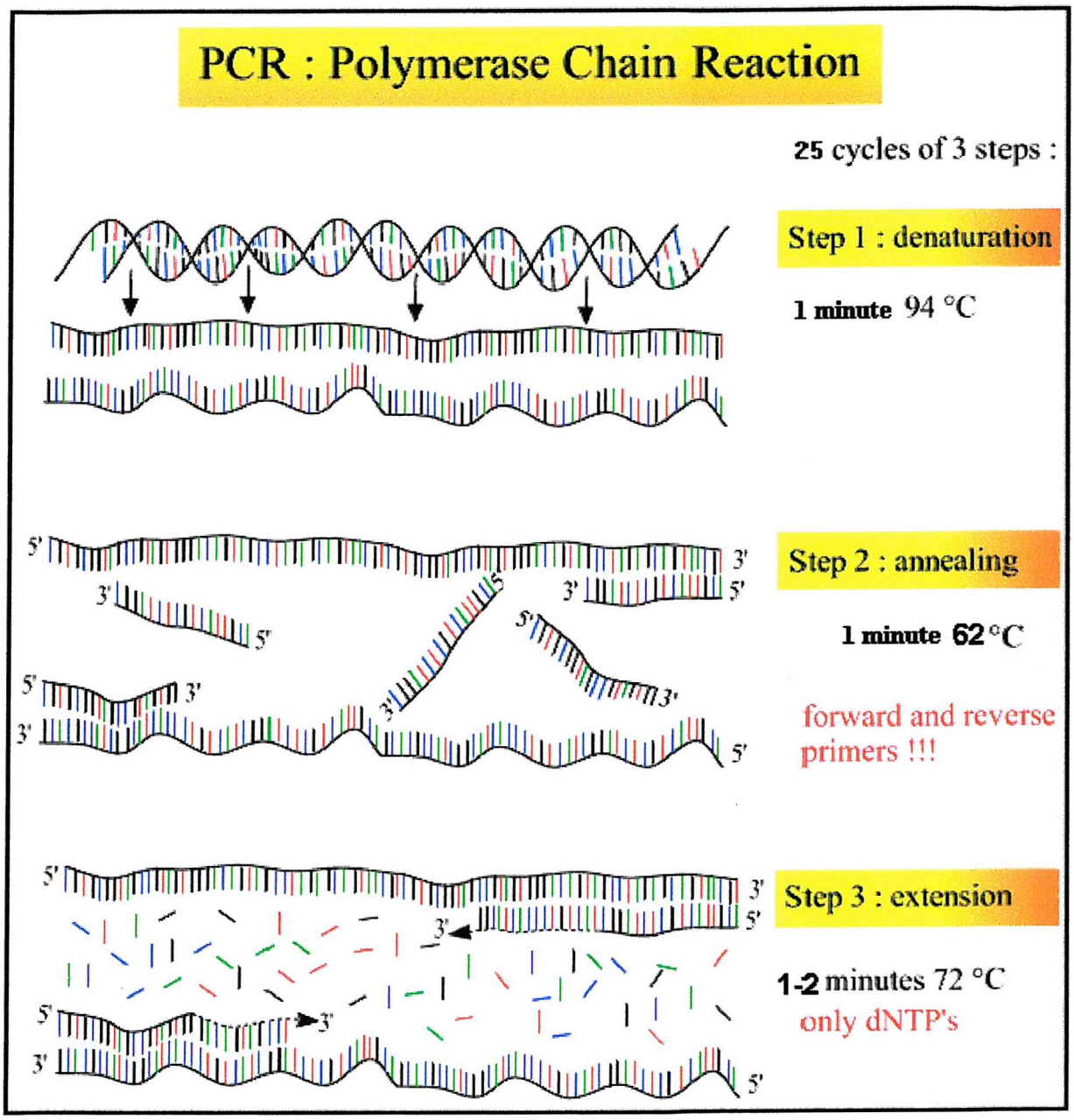

Figure 2.1 The different steps in the PCR.

2.3.3.6 Ligation of DNA

The insert DNA (40ng) and pTrcHisB vector were added to a sterile Eppendorf containing 1µl of 10x ligation buffer (30mM Tris, 1mM ATP, 10mM $MgCl_2$ and 10mM DTT, final concentration) and 1U of T4 DNA ligase was added to the mixture. The volume was made up to 10µl with sterile water and the ligation mixture was carefully mixed before overnight incubation at 14-16°C.

2.3.3.7 Enzymatic restriction of plasmid/insert DNA

In a sterile Eppendorf containing the vector, or PCR DNA (1-3 µg), 6µl of One Phor All Plus buffer (The stock is 10x buffer, which contain 100mM Tris acetate, pH 7.5, 100mM Mg acetate and 500mM potassium acetate) and 1.5µl (15 units) of each of the restriction enzymes, *Bam*HI and *Eco*RI, were added. The volume was adjusted to 30µl with sterile water. The tube was incubated at 37°C for 3 hours. The restricted DNA was then loaded onto an agarose gel, alongside DNA molecular weight markers. The DNA bands of interest were identified and excised. The DNA was recovered from the gel using the Geneclean II kit.

2.3.3.8 Electrophoresis of DNA

After the DNA had been digested with restriction enzymes, electrophoresis using agarose gels was used to identify and purify DNA fragments. Using a 100ml conical flask, 0.8ml of a 50x TAE solution was made up to 40ml with distilled water. Agarose was then added (0.30 g), the amount depending on the percentage gel required (Table 2.3). The smallest DNA fragment required the highest percentage of agarose.

Table 2.3 Agarose gel percent used according to the DNA size where the smallest size takes the highest percentage, The volume was made up to 40 ml in any percentage.

% Agarose in gel	Agarose added (g)
0.8	0.24
1.0	0.30
1.2	0.36

The agarose solution was melted in a microwave oven and the solution was allowed to cool before the addition of ethidium bromide (0.5μg/ml). The solution was then poured into a gel casting tray and the comb was inserted. The agarose gel was allowed to set and the comb was removed before being placed in the gel tank and immersed in 1x TAE buffer. The DNA sample, which contained loading buffer, was loaded into the wells and electrophoresis was carried out at 100V for 1hr. The DNA can be visualised by placing the gel on a UV-transilluminator.

2.3.3.9 DNA fragment size determination

The sizes of DNA fragments obtained from digests with restriction enzymes were estimated by comparing their relative mobilities with the mobilities of fragments of known size derived from the digestion of λDNA or ϕX174 DNA.

Table 2.4 The fragment lengths of DNA markers used in agarose gel electrophoresis

Bacteriophage λDNA digest with *Hin*dIII/*Eco*RI (kb)	ϕX174 DNA digest with *Hae*III (kb)
21.226	1.353
5.148	1.078
4.973	0.872
4.268	0.603
3.530	0.310
2.027	0.281
1.904	0.271
1.584	0.234
1.375	0.194
0.947	0.118
0.831	0.072
0.564	
0.125	

2.3.3.10 Recovery of DNA from agarose gels, using Geneclean II kit

DNA bands of interest were carefully excised from gels with a sterile razor blade taking as little of the gel as possible. The agarose containing the DNA was then transferred to a sterile Eppendorf and 3 volumes of sodium iodide (NaI) solution were added, followed by incubation in a water bath at 55°C for 5min. When the agarose had dissolved, 20µl of Glassmilk™ was added and the suspension was then placed on ice for 30min with mixing every 2 min. The tube was then centrifuged for 15 sec to pellet the silica-bound DNA and the supernatant was decanted off carefully. This was repeated 3 times to remove any remaining drops of supernatant, before washing the pellet with 500µl of ice-cold NEW WASH buffer 3 times. The pellet was resuspended in 30µl of sterile water and the DNA was dried using a speed vacuum centrifuge (UNIVAP) and stored at-20°C.

2.3.3.11 Transformation of competent cells with DNA

A 100µl sample from an overnight culture of *E.coli* DH5α was added to 10ml of LB media and grown up for 2-3 hrs until the O.D. at 600nm had reached 0.3. The cells were harvested by centrifugation at 3000rpm for 10 min at 4°C and the bacterial pellet was resuspended in 10ml of ice-cold 50mM $CaCl_2$. The cells were incubated on ice for 1hr, centrifuged at 3000rpm for 10 min at 4°C and then resuspended in 1ml of ice-cold 50mM $CaCl_2$. The mixture was incubated on ice for 30 min before use. Competent DH5α cells (200µl) were added to the DNA (0.5-1µl). The content was then mixed gently, prior to incubation on ice for 40 min. After incubation, the mixture was heat shocked by immersing the tube in water at 42°C for 2 min and immediately put on ice for 5min. LB (800µl) was added and the transformed culture was incubated at 37°C for 1hr. Finally, 150µl of the culture was spread on a LB-ampicillin plate with a sterile glass spreader.

2.3.3.12 Bacterial stock preparation

A single bacterial colony was picked off the plate and grown up overnight at 37°C in 10ml LB with ampicillin (100µg/ml). An aliquot of 800µl of culture was

added to 200µl of sterile glycerol and stored at -20°C. The culture was also used to prepare a LB ampicillin plate that was grown up overnight at 37°C and then stored at 4 °C.

2.4 Protein chemistry methods

2.4.1 Buffers and solutions

2.4.1.1 SDS-PAGE Running buffer (5x) pH 8.4

Tris	15 g
Glycine	72 g
SDS	5 g

Made up to 1L with distilled water.

2.4.1.2 SDS-PAGE disruption buffer

10% (w/v) SDS	2.0 ml
1M Tris/HCl, pH 6.8	0.5 ml
Glycerol	0.6 ml
β-Mercaptoethanol	0.5 ml
Bromophenol blue	0.01 g

Made up to 10 ml with distilled water.

2.4.1.3 SDS-PAGE Stain

Glacial acetic acid	70 ml
Methanol	400 ml
Coomassie brilliant blue R	0.25%

Made up to 1L with distilled water.

2.4.1.4 SDS-PAGE destain

Glacial acetic acid	70 ml
Methanol	400 ml

Made up to 1L with distilled water.

2.4.1.5 Modified Ehrlich's reagent

p-Dimethylaminobenzaldehyde	1 g
Glacial acetic acid	42 ml
Perchloric acid	8 ml

This solution was prepared freshly before use.

2.4.2 Methods used

2.4.2.1 Polyacrylamide gel electrophoresis (PAGE)

Polyacrylamide gel electrophoresis was carried out according to the method of Laemmlli (1970). The composition of the gel mixes is shown in Table 2.5A and 2.5B. The samples (30µl) were denatured by adding 10µl of 1.6x disruption buffer and then placed for 5 minutes in boiling water. The gel was run at a constant current of 35mA until the blue dye reached the bottom of the gel. The M_r of the protein was determined using protein standard markers (SDS-7 (Sigma); Table 2.6). To identify the protein, the bands of interest were excised and identified by "Peptide mass fingerprinting" using nanoelectrospray TOF MS. The normal process of polyacrylamide gel electrophoresis was carried out to separate protein the gel is stained with 0.2% Coomassie brilliant blue R-250 in 20% methanol and 0.5% acetic acid for 20 min. Then destained the gel using 30% methanol until the protein bands become visible (Hellman *et al.*, 1995).

Table 2.5A Separation gel contents

Stock solutions	Volume of stock solution required to make 12% polyacrylamide gel
1.5 M Tris/HCl, pH 8.8	2.0 ml
Acrylamide stock	3.2 ml
Water	2.8 ml
10% SDS	80 µl
10% Ammonium persulphate (fresh)	100 µl
TEMED	20 µl

* To run a native gel, SDS was excluded from the mixture and replaced by 80µl water.

Table 2.5B Stacking gel contents.

Stock solutions	Volume of stock solution required to make 12% polyacrylamide gel
0.5M Tris/HCl, pH6.8	1.0 ml
Acrylamide stock	1.0 ml
Water	3.0 ml
10% SDS	80 µl
10% Ammonium persulphate (fresh)	100 µl
TEMED	20 µl

* To run native gel, SDS was excluded from the mixture and replaced by 80µl water.

Table 2.6 Relative molecular mass markers (Sigma).

Protein standards	M_r
Bovine serum albumin	66000
Ovalbumin	45000
Glyceraldehyde 3-phosphate dehydrogenase	36000
Carbonic anhydrase	29000
Trypsinogen	24000
Soybean trypsin inhibitor	20100
α-Lactalbumin	14200

2.4.2.2 Determination of protein concentrations

The Bradford method (Bradford, 1972) was used to determinate the protein concentration at different stages of the purification of ALAS by adding the BioRad reagent (200µl) to the protein sample (10µl) and (790µl) distilled water. The mixture, of final volume 1ml, was incubated for 5 min at room temperature and the intensity of colour was measured at 595 nm (0.1 O.D=1.95µg of protein).

2.4.2.3 Purification of human ALA synthase (6 Histidine tag (6xHis) protein)

Inoculation

The bacterial colonies, transformed with pTrcHisB plasmid (figure 2.2), were grown up overnight in 10ml LB containing ampicillin (100μg/ml) at 37°C. The overnight cultures were inoculated into 4 x 2L baffled flasks, each containing 800 ml LB medium and ampicillin (100 μg/ml) and grown until the O.D. at 600nm had reached 0.6. IPTG (800μl) was then added to start induction and growth was continued until that final O.D. reached 1.0. The cells were harvested using a Beckman centrifuge (J2-21) at 5000 rpm (1000 x g) for 30 min at 4°C. The supernatant was discarded and the pellet was stored at -20 °C until required.

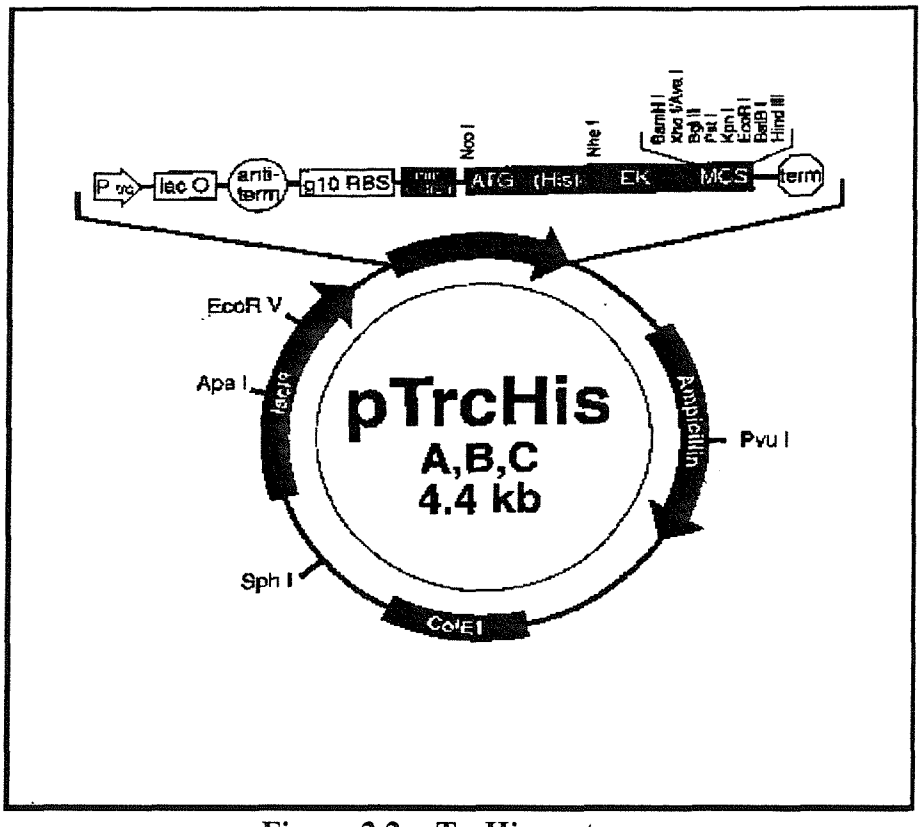

Figure 2.2 pTrcHis vector map

Sonication

The bacterial pellets from 4 flasks were resuspended in 100 ml of 50mM potassium phosphate buffer, pH 7.5, containing 20μM PLP, 500mM NaCl, 5mM imidazole, 5mM glycine and 10% glycerol. PMSF (0.2M) was added just prior to sonication as a protease inhibitor. The sonication was carried out for 20 cycle each 30 sec at an amplitude of 10 micron, with 90 sec cooling between.

Ultracentrifugation

The sonicated sample was centrifuged at 11,000 x g for 1hr at 4°C. The supernatant was then loaded onto a TALON metal affinity resin.

Batch column purification

The clarified sample, after ultracentrifugation, was added to 4ml of homogeneously resuspended TALON resin of 2ml bed volume. The resin had been previously equilibrated in 50mM potassium phosphate buffer, pH 7.5, (sonication buffer). The resin suspension was agitated gently at 4°C for 1hr on a platform shaker to allow the 6xHis ALAS protein to bind to the resin. The mixture was then centrifuged gently at 700 x g for 5 min to pellet the resin and the supernatant was discarded. The resin was then washed with 50mM potassium phosphate buffer, pH 7.5, containing 10% glycerol, 500mM NaCl, 5mM glycine and 5mM imidazole (20 ml) for 30 min at 4°C. The resin was recentrifuged for 5 min the supernatant was then discarded. This step was repeated 3 times.

The resin with the bound enzyme was transferred to a 2ml gravity-flow column with a filled end-cap and 1ml of the resin was allowed to settle. The end cap was then removed and the buffer was allowed to flow until it reached the top of the resin bed. The column was washed 3 times with sonication buffer (6 ml each), then with sonication buffer containing 15mM imidazole. Protein was eluted using increasing concentrations of imidazole, starting from 20mM, 30mM, 40mM, 50mM, 60mM, 70mM, 80mM, 90mM and increasing up to 100mM (12 ml for each concentration). The same technique was repeated once using the initial flow-through from the column. This resulted in an increased recovery of the protein. After checking the

purity of the fractions using SDS gel electrophoresis, they were pooled and concentrated to 2.5ml in an Amicon ultrafiltration cell fitted with a PM30 membrane.

2.4.2.4 Storage of purified protein

The enzyme was desalted on a PD10 column equilibrated with 50mM potassium phosphate buffer, pH 7.5, containing 20μM PLP and 10% glycerol. The enzyme was stable for several days when stored at -20°C.

2.4.2.5 Enzyme assay

The assay method used was originally described by Mauzerall and Granick, (1956), and depends on the formation of a pyrrole in a Knorr-type reaction between ALA and acetylacetone (scheme 2.1). In this assay two blanks were used, one without protein and one without succinyl-CoA. The assay was carried out on all protein samples at different stages of the purification. In a 1.5ml Eppendorf, human ALAS2 enzyme (6-10μM) was added to 50 μl of stock reaction buffer containing glycine (250mM) and pyridoxal 5'-phosphate (250μM) final concentration. Finally, 25μl of (2.5mM) succinyl-CoA was added and the volume was adjusted to 100μl. The reaction mixture was carefully mixed before incubated at 37°C for 30min. After the incubation, 150μl of 10% trichloroacetic acid (TCA) was added, the samples were mixed and centrifuged for 3min at room temperature. The supernatants were transferred to new Eppendorf tubes and 300μl of sodium acetate buffer (1M), pH4.6, and acetylacetone (25μl) were added to 250μl of the supernatant. The tubes were mixed thoroughly and heated in a boiling water bath for 10min. Finally, after cooling the tubes, Ehrlich's reagent was added (575μl), to give a final volume of 1.20ml. The intensity of colour was measured at 553nm immediately.

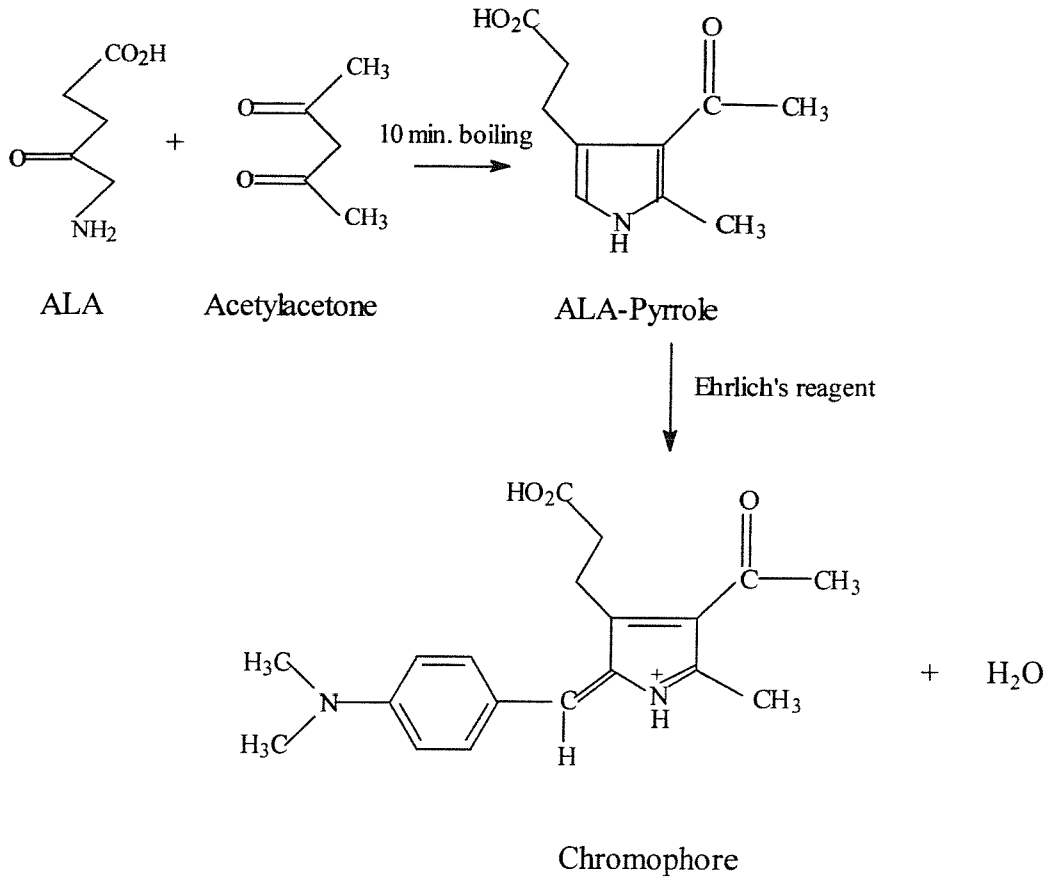

Scheme 2.1 Conversion of ALA into a pyrrol by reaction with acetylacetone and reaction with modified Ehrlich's reagent produce a chromophore (Mauzerall and Granick, 1956).

2.4.2.6 A continuous spectrophotometric assay for 5-aminolaevulinic acid synthase

The most widely referenced assay for ALAS involves the chemical conversion of ALA to a pyrrole, which is quantitated spectrophotometrically following reaction with Ehrlich's reagent, as mentioned above. The continuous spectrophotometric assay differs from those previously reported in that it measures the rate of CoASH liberation in the presence of 5-aminolaevulinic acid synthase. CoASH is determined enzymatically using excess α-ketoglutarate dehydrogenase (α-KGD), which couples the reaction of CoASH to succinyl-CoA to the reduction of NAD^+ to NADH. The rate of NADH production is followed spectrophotometrically at 340nm. This assay usually used to determine the K_m of the succinyl-CoA.

$$\text{Glycine} + \text{Succinyl-CoA} \xrightleftharpoons{\text{ALAS}} \text{5-Aminolaevulinic acid} + \text{CoASH} + CO_2 \qquad (1)$$

$$\text{CoASH} + NAD^+ + \alpha\text{-Ketoglutarate} \xrightleftharpoons{\alpha\text{-KGD}} \text{Succinyl-CoA} + \text{NADH} + CO_2 \qquad (2)$$

In a 1ml quartz cuvette, 18μg of ALAS2 was added to 20mM Hepes buffer, pH 7.2, 100mM glycine, 1 mM α-ketoglutarate, 1mM NAD^+, 3mM $MgCl_2$, 0.25mM thiamine pyrophosphate, 0.25units α-ketoglutarate dehydrogenase and succinyl-CoA. To determine the K_m values for glycine and succinyl-CoA the concentration of these substrates were varied using the same assay (Hunter and Ferreira, 1995).

Chapter 3

Model structure of human 5-aminolaevulinic acid synthase

Despite the development of techniques in molecular biology that allow rapid identification, isolation, and sequencing of genes, it is still a time-consuming task to obtain the three-dimensional structures of these proteins.

However, alternative strategies are being applied to develop models of protein structures when X-ray or NMR structures are not yet available. One method that can be applied to generate reasonable models of protein structures is homology modelling. This procedure, also termed comparative modelling or knowledge-based modelling, develops a three-dimensional model from a protein sequence based on the structures of homologous proteins.

In the absence of an X-ray structure for human 5-aminolaevulinic acid synthase (hALAS2), a model structure has been obtained for the core region of hALAS2 encompassing exons 5-11. The 8-amino-7-oxononanoate synthase (AONS) structure was used as a template using the programme MODELLER version 6 (Šali and Blundell, 1993).

3.1 The MODELLER

MODELLER is a computer program that models protein 3D structure. In MODELLER, spatial and stereochemical restraints derived from the template structures and the sequence alignment are combined to form an objective function and the model structure are created by optimising this function. Briefly, homology modelling procedure begins with an alignment of a known sequence with an unknown structure (target) with related known structure (template). This alignment is usually the input to the program, and the output is a 3D model for the target sequence containing all main chain and side chain non-hydrogen atoms. The model is obtained without any user intervention and many distance and dihedral angle

restraints on the target sequence are calculated from its alignment with template 3D structures. Next, the spatial restraints and stereochemistry are combined into an objective function. Finally, the model is obtained by optimising the objective function.

3.2 Human erythroid 5-aminolaevulinic acid synthase (ALAS2) and 8-amino-7-oxononanoate synthase (AONS)

AONS is a homodimer enzyme with each monomer consisting of three domains. This enzyme is encoded by *bioF* and catalyses the first committed step in biotin biosynthesis, which is the decarboxylative condensation of L-alanine and pimeloyl-CoA, with K_m values for the substrates of 0.9mM and 60μM, respectively (Alexeev *et al.*, 1998). Both AONS and ALAS belong to unique group of pyridoxal 5'- phosphate dependent enzymes, which catalyse condensations between an amino acid and an acyl-CoA substrate. Serine palmitoyl transferase and 2-amino-3-oxobutyrate-CoA ligase are other enzymes that belong to the same group.

Attempts to model the structure of ALAS2 using other PLP-dependent enzymes proved to be problematic due to poor homology and the existence of insertions and deletion. A major breakthrough in understanding the structure of ALAS has come from the determination of the X-ray structure of AONS. The identity between the amino acids sequences of ALAS2 and AONS is approximately 30% with similarities over 60%. Many invariant amino acids exist in the vicinity of the substrate glycine and pyridoxal 5'-phosphate binding regions (figure 3.1). This suggests that the two enzymes have very similar overall structures, similar active sites geometries and follows the same reaction mechanism. Therefore, an ALAS2 model based on AONS is likely to be reliable. Mapping the mutations that cause X-linked sideroblastic anaemia on the ALAS2 model may give reasons why, in some cases pyridoxine treatment is a success, but in others is not. The model is also important for making knowledge-based mutations for determining the function of individual amino acids.

This chapter describes the modelling of ALAS2 on AONS and uses the model to predict the outcome of human mutations that cause X-linked sideroblastic anaemia. Furthermore, this chapter determines whether each subunit of ALAS2 contains an independent active site (intrasubunit arrangement) or the active site resides at the subunit interface (intersubunit arrangement).

Figure 3.1 The sequence alignment of ALAS2 and AONS. The blue colour refers to the hydrophobic amino acids, the green colour to the hydrophilic amino acids, the pink colour refers to the negatively charged amino acids, the orange colour refers to the positively charged amino acids and the yellow colour refers to the α-imino acid proline. The symbol * refers to the identical amino acids and . - : refers to the similar amino acids.

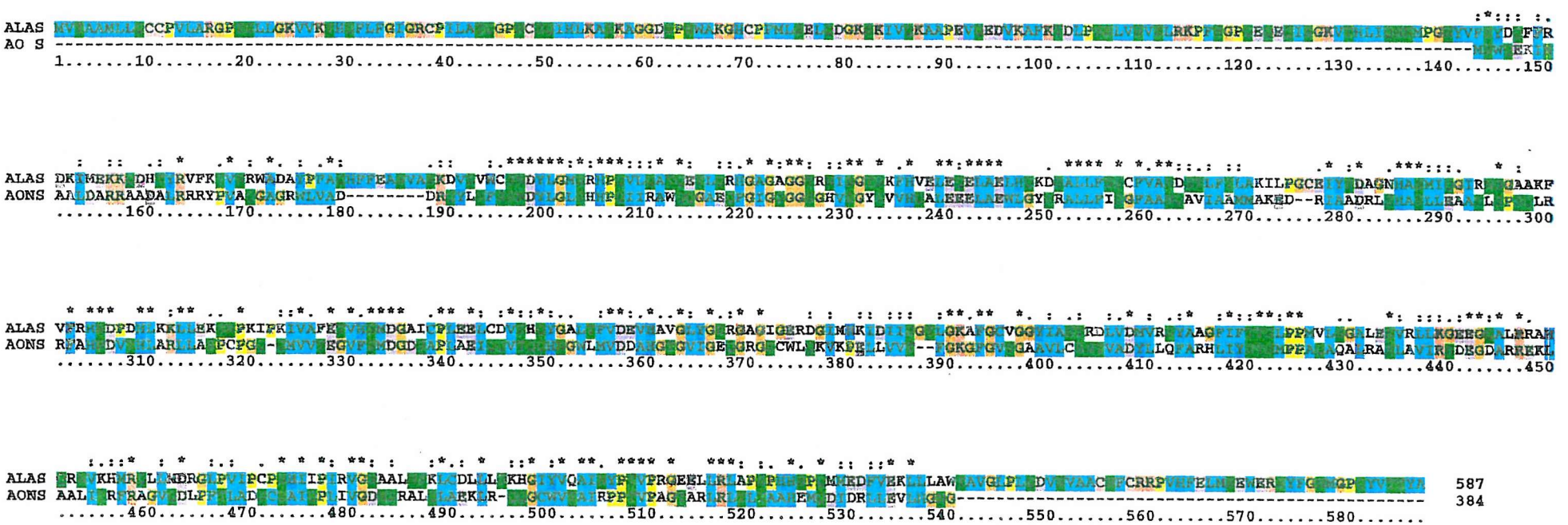

3.3 Determination of a structural model of human ALAS2

3.3.1 Methods

With the structure of AONS as a template, the initial model of human ALAS was obtained using the standard comparative modelling procedure. Spatial restraints of the target sequence were first calculated from the input sequence alignment (figure 3.2) and a statistical analysis of relationships between many pairs of homologous structures in the programme database. The spatial restraints were then combined with stereochemistry to produce an objective function, which was used to create the initial model.

The initial model of ALAS2 was very similar to that of the AONS structure, especially in the region around the active site where the sequence alignment is almost identical. Small adjustments around the active site were required to maintain a reasonable distance between Cys258 and Val359 and the coenzyme. The coenzyme was therefore moved from the position that it would occupy in the AONS structure towards the protein surface in order to avoid steric clashes. The residues around the coenzyme were also shifted to maintain reasonable protein geometry and to preserve bonding between the coenzyme and key residues, such as His. The whole model was energy minimised against ideal protein geometry using X-PLOR after the changes mentioned which is the adjustment around the active site.

```
ALAS    CSNDYLGMSRHPQVLQ---AT-QETL--QRH--
AONS    SSNDYLGLSHHPQ---IIRA-WQQ--GAE--QF

ALAS    GA-GA-GGTRNI----SGT-SKF--HVE--LEQELAELHQK--DS
AONS    G-IG-SGG----SGHVSG-YS--VVH--QALEEELAEWL--GYSR

ALAS    ALLFSSCFVANDST--LF-TLAKILPGCE------IYS--DAGN---
AONS    ALLFISGFAANQ--AVI-AAM--------MAKEDRI--AAD---RLS

ALAS    HASMIQGI-RN--SG-AAKFV----FR-HNDPD--HLK-KLL
AONS    HASLLEA-A--SLS-PS----QLRRF-AHND--VTHL-ARLL

ALAS    EKSNPK------IP--KIVAF--ET-VHSMDGA-
AONS    ------ASPCPG--QQ-MV--VTE-GVFSMDG-D

ALAS    IC--PLE-ELC-DVSH--QYGA--
AONS    --SAPL-AEI-QQV--TQQH--NG

ALAS    LT--FVDEV-HAV--GLY--GSR--GA-G
AONS    --WLMVDD-AH--GTG--VIG--EQG-RG

ALAS    IG--ER--DGIMHKIDIISGTLGK-AFGCV-
AONS    --SC--WL-QKVK-PELLVVTFGKGFG--VS

ALAS    GGYIASTRD--------LV-DM-VRS--YAAGF---IFTTSLPP
AONS    G--------AAVLCSSTV-AD-YL--LQFA---RHLIYSTSMPP

ALAS    MVLSGALE--------SVR-LLKG-EEGQAL-RRAHQRNV-------KHM
AONS    --------AQAQALRASL-AVIR-SDEGDA-RR-------EKLAALITRF

ALAS    RQL--LMDRG----LPVIPCPSH------
AONS    R--AGV----QDLPFTL------ADSCSA

ALAS    IIPIRVGNAALNSK------LCDL---LLSK---H
AONS    IQPLIVGD------NSRALQL---AEKL---RQQ-

ALAS    GIY--VQ-AIN-YPTVPR-GEEL---LRLAP--SPH--HS-
AONS    G--CWV-TGI-RPPTVP-AG---IARLRL--TLT--AAH-E

ALAS    PQM---MEDF--VEK-LLLA---
AONS    ---MQDID--RLLE-VL---HGN
```

Figure 3.2 The sequence alignment of ALAS and AONS, which was used for the modelling.

3.3.2 Results

The final model has 73.2% of its non-glycine and non-proline residues fitted into the most preferred region of the Ramachandran plot with none in the disallowed region (figure 3.3). The overall bond lengths and angles of the model deviate from the ideal values for 0.006Å and 0.991 degrees, respectively.

The overall structure of the initial ALAS2 model is very close to the AONS structure (figure 3.4) except in ALAS2 model the PLP coenzyme is shifted more towards Arg517. The similarities increase in the regions around the active site, where the sequence alignment is very similar. In the vicinity of the PLP binding site (figure 3.5), residues His285, His360, Asp357, and Lys391, all of which have key roles in binding and positioning PLP, occupy identical positions as AONS. Two residues, Cys258 and Val359, may play a role in amino acid substrate specificity since there are interesting comparisons to be made at these two positions among four PLP-dependent enzyme (Table 3.1). In ALAS2, these residues have larger side chains than the corresponding residues in AONS (Gly258 and Ala359) and require the coenzyme to be moved slightly to avoid steric clashes. It was therefore necessary to make small adjustments around the active site to satisfy the requirements of bonding between key residues (His285, His360, Asp357, and Lys391) and PLP and also to maintain a reasonable distance between Cys258 and Val359 residues and PLP. This results in a smaller gap in the active site that can be occupied by glycine.

Table 3.1 The 359 and 258 residues in the four related oxoamine synthases and their substrate

Enzyme	Substrate	Residue 359	Residue 258
SPT	Ser	Ala	Gly
AONS	Ala	Ala	Gly
AKB	Gly	Ser	Cys
ALAS2	Gly	Val	Cys

Abbreviation: SPT, serine palmitoyltransferase; AKB, 2-amino-3-oxobutyrate CoA ligase.

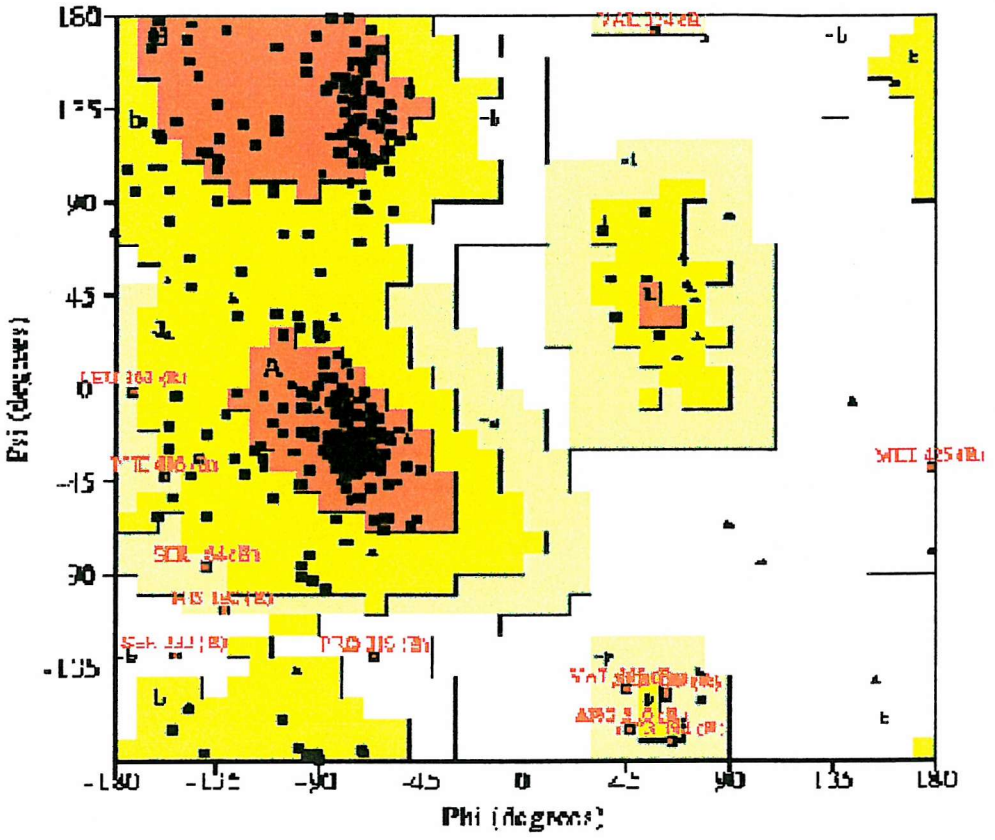

Plot statistic

Residues in most favoured regions [A, B, L]	454	73.2%
Residues in additional allowed regions [a, b, l, p]	142	22.9%
Residues in generously allowed regions [~a, ~b, ~l, ~p]	24	3.9%
Residues in disallowed regions	0	0.0%
Number of non-glycine and non-proline residues	620	100%
Number of end-residues (excluding Gly and Pro)	6	
Number of glycine residues (shown as triangles)	62	
Number of proline residues	34	
Total number of residues	772	

Figure 3.3 Ramachandran plot where the main chain is fitted in the most preferred A, B and L regions

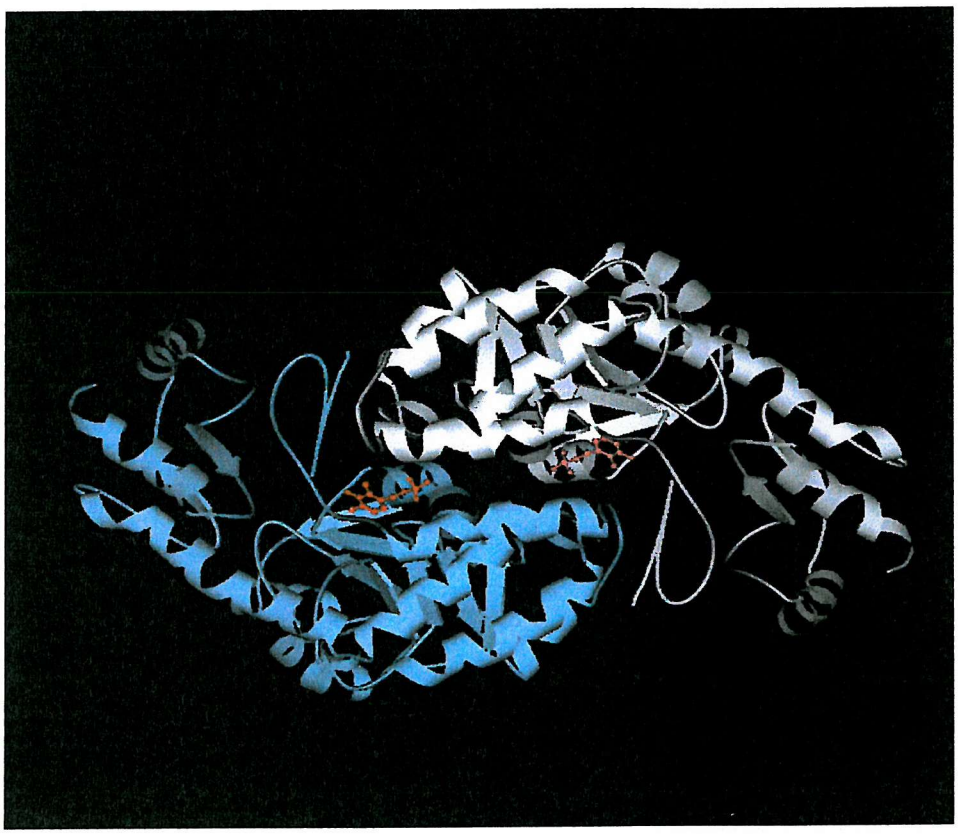

Figure 3.4 The model of human ALAS2 showing the homodimeric enzyme with PLP (in red) bound in the active sites.

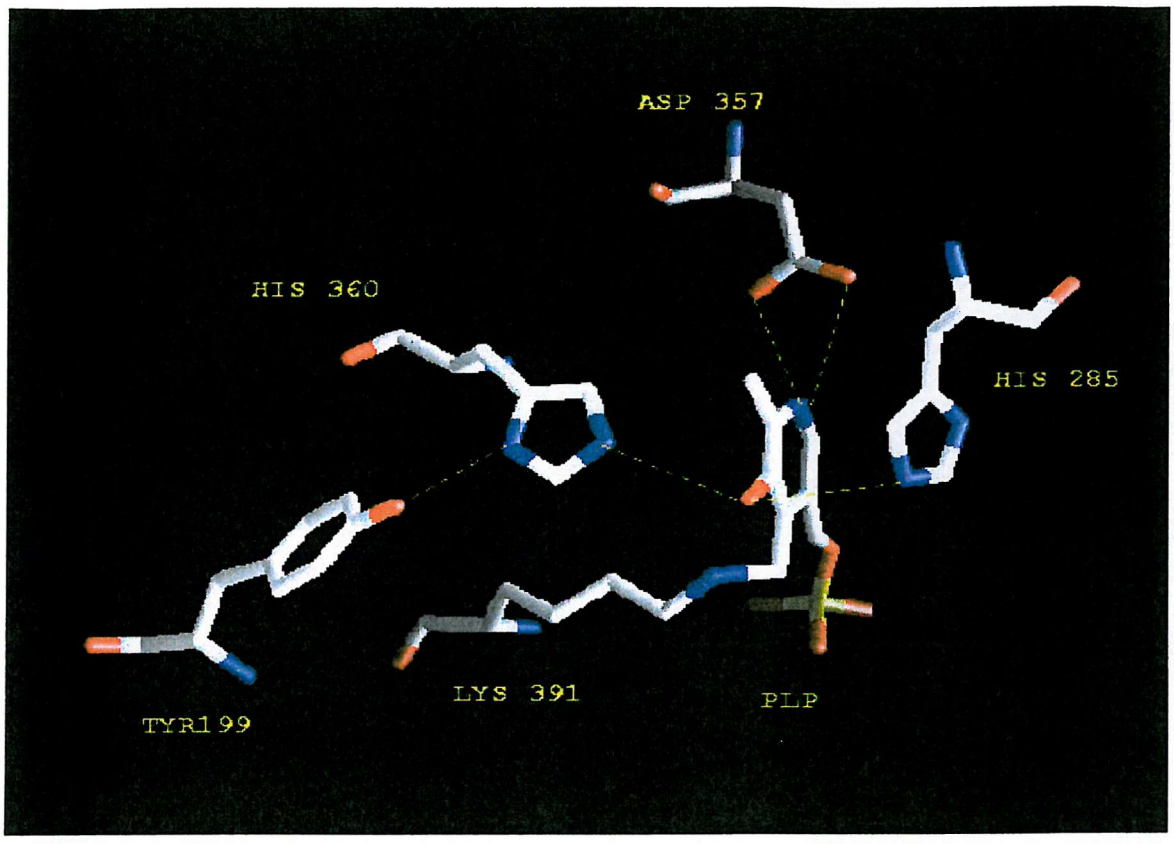

Figure 3.5 The pyridoxal 5'-phosphate binding site of ALAS2. The coenzyme PLP is attached to Lys391 and Asp357 binds to the PLP by two hydrogen bonds. Two histidine residues, His285 and His360, bind to PLP by hydrogen bonds. His285 occupied a parallel position and His360 binds to Tyr199 by another hydrogen bond.

3.4 Studies on human ALAS2 mutants

About 30 mutations have been described in nearly 40 families that lead to X-linked sideroblastic anaemias of differing severity (table 3.2) (May and Bishop, 1998). Some of these mutations have been mapped onto the model. One of the most interesting aspects of X-linked sideroblastic anaemia is the relationship between the location of the mutation in ALAS2 enzyme and the responsiveness to pyridoxine treatment. Those in which the mutant protein is responsive to vitamin therapy *in vivo* are generally clustered in the vicinity of the coenzyme binding site unless involving a key catalytic group. Others, more refractory to pyridoxine treatment, are often found on the periphery of the pyridoxal 5'-phosphate binding site or distant from the active site. The model structure of ALAS2 can be used to help explain the different responses of the disease to pyridoxine treatment as follows.

3.4.1 Mutations in ALAS2 refractory to pyridoxine therapy

A number of mutations have been identified from patients where the disease is refractory to pyridoxine treatment (figure 3.6). Asp190 is a poorly conserved residue in the ALAS2 enzyme. The model suggest that introduction of a hydrophobic residue in D190V mutant in the vicinity of the *N*-terminus could reduce the half-life *in vivo*. However recent investigations have shown that D190V has normal activity but is defective in transport into mitochondria (Furuyama and Sassa, 2000). Thus the mutation may affect the structure in the vicinity of the mitochondria transport recognition site. Another refractory anaemia is caused by the mutation of Arg204 to a termination codon in exon 5, the result is a truncated protein with no activity. The Arg227Cys mutation located in a positive charged region near the active site of the enzyme that may be important in charge balance. This residue is also near the monomer-monomer interface and loss of the strong +ve side chain would be likely destabilising the protein. The Arg517 residue almost certainly forms the glycine substrate carboxyl binding site and loss of this residue to

cysteine would result in a total loss of the activity that could not be recovered by increasing the coenzyme (figure 3.7).

Table 3.2 Defects of the human erythroid ALAS2 gene in patients with X-linked sideroblastic anaemia (Cotter et al, 1999).

Exon	Mutation	Amino acid substitution	Sex	Response to pyridoxine	Reference
5	TTC-TTA	F165L	M	+	Cotter et al (1994)
5	GCT-ACT	A172T	F	++++	Cotter et al (1995)
5	CGC-CTC	R170L	M	++	Edgar et al (1998)
5	GAT-GTT	D190V	M	Refractory	Furuyama et al (1997)
5	TAC-CAC	Y199H	M	++	Cotter et al (1999)
7	GGT-AGT	G291S	M	+++	Prades et al (1995)
7	AAG-GAG	K299Q	M	++++	Cotter et al (1995)
8	ACT-AGT	T388S	M	++	Cox et al (1994)
9	CGC-TGC	R411C	M	+++	Cotter et al (1999)
9	CGA-CAA	R448Q	M	++	Cotter et al (1999)
9	CGC-TGC	R452C	M	+	Cotter et al (1999)
9	CGC-CAC	R452H	M	+	Edgar et al (1997)
9	ATC-AAC	I476N	M	+++	Cotter et al (1992)
9	ATG-GTG	M426V	M	+++	Furuyama et al (1997)
10	CGC-TGC	R517C	F	Refractory	May and Bishop (1998)

Abbreviations: M, male; F, female; + - ++++, response to B_6.

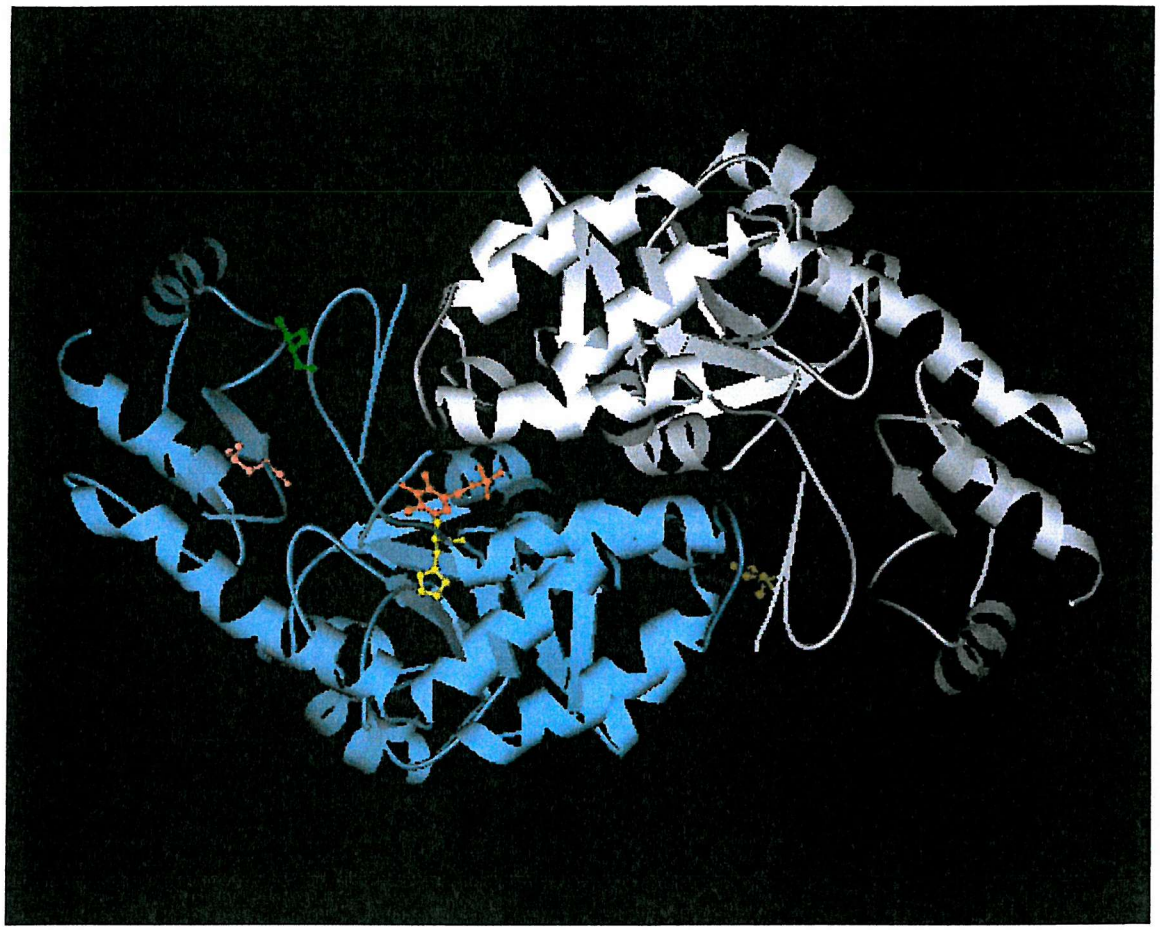

Figure 3.6 The position of the mutations that cause refractory anaemia in ALAS2. The picture shows the position of residues in one monomer. The pink colour represents the Arg517 residue, which play a role in glycine binding, Asp190 green, Arg204 yellow (the mutation leading to a stop codon) and Arg227 brown. PLP is shown in red in one monomer.

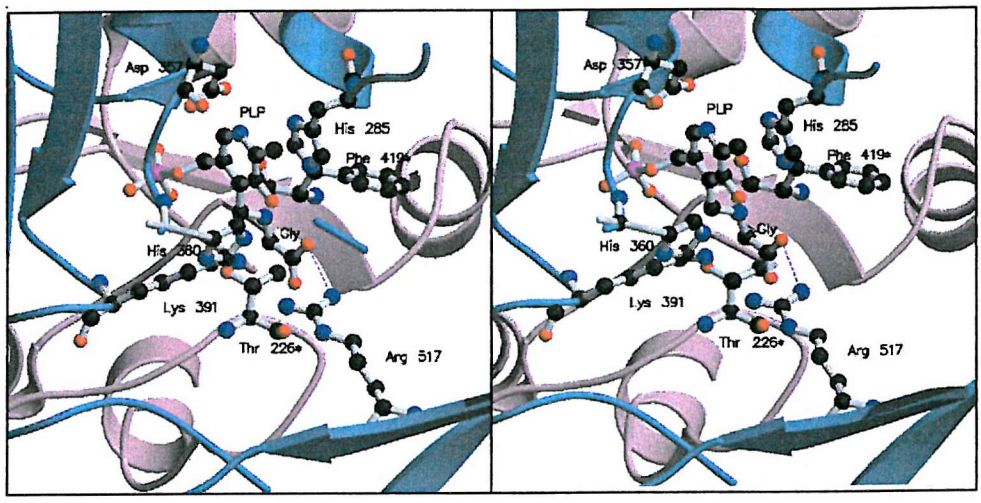

Figure 3.7 The location of R517 at the active site of human ALAS2 showing the interaction with the carboxyl group of the substrate glycine in the external aldimine.

3.4.2 Mutations partially responsive to pyridoxine therapy

Some of mutations have been described as a partially response to pyridoxine treatment and can be located in the ALAS2 model. Several of these are relatively easy to explain although others are less easy to predict (figure 3.8).

Tyr199 is a residue that forms contact with His360, one of the two histidine residues that hold the coenzyme in the correct orientation in the active site. Mutation of tyrosine to histidine is likely to force its neighbouring His360 to move away from its optimal coenzyme binding position. By increasing the concentration of the coenzyme, the defect in the binding affinity could be overcome.

Arg411 is another residue located in a positively charged area. Mutation of this residue to cysteine or histidine is likely to alter the charge distribution and destabilise the enzyme. Furthermore Arg411 is located in a region very closed to the PLP binding site on the other subunit in the dimer and the affinity of PLP could be adversely affected. Similar, Gly416 is also located in this region. Gly416 is a conserved residue forming a beta-turn. The Gly416Asp mutation could destabilise the protein, since the larger Asp could cause movement of other residues. Higher levels of PLP probably contribute by stabilising this intersubunit region.

Two residues, Arg452 and Arg448, are located on the surface of the enzyme in a patch where several positively charged residues are present (figure 3.9). Their roles are not clear but they may be involved in stabilising the hydrogen-bonding network of the enzymes. Three mutations have been described for this residue, Arg452His/Cys/Ser.

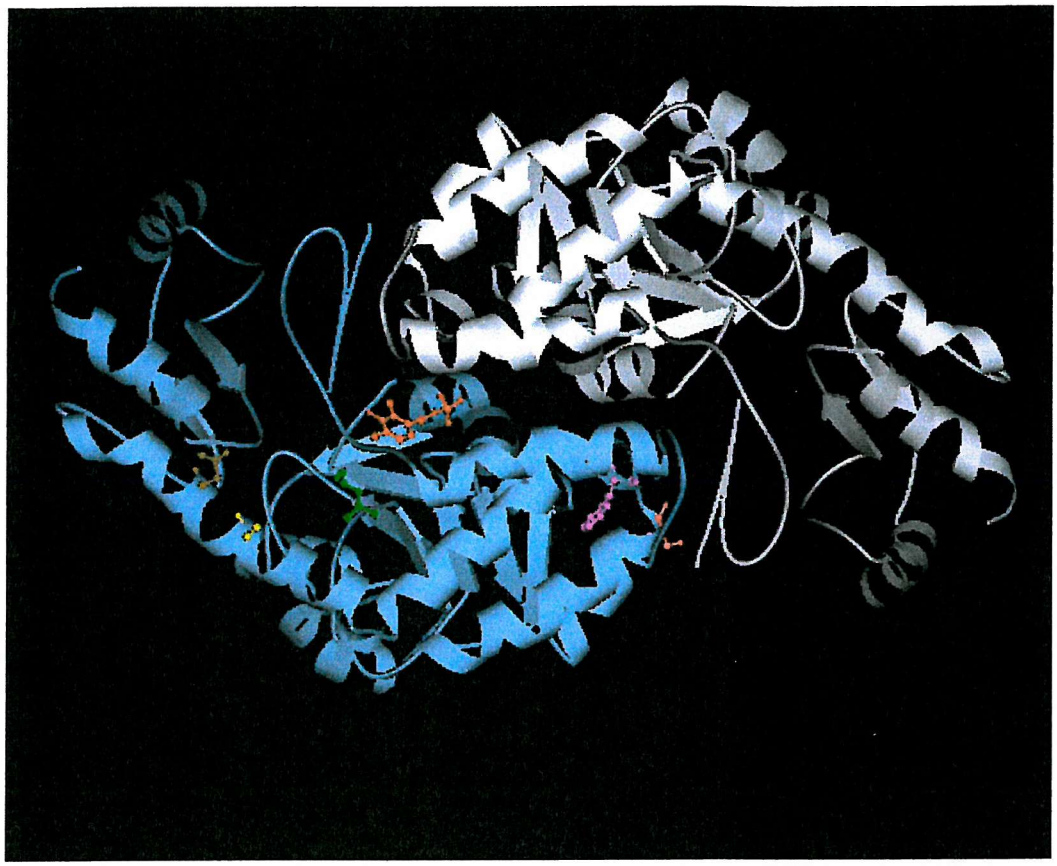

Figure 3.8 The positions of the mutations in the ALAS2 model that partially respond to pyridoxine treatment. Tyr199 (green) is close to the PLP (red), Arg411 (pink), Arg452 (brown) and Arg448 (yellow) are located in a positively charged area. Gly416 (magenta) is located at beta-turn. Arg411 and Gly416 are located close to the PLP binding site in the other subuint.

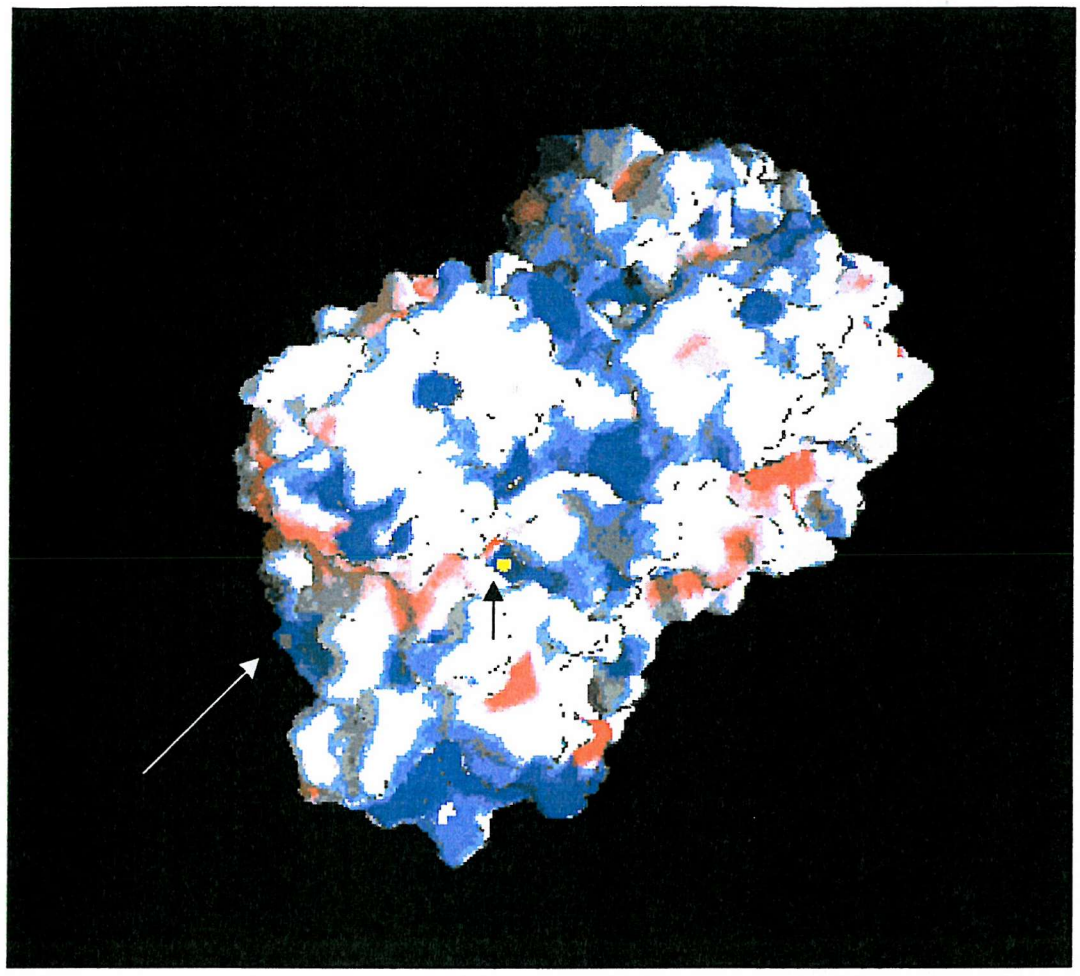

Figure 3.9 The surface of the ALAS2 highlighting the position of the Arg452 residue. The surface of the ALAS2 is shown, as calculated and displayed by GRASP (Nicholls *et al*, 1993). The blue colour corresponds to positive potential and the red to negative. The yellow square represents the active site and the grey square on the left represents the Arg452 residue, both of which are in positively charged areas.

3.4.3 Mutations that respond well to pyridoxine therapy

From the model, the mutations that respond well to pyridoxine treatment appear to be located largely in the vicinity of the coenzyme-binding site or close to this region (Figure 3.10 and 3.11). In Thr388 residue, the model shows the contacts made by the hydroxyl group with one of the phosphate oxygen atoms of pyridoxal 5'-phosphate and the main chain of Cys258 (Figure 3.12). Replacing the threonine side chain with the smaller side chain serine, could allow a water molecule to bind in the vicinity of the coenzyme and interfere with the binding of the OH group with the coenzyme phosphate. Gly291 is located on a helix in the vicinity of the coenzyme and in the Gly291Ser mutant the larger side chain of serine introduced into a helix could cause some steric effects on the coenzyme. The Met426 side chain sulphur atom forms a hydrogen bond with Ser395 from the other subunit within the dimer. Mutation of this residue to valine in the Met426Val mutant would remove the hydrogen bond and destabilise the intersubunit region in the vicinity of the coenzyme. It is difficult to predict the affect of introduction a hydrophilic residue in Ile476Asn on the stability of the enzyme, although the N-terminus does contribute some residues to the vicinity of the PLP active site. Finally, K299Q is a mutant that responds completely to pyridoxine therapy. Lys 299 contributes to a positively charged region close to the active site that is involved in coenzyme binding (figure 3.13). The affinity of the coenzyme is likely to be lower in Lys299Gln, thus increasing the coenzyme concentration could overcome the lowered affinity.

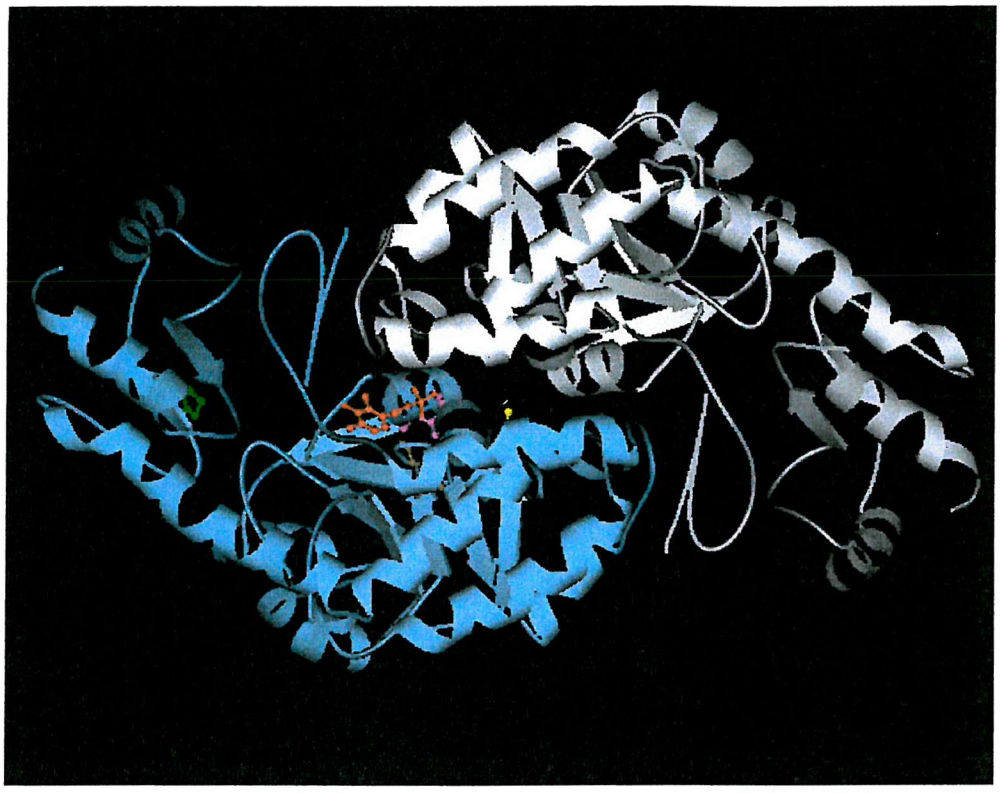

Figure 3.10 The positions of the mutations in human ALAS2 that respond well to pyridoxine therapy. Three residues are close to the PLP, Gly291 (magenta), Thr388 (brown) and Met426 (yellow). Ile476 is a hydrophobic residue (green).

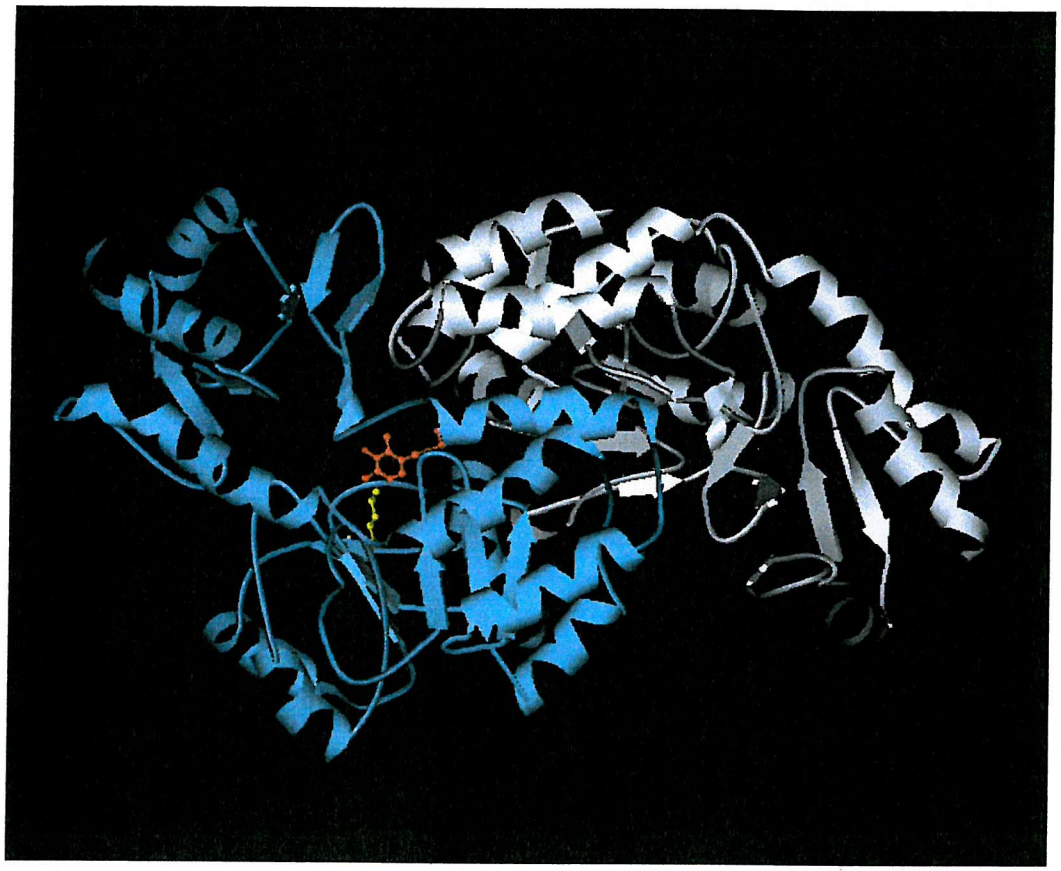

Figure 3.11 The position of the K299 in human ALAS2 that respond well to pyridoxine therapy. K299 (yellow) residue is close to the PLP (red).

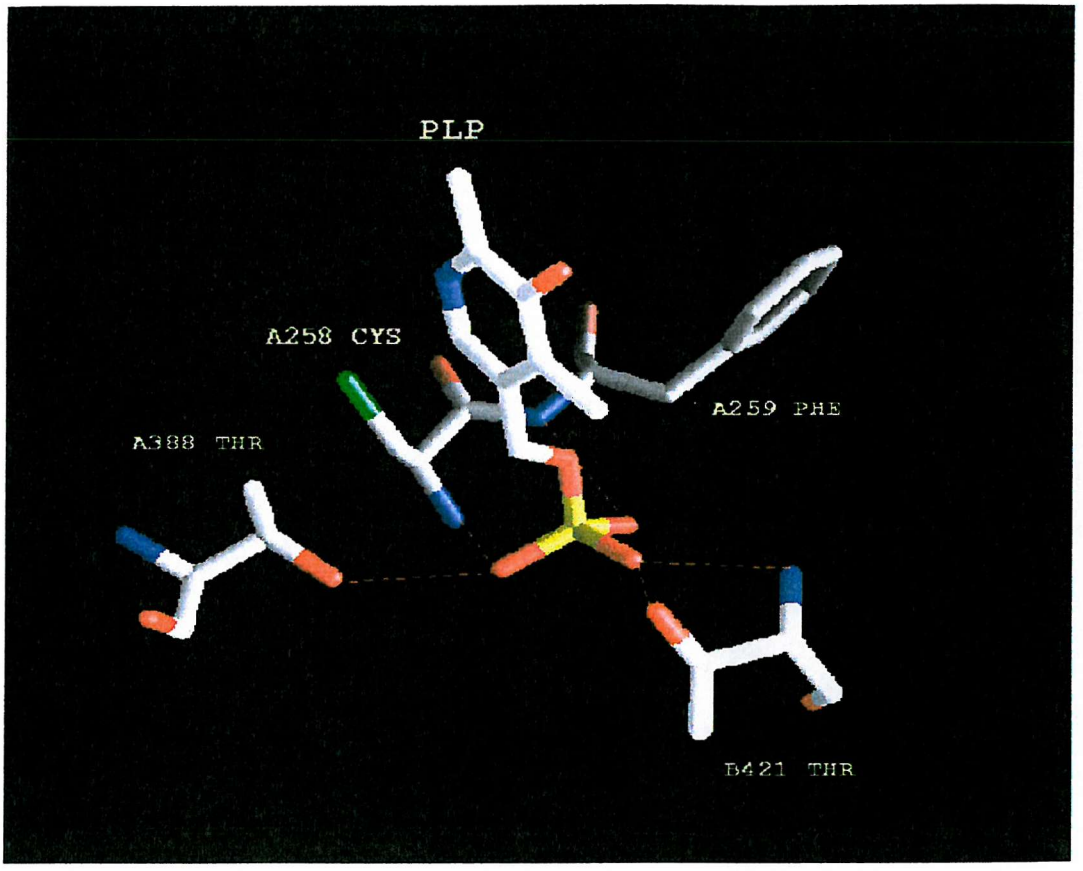

Figure 3.12 The environment of Thr388 in human ALAS2. Thr388 is bound to the PLP-lysine complex by a hydrogen bond, which is part of a hydrogen bond network system that also includes Cys258 and Thr421. A and B refer to residues from the two subunits of the dimer.

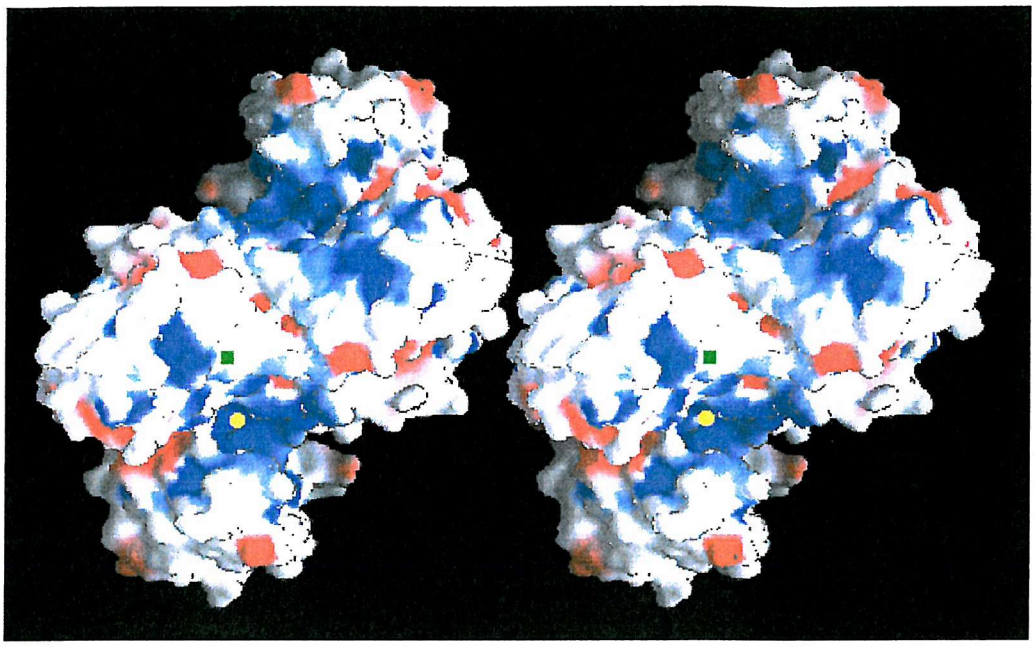

Figure 3.13 Stereo view of the human ALAS2 surface as calculatated and displayed by GRASP (Nicholls *et al*, 1993). The blue colour corresponds to positive potential and the red to negative. The yellow circle represents the active site and the green square represents the K299 residue, which is located in a neutral region.

3.5 Some other important and conserved residues in humanALAS2

A detailed look at the sequences of ALAS2 and other related enzymes such as AONS reveal several invariant amino acids that are located in the active site region. Because of the confusing differences in the numbering of these enzymes a table 3.3 is shown for a comparison.

Table 3.3 The important amino acid residues in human ALAS2 and their equivalent residues in mouse, *R.sphaeroides* and AONS.

Residues	H	D	H	T	K	R	R
HumanALAS2	285	357	360	388	391	452	517
Mouse ALAS	207	298	283	310	313	374	439
R.sphaeroides	142	233	217	245	296	-	372
AONS	155	227	230	-	261	-	387

Lysine 391 of the human ALAS2 (Lys313 of the mouse) is an invariant residue among all organisms. The ε-amino group of this lysine residue has been identified to forming the vital Schiff base linkage with the coenzyme PLP in the *C*-terminal core region of the enzyme (Ferreira *et al.*, 1993). Ferreira and her co-workers (Ferreira *et al.*,1995 and Hunter and Ferreira 1999a) established that the replacement of lysine 313 by alanine, histidine and glycine, using site-directed mutagenesis, yields enzymes that cannot form the internal aldimine with the coenzyme but can form the external aldimine by the addition of glycine. The mutant proteins exhibit no spectral evidence for any quinonoid intermediate formation in the presence of glycine and succinyl-CoA, which suggests that lysine 313 also acts as a general base during the ALAS catalytic cycle. As a consequence the mutant enzymes have no measurable activity.

The sequence alignments of ALAS enzymes also indicate the presence of a conserved glycine-rich sequence (GAGAGG). A similar sequence motif (GXGXXG) has been found in some other PLP-dependent enzyme as well as in the

ALAS. The role of this sequence motif is shown in the ALAS2 model to form a loop between a β-sheet and an α-helix in the region near the active site. The first glycine residue in the sequence is thought to be essential for the tightness of αβ-turn (Scrutton *et al.*, 1990). This motif has also been suggested as being involved in PLP and CoA binding (Neidle and Kaplan, 1993), however, since the sequence is not conserved in other members of the family this seems unlikely.

Tyr121in mouse, which is equivalent to Tyr199 in human ALAS2, is another conserved residue in all known sequences of ALAS. Using site-directed mutagenesis, kinetic studies and coenzyme titration Ferreira and her co-workers (Tan *et al.*, 1998) determined that Tyr121 in murine erythroid ALAS plays an important role in coenzyme binding.

Tan and Ferreira (1996) also established that the mouse ALAS active site is located at the subunit interface and contains catalytically essential residues from the two subunits. This is predicted from the model of human ALAS2 that shows the two subunits contain residues at the subunit interface that border the active site of the other subunit. This account for the destabilising effect in human mutants such as Gly416Asp and Arg411Cys/His, that form key interactions in the other subunit.

The value of ALAS2 model is that it allows an analysis to be made of why in some cases pyridoxine treatment is a success, but in others is not. One of the most interesting aspects of X-linked sideroblastic anaemia is the relationship between the location of the mutation in the ALAS2 enzyme and the responsiveness to pyridoxine treatment. In the mutations that response well to pyridoxine therapy *in vivo* are generally, but not always, clustered in the vicinity of the coenzyme binding site unless involving a key catalytic group. Others, more refractory to pyridoxine treatment, seem to be found on the periphery of the pyridoxal 5'-phosphate binding site. The model is also important for making knowledge-based mutations for determining the function of individual amino acids and, also, to explain the results represented in the next two chapters.

Chapter 4

X-Linked sideroblastic anaemias due to mutations in the erythroid 5-aminolaevulinic acid synthase gene

4.1 Introduction

X-Linked sideroblastic anaemias are some of the most common forms among the inherited types of the disorder (Bottomley, 1995) and many have been shown to be caused by missense mutations in the ALAS2 gene (May and Bishop, 1998). The groups of Bottomley and Bishop have been largely responsible for investigating the relationship between mutations in ALAS2 and X-linked sideroblastic anaemia. There are over 22 mutations described in more than 30 kindreds with all the mutations being found in exons 5 to 11, the functional core of the protein. Following the discovery that some patients with X-linked sideroblastic anaemia responded to pyridoxine (vitamin B_6), vitamin therapy has been adopted as one of the most important ways of treating the disease. The therapy centres on the fact that 5-aminolaevulinic acid synthase is a pyridoxal 5'-phosphate-dependent enzyme and that increased amounts of dietary pyridoxine lead to raised circulating levels of the coenzyme. It is thought that the increased level of the coenzyme may help to stabilise the ALAS2 protein or overcome any lowered affinity of the enzyme for the coenzyme. The way in which X-linked sideroblastic anaemias respond to pyridoxine therapy is very different, with some patients responding completely, others partially but a lower percentage being completely refractory to the therapy. In chapter 3, a model of ALAS2 was constructed to investigate the relationship between point mutations in the enzyme and the response to pyridoxine therapy. This indicated that patients with mutated residues in the vicinity of the coenzyme binding site generally responded well to vitamin therapy.

In this chapter we have investigated two ALAS2 human mutants, T388S (Cox *et al.*, 1994) and R452H (Edgar *et al.*, 1997). Threonine 388 and arginine 452 have been shown to be conserved residues among all ALAS enzymes. This is illustrated by the sequence alignment of arginine 452 (figure 4.1A) and threonine 388 (figure 4.1B) within the coding sequence. Figure 4.2 shows the structure of the residues investigated in this study.

QRNVKHMRQLLMDRGLPVIP	Human ALAS2
QRNVKHMRQLLMDRGFPVIP	Mouse ALAS2
QRNVKYMRQLLMDKGLPVVN	Toadfish
QRNVKLMRQMLMDAGLPVVH	Chicken ALAS1
QRNVKLMRQMLMDAGLPVVH	Human ALAS1
QRNVKLLRQMLMDSGLPVVH	Toadfish ALAS1
QRNVKLMRQMLMDAGLPVIH	Rat ALAS1
QRHAKHLRVLLRDRGLPAL.	Chicken ALAS2

Figure 4.1 A) An alignment of amino acid sequences in human ALAS2 the region of the Arg452 residue. The amino acids that are conserved in all species are shown in bold. The Arg452 residue is shown in red (Edgar *et al.*, 1997).

IMHKIDIISGTLGKAFGCVGGYIAS	Human ALAS2
IMHKLDIISGTLGKAFGCVGGYIAS	Mouse ALAS2
VQHKVDVVSGTLGKALGAVGGYIAS	Chicken ALAS2
VMPKMDIISGTLGKAFGCVGGYIAS	Human ALAS1
VMPKMDIISGTLGKAFGCVGGYIAS	Rat ALAS1
VMHKMDIISGTLGKAFGCVGGYIAS	Chicken ALAS1
VMDRVDMITGTLGKSFGSVGGYVAA	Saccharomyces cerevisiae ALAS
LMHRIDIFNGTLAKAYGVFGGYIAA	*Rhodobacter capsulatus* ALAS

B) The conservation of the amino acid sequences surrounding Thr388 of human ALAS compared to other ALAS enzymes. Amino acid residues that are conserved across all species are bold, Thr388 residue in red (Cox *et al.*, 1994).

Threonine 388, encoded within exon 8, is shown by the model (chapter 3) to be hydrogen bonded to the phosphate group of pyridoxal 5'-phosphate (figure 4.3). In one of the X-linked sideroblastic anaemias, this residue is conservatively mutated to serine (figure 4.4). Patients with this mutation respond completely to pyridoxine therapy. In the case of arginine 452, encoded within exon 9, this residue is located on the surface of the enzyme in a region containing several positively charged residues (figure 4.5). The replacement of arginine 452 by histidine, a semi-conservative mutation, leads to a relatively mild anaemia, although the pyridoxine response is small and only partial. Both the T388S and R452H mutants have been expressed in recombinant form in *E.coli* and appear to be relatively stable. As representatives of classes of X-linked sideroblastic anaemias that respond to pyridoxine therapy to different extents these mutants they are therefore of interest to study in detail with respect to substrate and coenzyme affinity, thermostability and protein conformation. The information from the ALAS2 model described in chapter 3 has been used in an attempt to explain the findings obtained.

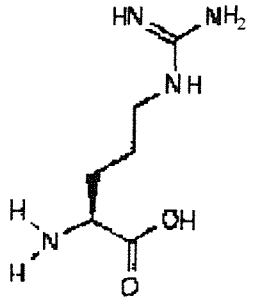

Arginine

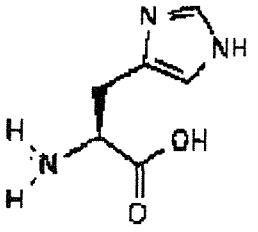

Histidine

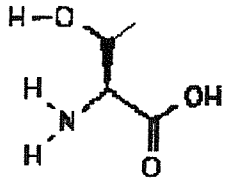

Threonine

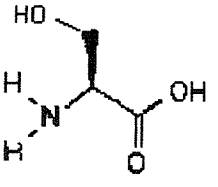

Serine

Figure 4.2 The structure of the amino acids involved in T388S and R452H mutants.

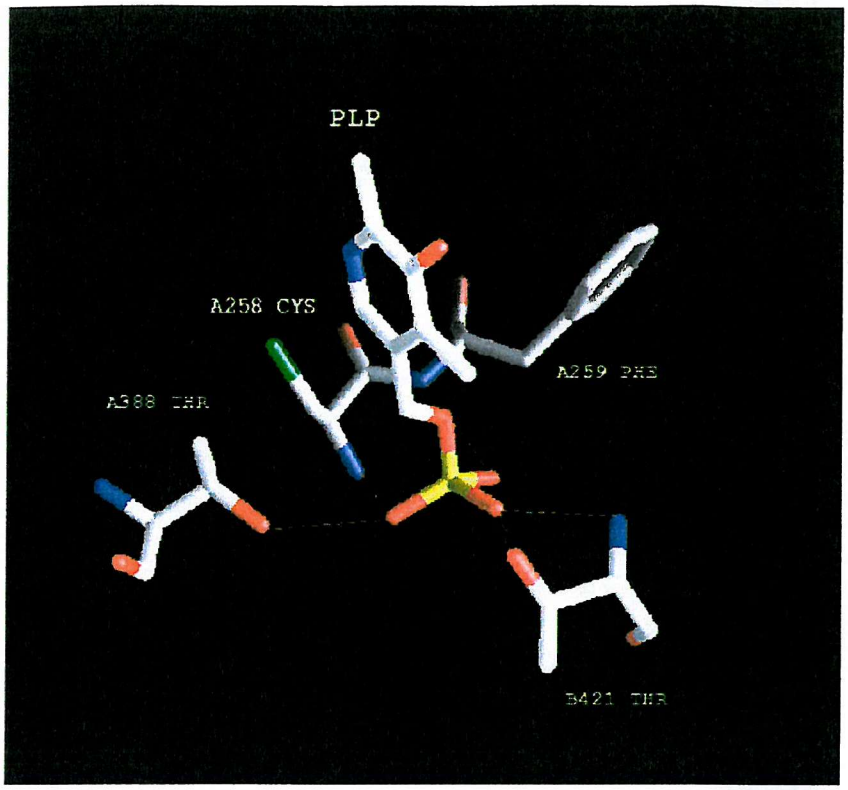

Figure 4.3 The environment of the threonine 388 residue in human ALAS2.

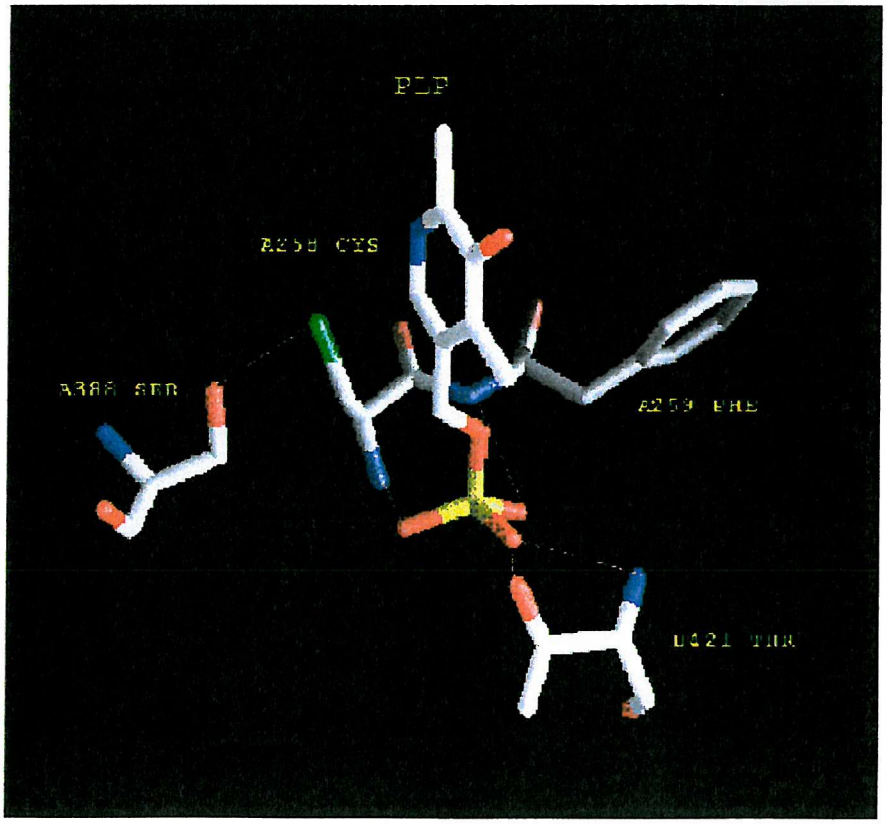

Figure 4.4 In the T388S threonine residue is replaced by serine and may form a hydrogen bond to cysteine instead of PLP, as suggested by the model.

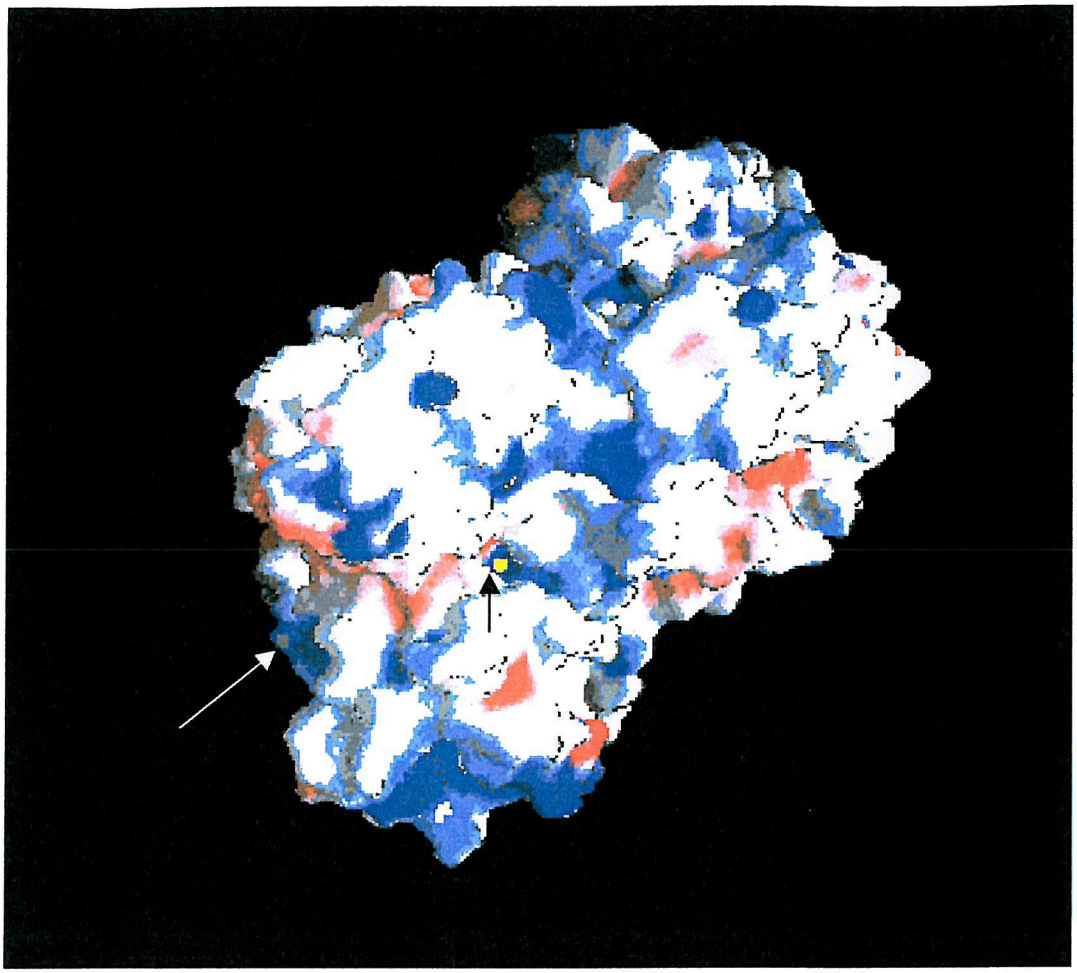

Figure 4.5 The surface of the ALAS2 dimer showing the position of the Arg452 residue. The surface charge of human ALAS2 as calculated and displayed by GRASP (Nicholls *et al.*, 1993). The blue color corresponds to positive potential and the red to negative. The yellow square represents the active site (black arrow) and the grey square in the left represents the Arg452 residue (white arrow). Both are in the positively charged region.

4.2 PCR and cloning of recombinant human ALAS2

PCR was carried out using the T388S mutant cDNA to generate the native ALAS. PCR was made in two sets; the first set with coding primers had 1032 bp and the second set with noncoding primers has 612 bp. Figure

4.6A shows PCR 1 using *Bam*HI and *Eco*RI coding primers, and figure 4.6B shows PCR 1 with noncoding primers.

A) Coding primers using λDNA marker

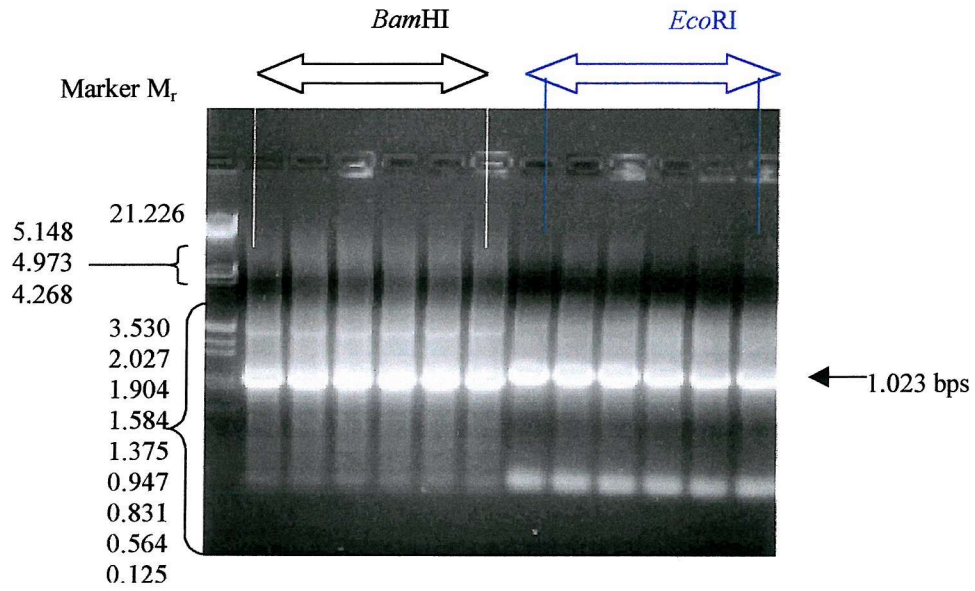

B) Non-coding primers using ϕX174 DNA marker

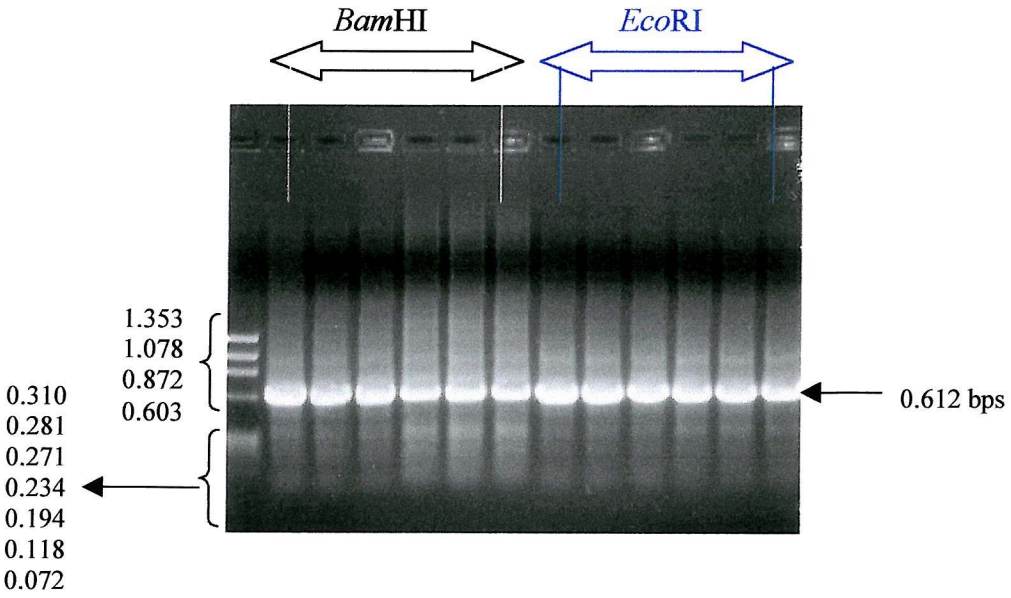

Figure 4.6 PCR 1 to generate the native ALAS2 using T388S DNA as a template with *Bam*HI and *Eco*RI sites

In the second PCR, the product of the PCR 1 was used to generate the native DNA with *Bam*HI-*Eco*RI sites (figure 4.7).

Figure 4.7 PCR 2 to generate the native ALAS using T388S DNA as a template with PCR primers containing *Bam*HI and *Eco*RI sites

4.3 Purification of ALAS and protein determination

Recombinant human ALAS was purified as a His-tag protein using TALON resin as described in chapter 2. SDS/PAGE (12%) was performed as described by Laemmli (1970). The degree of purification and the M_r of 59k for the R452H and T388S enzymes were similar to those for the native ALAS (figure 4.8 A, B and C). Protein concentrations were determined using the BioRad reagent kit. The amount of enzyme from 1L of overproducing bacterial cells was usually about 0.5 mg for the native enzyme and the mutants. Apo-enzymes, were purified using the same procedure used for the holo enzymes, but without addition the PLP to the buffer. Apo-enzymes show a similar M_r (59k) and a similar pattern of bands to those of holo-enzymes (figure 4.9 A, B and C).

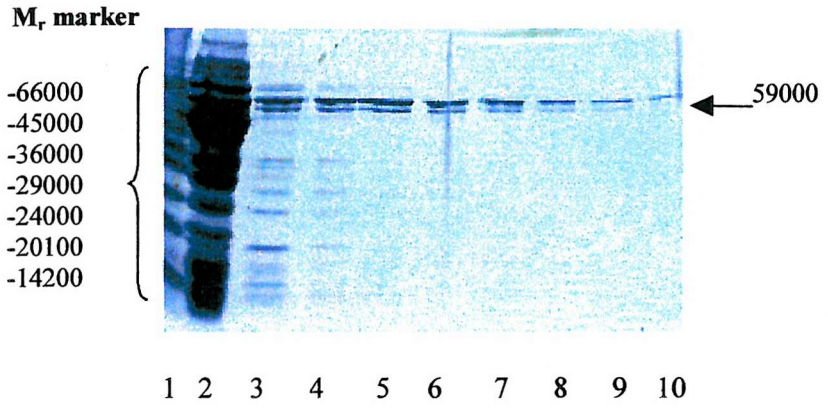

Figure 4.8 A Purification of recombinant holo-form of the native ALAS2 protein by TALON resins. Enzyme was analysed by SDS/PAGE and detected by staining with fast stain. Lane 1, the molecular mass marker; lane 2, crude extract; lane 3, elution with 15mM imidazole; lane 4, elution with 20mM imidazole; lane 5, elution with 30mM imidazole; lane 6, elution with 40mM imidazole; lane 7, elution with 50mM imidazole; lane 8, elution with 60mM imidazole; lane 9, elution with 70mM imidazole and lane 10, elution with 80mM imidazole.

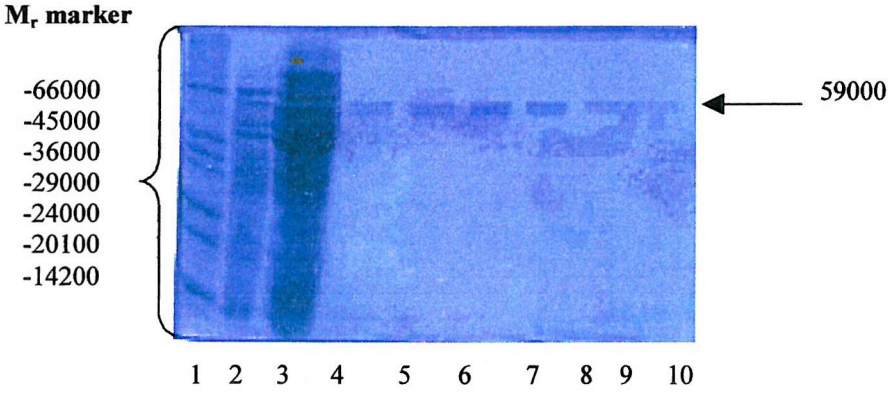

Figure 4.8 B Purification of recombinant holo-R452H mutant ALAS2 protein using TALON resin. R452H mutant enzyme was analysed by SDS/PAGE. Lane 1, the molecular mass marker; lane 2 elution with 15mM imidazole; lane 3, crude extract; lane 4, elution with 20mM imidazole; lane 5, elution with 30mM imidazole; lane 6, elution with 40mM imidazole; lane 7, elution with 50mM imidazole; lane 8, elution with 60mM imidazole; lane 9, elution with 70mM imidazole and lane 10, elution with 80mM imidazole.

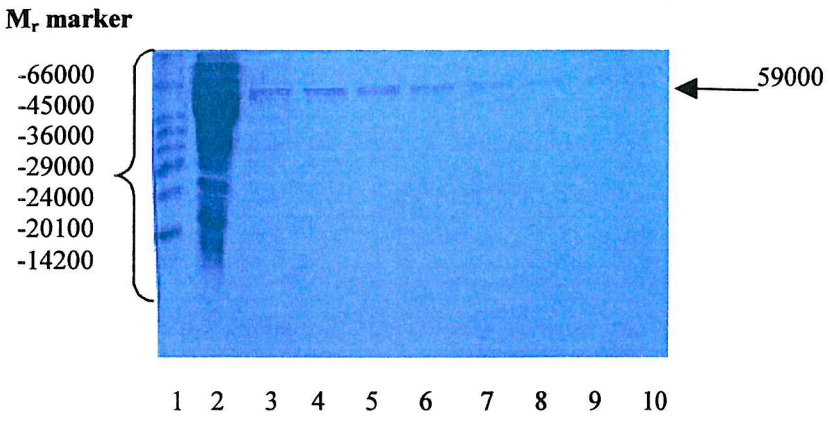

Figure 4.8 C Purification of recombinant holo-T388S mutant ALAS2 protein by TALON resin. T388S mutant enzyme was analysed by SDS/PAGE. Lane 1, the molecular mass marker; lane 2, crude extract; lane 3 elution with 15mM imidazole; lane 4, elution with 20mM imidazole; lane 5, elution with 30mM imidazole; lane 6, elution with 40mM imidazole; lane 7, elution with 50mM imidazole; lane 8, elution with 60mM imidazole; lane 9, elution with 70mM imidazole and lane 10, elution with 80mM imidazole.

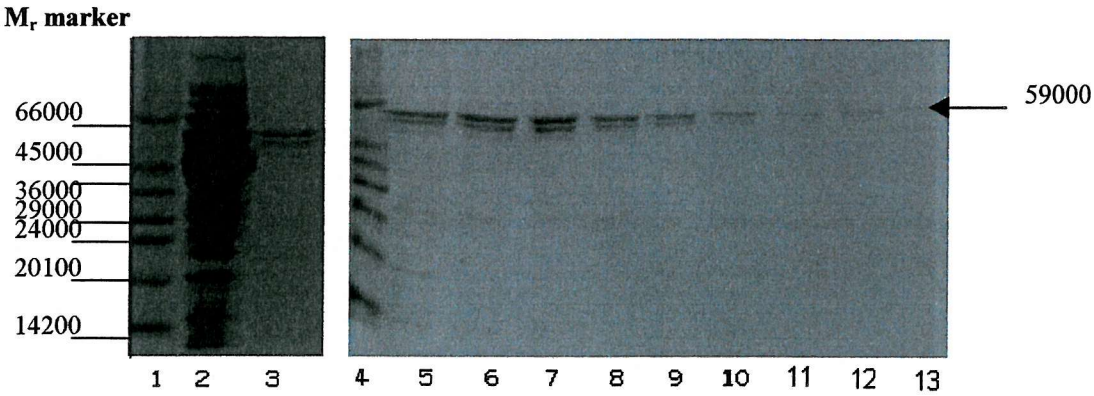

Figure 4.9 A Purification of recombinant apo-form of native ALAS2 protein by TALON resin. Native apo-ALAS2 analysed by SDS/PAGE and detected by staining with fast stain. Lane 1, the molecular mass marker; lane 2, crude extract; lane 3, elution with 15mM imidazole; lane 4, the molecular mass marker; lane 5, elution with 20mM imidazole; lane 6, elution with 30mM imidazole; lane 7, elution with 40mM imidazole; lane 8, elution with 50mM imidazole; lane 9, elution with 60mM imidazole; lane 10, elution with 70mM imidazole; lane 11, elution with 80mM imidazole; lane 12, elution with 90mM imidazole and lane 12, elution with 100mM imidazole.

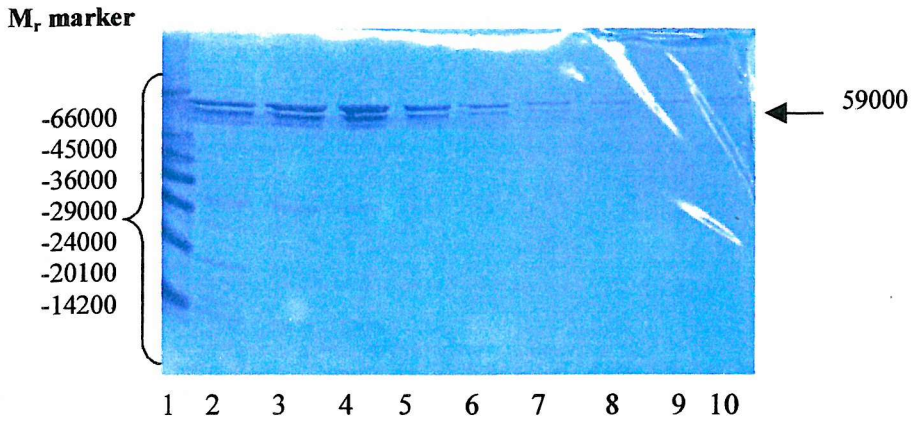

Figure 4.9 B Purification of recombinant apo-form of R452H ALAS2 mutant protein by TALON resin Apo-R452H mutant was analysed by SDS/PAGE. Lane 1, the molecular mass marker; lane 2 elution with 15mM imidazole; lane 3, elution with 20mM imidazole; lane 4, elution with 30mM imidazole; lane 5, elution with 40mM imidazole; lane 6, elution with 50mM imidazole; lane 7, elution with 60mM imidazole; lane 8, elution with 70mM imidazole and lane 9 the elution with 80mM imidazole; lane 10, elution with 90mM imidazole.

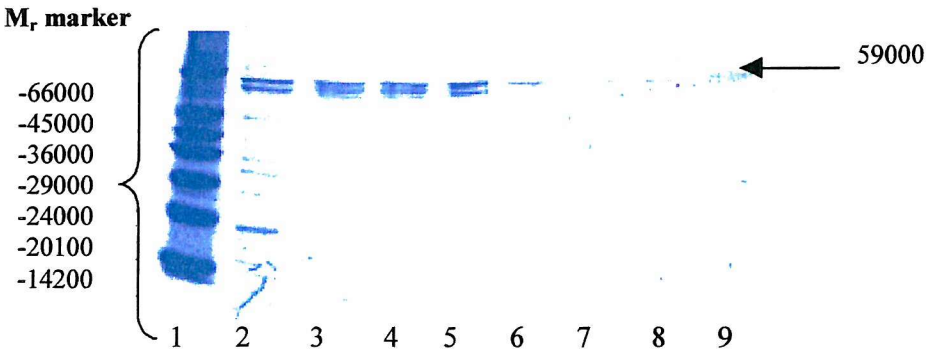

Figure 4.9 C Purification of recombinant apo-form of T388S ALAS2 mutant protein by TALON resin Apo-T388S mutant was analysed by SDS/PAGE. Lane 1, the molecular mass marker; lane 2 elution with 15mM imidazole; lane 3, elution with 20mM imidazole; lane 4, 30mM imidazole elution; lane 5, 40mM imidazole elution; lane 6, 50mM imidazole elution; lane 7, 60mM imidazole elution; lane 8, elution with 70mM imidazole; lane 9, elution with 80mM imidazole; lane 10, elution with 90mM imidazole.

From the SDS/PAGE analysis, shown in figure 4.8 A, the recombinant native human ALAS2 appears as a double band. Analysis of the native enzyme using non-denaturing gel electrophoresis revealed a single protein band (figure 4.10). The reason for the double band on SDS gels was not known initially.

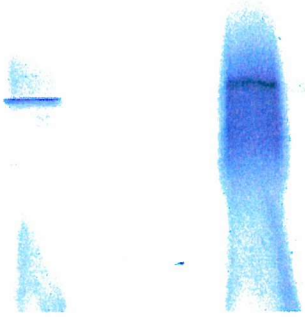

1 2

Figure 4.10 Non-denaturing gel electrophoresis for the native recombinant ALAS2. The non-denaturing gel was run to detect whether the native ALAS2 shows more than one band. The gel revealed a single protein band. Lane 1, native ALAS sample (10μg); lane 2 native ALAS sample (20μg).

Further investigation of the double band from SDS/PAGE (figure 4.8A) was carried out by removal of each band from the gel followed by tryptic digest procedure that involved sequencing the resulting peptide. Some of the data obtained yielded sequences similar to those characteristics of GroEl. GroEl is an ATP-dependent enzyme and dissociates into subunits if incubated with ATP. To see the effect of ATP on the ALAS2 double bands, the enzyme was incubated with 1mM ATP and 10mM MgCl, following by electrophoresis of the mixture using a native gel. The native gel did not show any difference between the control native sample and the native sample incubated with ATP (figure 4.11). The result obtained from the native gel, in addition to the ALAS2 activity, may indicate that the GroEl is not binding to the ALAS and might be present as a contaminant. The apo-form of the enzyme shows the same pattern of bands when run in SDS/PAGE electrophoresis, which indicate that the double bands do not represent the apo-form and holo-forms of the ALAS2.

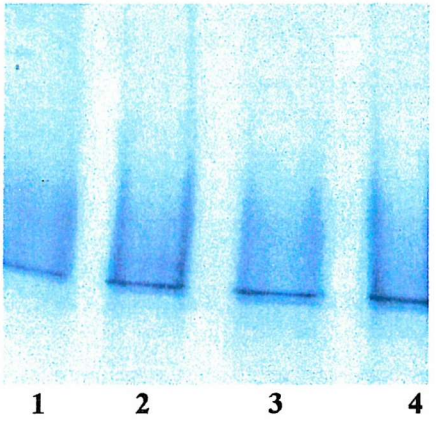

Figure 4.11 Non-denaturing gel electrophoresis of native ALAS2 incubated with ATP. Since GroEl is an ATP-dependent enzyme and dissociates when incubated with ATP, non-denaturing gel electrophoresis was used to analyse the native ALAS2 after incubation with ATP. The bands of the ALAS2 incubated with ATP are similar to those of the control. The native ALAS2 was incubated with 1mM ATP and 10mM MgCl for different time. Lane 1, control without ATP (native ALAS2); Lane 2, native ALAS2 incubated with ATP for 20 minutes; Lane 3, native ALAS2 incubated with ATP for 30 minutes; Lane 4, native ALAS2 incubated with ATP for 1hour.

A sample of ALAS2 (10mg/ml) was loaded onto an FPLC column of Superdex G-200 to separate the two bands (figure 4.12). Electrophoresis using SDS/PAGE was then used to monitor the elution fractions. The two bands of ALAS2 were separated (figure 4.13) and, by assaying the fractions, the activity was detected in each.

An electrospray mass spectrometer, fitted with a nano-spray, was used to investigate the molecular weight of each of the ALAS2 bands. Unfortunately, neither the mass spectrometer nor the nano-spray techniques successfully determined the molecular weight of the two bands.

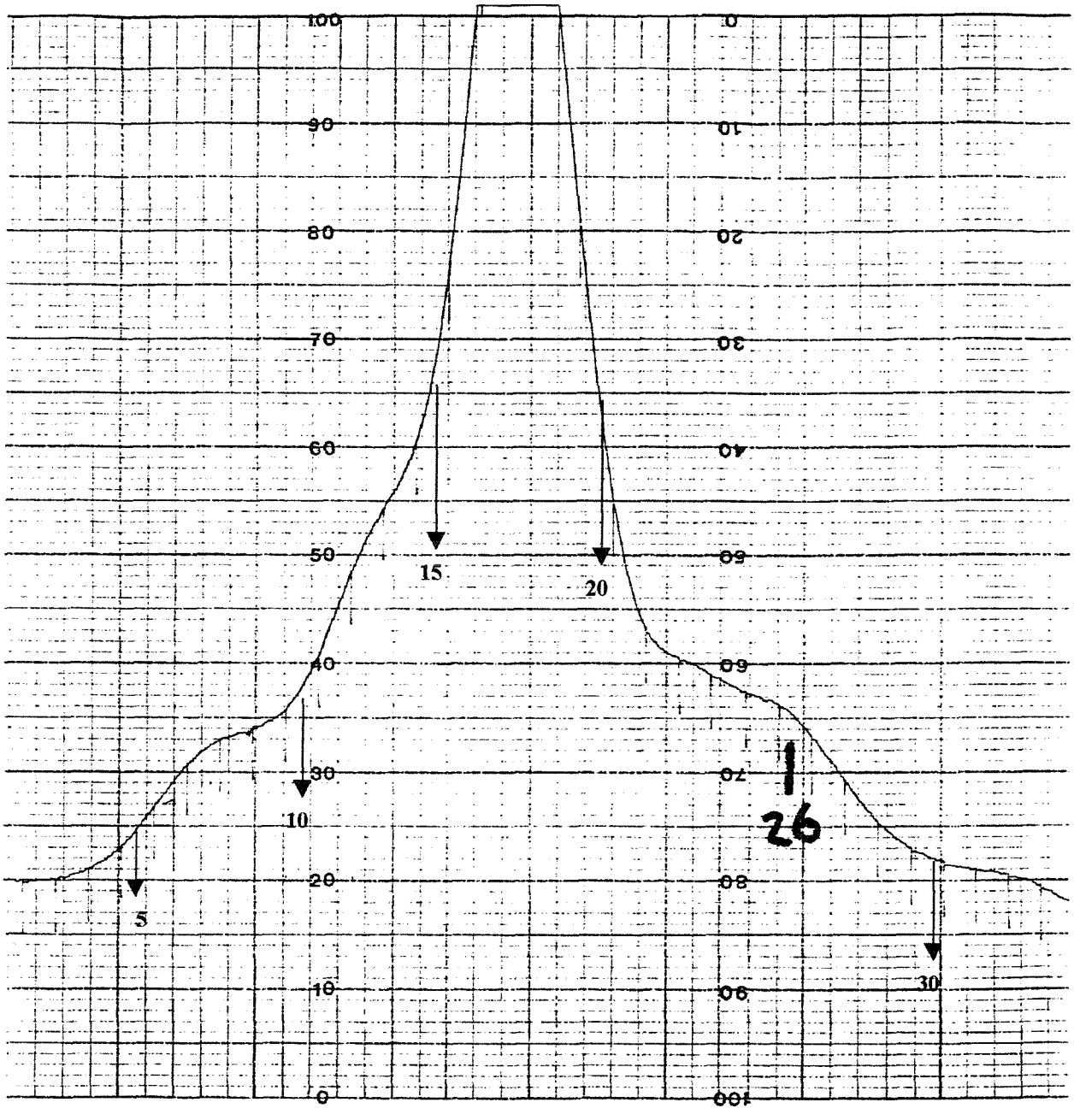

Figure 4.12 Native human ALAS2 protein bands separated by FPLC technique. This technique was carried out to separate the double bands of ALAS2 and to assay them separately. The double band was successfully separated on the FPLC and fractions were assayed. Both the upper and lower bands were active. Native ALAS2 (10 mg) was loaded onto a FPLC Superdex G-200 and eluted using 50mM phosphate buffer, pH 7.5, containing 20μM PLP, 10% glycerol, 5mM glycine and 100μM PMSF. The FPLC chart shows two peaks; the first peak (the small peak) starts from fraction 5, and this peak represents the bottom band. The second peak is the largest and represents the top band. Both samples had similar activity. The peak at 25 was inactive.

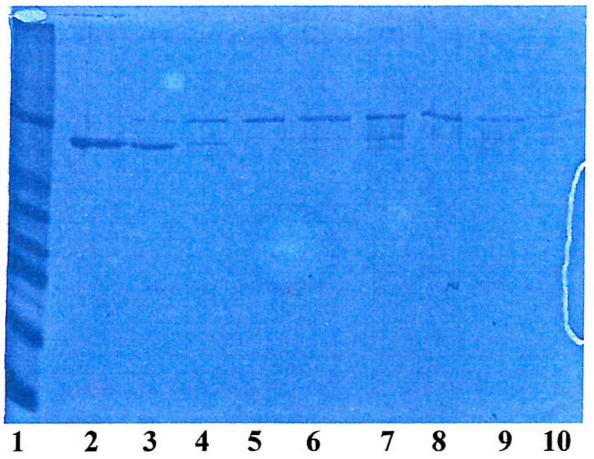

Figure 4.13 SDS/PAGE gel of native human ALAS2 fractions after FPLC. The two peaks (Fraction 4-8 and 9-20) were analysed by SDS/PAGE to determined the mobility of the bands after the FPLC. The two bands were separated. Lane 1, the marker; lane 2, fraction no.6; lane 3, fraction no. 7. Lanes 4-10 represent the second peak, lane 4, fraction no. 12; lane 5, fraction no. 15; lane 6, fraction no. 17; lane 7, fraction no. 18; lane 8, fraction no. 19; lane 9, fraction no. 20; lane 10, fraction no. 21.

4.4 Activity of the native and R452H and T388S mutant human erythrocyte ALAS

The assay traditionally used for ALAS2 (Mauzerall and Granick, 1956) involves termination of the reaction by the addition of trichloroacetic acid. After reaction with acetylacetone, ALA formation can then be measured as the "ALA" pyrrole, that is detected quantitatively using the chromophore generated by reaction of this pyrrole with Ehrlich's reagent at 553 nm. Enzyme assays were performed in a final volume of 1ml. Native human ALAS2 was active in

the assays described with a final specific activity of 18 μmol/hr/mg, where one unit of enzyme catalyses the formation of 1 μmol ALA product in 60 min at 37^0C. However, the specific activity of human ALAS is lower than that reported for ALAS purified from recombinant mouse ALAS2 (145 U/mg) (Ferreira and Daily, 1993) and that reported for purified *R. sphaeroides* ALAS (130 U/mg) (Warnick and Burnham, 1971), but higher than the activity of recombinant *R. sphaeroides* ALAS (13 U/mg) (Bolt *et al.*, 1999) (Roy and Shoolingin-Jordan, unpublished results). Mutants, R452H and T388S, showed 61% and 56% of the native enzyme activity, respectively. Tables 4.1 (A, B and C) shows the purification steps of the holo-form of the native and mutants ALAS2 enzymes.

Table 4.1 The purification table of the holo-form of human native, R452H and T388S ALAS2 enzyme . The assay was carried out to determine the activity of the native and mutant ALAS2 enzymes. The specific activity of the native ALAS2 is 18μmol/hr/mg whereas the activity is reduced to 61 and 56% in the R452H and T388S mutants, respectively. The assays were carried out using 50mM potassium phosphate buffer, pH 7.5, containing 250mM glycine, 2.5mM succinyl-CoA, 250μM PLP and 7μM ALAS.

A) Native ALAS2

Stage	Volume (ml)	Protein (mg/ml)	Total protein (mg)	Specific activity (μmol/hr/mg)	Total activity (μmol/hr)	% Yield
Crude extract	50	14.5	725	0.93	674.25	100
Pure ALAS2	3.5	0.70	2.46	18	44.15	7

B) R452H ALAS2

Stage	Volume (ml)	Protein (mg/ml)	Total protein (mg)	Specific activity (μmole/hr/mg)	Total activity (μmol/hr)	%Yield
Crude extract	100	10.51	1051	0.31	324.7	100
Pure ALAS2	3.5	0.32	1.1	11	12	4

C) T388S ALAS2

Stage	Volume (ml)	Protein (mg/ml)	Total protein (mg)	Specific activity (μmole/hr/mg)	Total activity (μmol/hr)	%Yield
Crude extract	100	10.06	1006	0.38	382.3	100
Pure ALAS2	3.5	0.532	1.86	10	10.2	5

Purification of the human recombinant ALAS2 enzymes in their apo-forms was carried out without addition of PLP to any of the purification steps. Two kinds of assays were performed to measure the specific activity of the apo-form. The first assay was carried out in the absence of the coenzyme PLP in the assay buffer. The apo-enzyme exhibited only 10% (2.6 μmole/hr/mg) of the holo-enzyme activity (18 μmole/hr/mg) when assayed in the presence of 250μM PLP. In the R452H and T388S mutants, the specific activities of the apo-enzymes were 2.0 and 1.39 μmole/hr/mg, respectively, compared to the mutant holo-forms (11 and 10 μmole/hr/mg, respectively) (table 4.2). Therefore the presence of PLP was found to be essential for maximal activity of human ALAS.

Table 4.2 Comparison of the activity of the native and mutant human recombinant ALAS2 in the absence and presence of the coenzyme PLP. The assays were carried out using 50mM potassium phosphate buffer, pH 7.5, containing 250mM glycine, 2.5mM succinyl-CoA and 7μM ALAS.

Enzyme	Specific activity -PLP	Specific activity +PLP
WT	2.6 μmole/hr/mg	18 μmole/hr/mg
R452H	2.0 μmole/hr/mg	11μmole/hr/mg
T388S	1.39 μmole/hr/mg	10 μmole/hr/mg

Another assay was carried out for the enzymes in their apo-form to see the effect of incubating the enzymes with 500μM PLP for 30 min at room temperature, before starting the actual assay. This was accomplished by the presence of 250μM PLP in the stock reaction buffer. The specific activity measured in this assay was similar to that recorded for the native ALAS2 isolated as its holo-form. The maximum activity of the mutants ALAS2 enzymes incubated with PLP also was similar to the holo-enzymes isolated by purification (table 4.3).

Table 4.3 The purification table of the apo-form of the native, R452H and T388S recombinant human ALAS2. The ALAS enzymes were purified in their apo-form and before the assay was carried out the enzymes (7μM) were first incubated with 500μM PLP for 30 min at room temperature. The activity obtained from this assay was close to that recorded for the enzymes in their holo-form.

A) Native ALAS2

Stage	Volume (ml)	Protein (mg/ml)	Total protein (mg)	Specific activity (μmol/hr/mg)	Total activity (μmol/hr)	%Yield
Crude extract	95	13.7	1301.4	0.626	815	100
Pure Protein	3.5	0.93	3.25	18	58.5	7

B) R452H ALAS2

Stage	Volume (ml)	Protein (mg/ml)	Total protein (mg)	Specific activity (μmole/hr/mg)	Total activity (μmole/hr)	% Yield
Crude extract	100	8.9	890	0.42	382.4	100
Pure protein	3.5	1.9	6.6	9.3	61.8	16.1

C) T388S ALAS2

Stage	Volume (ml)	Protein (mg/ml)	Total protein (mg)	Specific activity (μmole/hr/mg)	Total activity (μmole/hr)	%Yield
Crude extract	100	10.7	1070	0.36	385.2	100
Pure Protein	3.5	1.2	4.2	9.8	41.5	10.7

4.5 Kinetic characterisations

Kinetic parameters were determined for the purified human recombinant native and mutant ALAS2 enzymes. Assays were carried out by varying the concentration of substrates or coenzyme and keeping the concentrations of other components constant. A range of concentrations of glycine (1-100mM), succinyl-CoA (0.02-40μM) and pyridoxal 5'-phosphate (0.2-30μM) were used. The line equations derived from Eadie-Hofstee plots were used to calculate the K_m values of the substrates and the coenzyme, PLP. The K_m values for the substrate glycine was 10.55 and 10.37 in R452H and T388S, respectively, compared to the value for native ALAS2 of 13.9mM (figure 4.14A, B and C). The K_m value for succinyl-CoA was 0.8μM for the native ALAS2, lowered to 0.58 in R452H and 3-fold higher in the T388S mutant (figure 4.15 A, B and C). Native ALAS2 has the highest affinity toward the PLP whereas the lowest affinity recorded was for the T388S mutant (figure 4.16 A, B and C). Table 4.4 summarises the data from figures 4.14, 4.15 and 4.16 respectively.

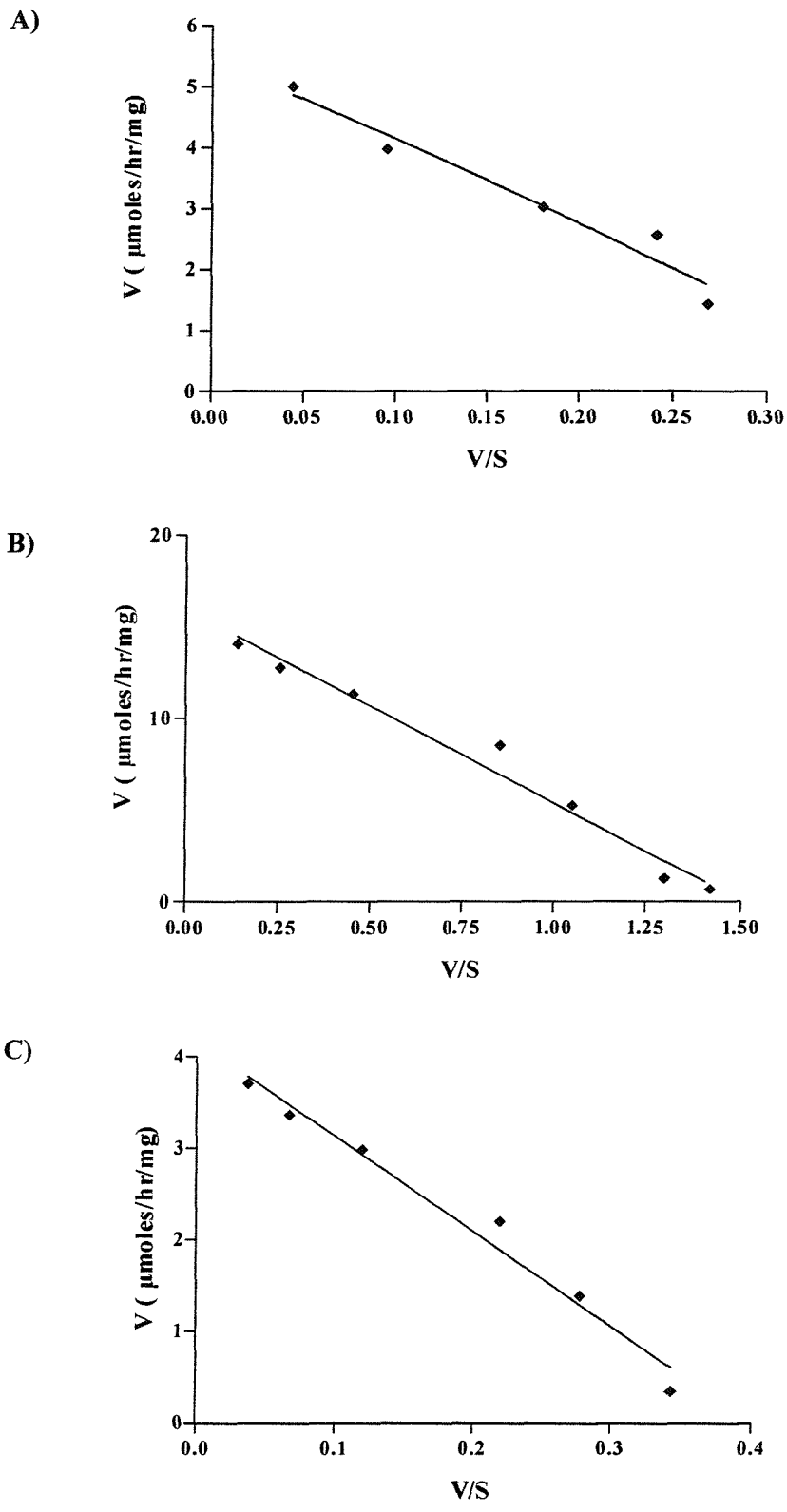

Figure 4.14 Eadie-Hofstee plots for glycine for the native human ALAS2 and R452H and T388S mutants. The K_m value for glycine was calculated from the slope derived from these plots using various concentration of glycine (1-100mM) at 2.5mM succinyl-CoA and 250µM pyridoxal 5'-phosphate. A) Native ALAS2 ; B) R452H; C) T388S.

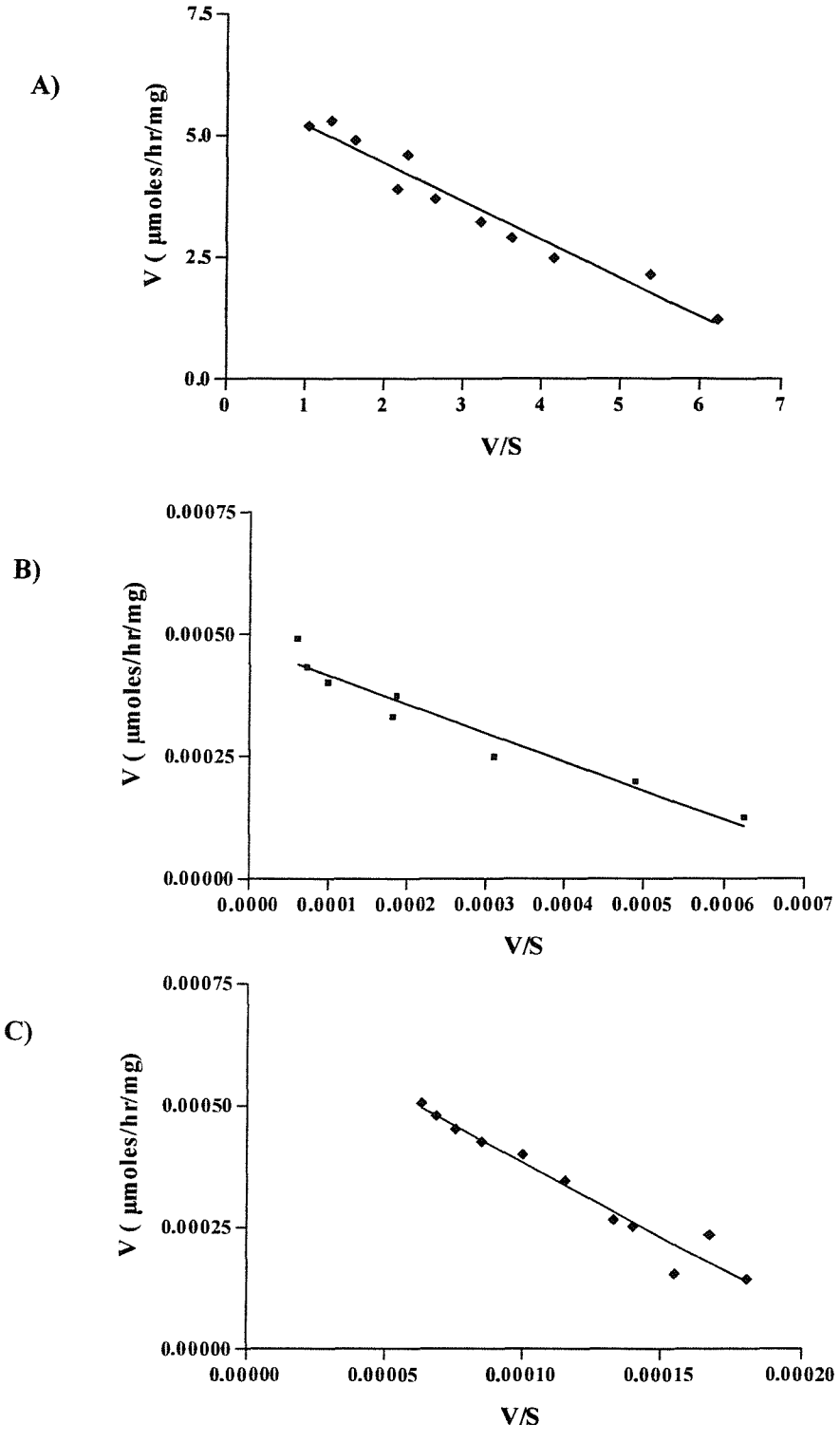

Figure 4.15 Eadie-Hofstee plots for succinyl-CoA for the native human ALAS2 and R452H and T388S mutants. The K_m value for succinyl-CoA was calculated from the slope derived from these plots using various concentration of succinyl-CoA (0.02µM-40M) at 250mM glycine and 250µM pyridoxal 5'-phosphate. A) Native ALAS2 ; B) R452H; C) T388S.

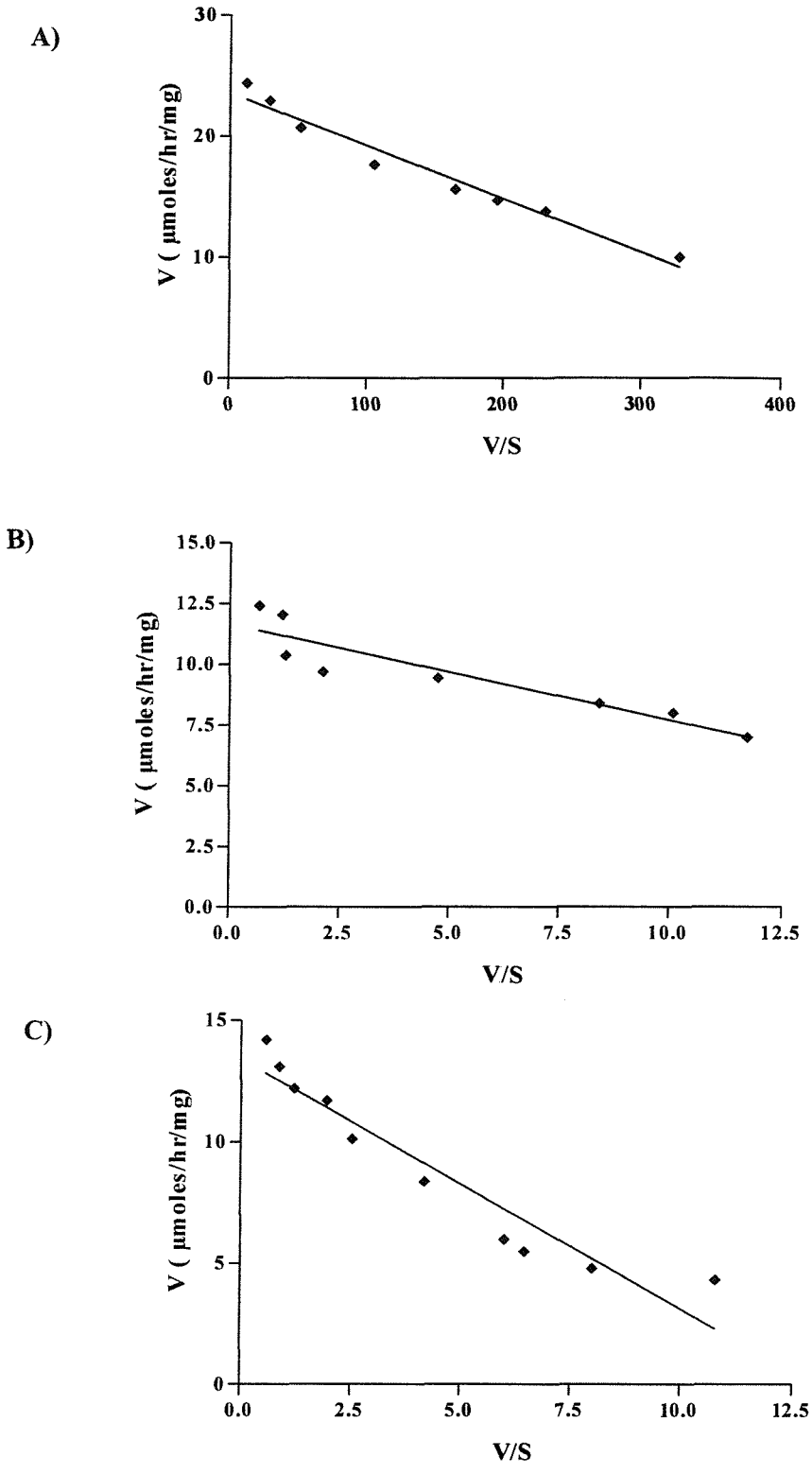

Figure 4.16 Eadie-Hofstee plots for pyridoxal 5'-phosphate for the native human ALAS2 and R452H and T388S mutants. The K_m value for the coenzyme was calculated from the slope derived from these plots using variouse concentration of Pyridoxal 5'-phosphate (0.2µM-30µM) at 250mM glycine and 2.5mM succinyl-CoA. A) Native ALAS2; B) R452H; C) T388S.

Table 4.4 Summary of the data from figures 4.15, 4.16 and 4.17, respectively, to compare the kinetic parameters for native human ALAS2 and the R452H and T388S mutants.

Enzyme	K_m Glycine (mM)	K_m Succinyl-CoA (μM)	K_m PLP (μM)
Native	13.90mM	0.80μM	0.05 μM
R452H	10.55mM	0.58μM	0.43 μM
T388S	10.37mM	3.00 μM	1.00 μM

The turnover number (k_{cat}), is defined as the maximum number of moles of substrate that can be converted to product per mole of enzyme in a unit of time under conditions of complete saturation. The k_{cat} for glycine for both native ALAS2 and T388S is almost similar (5 and 4 m^{-1}, respectively), whereas it is increased to 15.8 m^{-1} in R452H. Both mutants show lower k_{cat} values for succinyl-CoA compared to native ALAS2. In the PLP case the different in the k_{cat} values between the native and mutant enzymes are significant (table 4.5).

Table 4.5 The k_{cat} of the ALAS2 enzymes for the substrate and the coenzyme. The k_{cat} obtained from the following equation: $k_{cat} = V_{max}/[E_t]$.

Enzyme	k_{cat} (m^{-1}) Glycine	k_{cat} (m^{-1}) SCoA	k_{cat} (m^{-1}) PLP
Native ALAS2	5	6	23.5
R452H	15.8	0.0005	11.6
T388S	4	0.0006	13.3

4.6 Thermostability characterisation

Thermostability experiments were conducted to determine the relative thermostability of R452H and T388S mutant enzymes compared to the native

enzyme. The enzymatic activity was plotted as a function of temperature. The thermotransition temperature $T_{1/2}$, defined as the temperature needed to achieve a 50% activity loss, was 48.5 ^{0}C for the holo-form of the native ALAS2 and R452H and 50 ^{0}C for the holo-form of the T388S (figure 4.17). For the apo-form of the ALAS enzymes, the $T_{1/2}$ was 37.5 ^{0}C for the native, R452H and 40 ^{0}C for T388S (figure 4.18).

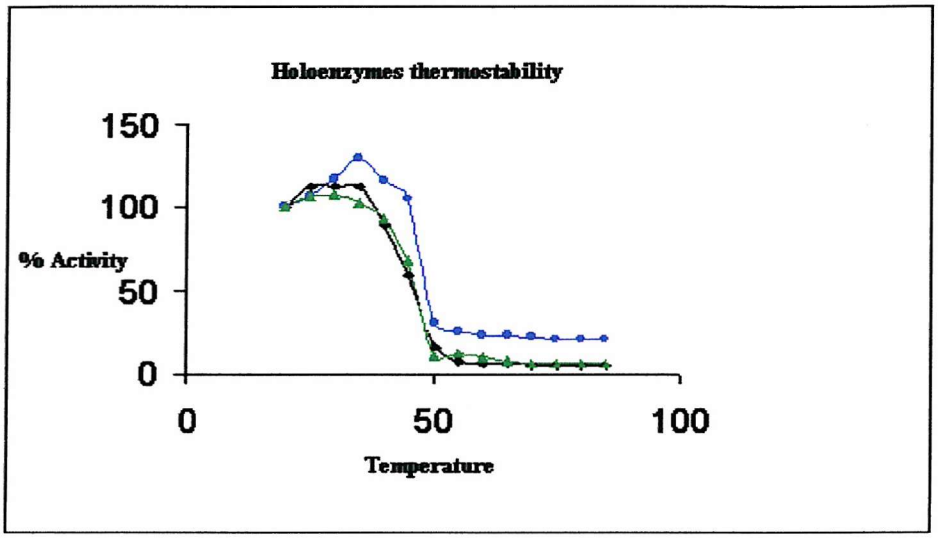

Figure 4.17 Thermostability of native ALAS and mutant enzymes. Thermostability was measured for the holo-enzymes to find the difference in the stability of the enzymes between the native ALAS2 and the mutants. Human ALAS2 enzymes were incubated at a given temperature for 5 min then cooled to 0°C, and activity assays performed. The enzymatic activity from the sample treated at 0°C was set as 100%. Black curve, native; green curve, R452H; blue curve, T388S.

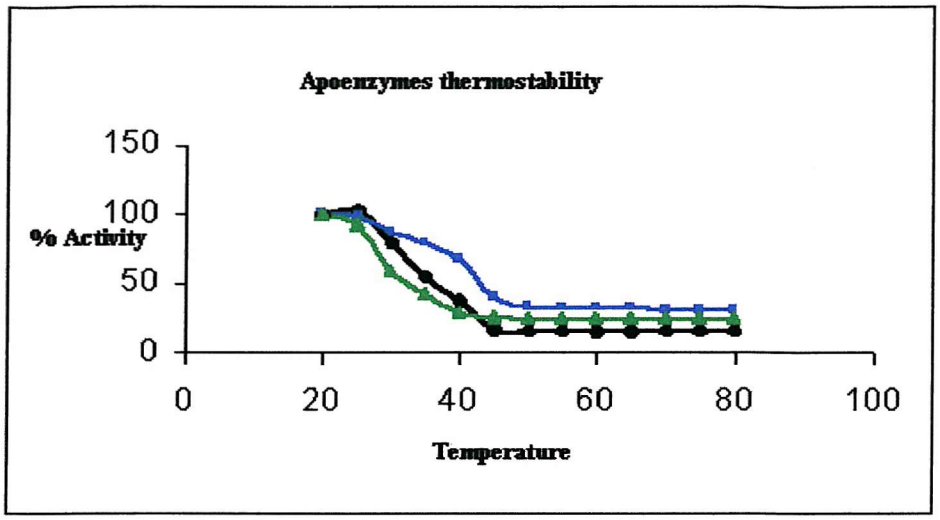

Figure 4.18 Thermostability of native ALAS and mutant enzymes. Thermostability was measured for the native ALAS2 and the mutants in their apo form to see the different in the stability among them. Human ALAS2 enzymes were incubated at a given temperature for 5 min then cooled to 0°C, and activity assays performed. The enzymatic activity from the sample treated at 0°C was set as 100%. Black curve, native; green curve, R452H; blue curve, T388S.

4.7 UV-visible spectroscopic analysis of PLP binding to human recombinant ALAS2, native and mutant enzymes

All PLP dependent enzymes, as mentioned in chapter 1 section 1.9, form a Schiff base linkage between the coenzyme and the ε-nitrogen atom of a lysine residue (lysine 391 for the human) in the active site. This complex is called the "internal" aldimine to distinguish it from the "external" aldimine, formed between the coenzyme and the amino acid upon the substrate binding. The formation of internal and external aldimines can be followed spectroscopically by their characteristic absorption spectra at about 430nm, (using a Hitachi 3010U spectrophotometer). The purified human ALAS has been shown to form an internal aldimine with PLP. The recombinant human ALAS2 was purified in its apo-forms (absence of PLP). On addition of 20μM PLP, the native and T388S mutant displayed absorption maxima at 430nm (A=0.07 and A=0.04, respectively), whereas the R452H mutant exhibited absorption

maxima at 416nm (A=0.05). This pattern of absorbance is typical of an internal aldimine linkage between the aldehyde group of the coenzyme and the lysine amino group of the enzyme. Both mutants showed absorption maxima at 330 nm. The wavelengths 330nm and 430nm, correspond to different ionisation states of the internal aldimine bond between the PLP and the ALAS, these two absorption maxima, 330nm and 430nm, represent the unprotonated and protonated forms, respectively (Ferriera *et al.*, 1995). The spectroscopic data indicate that the R452H and T388S mutants have impaired binding of PLP since the internal aldimine is reduced compared to the native enzyme. These finding are consistent with the K_m data (table 4.4) that shows the mutants have a lower affinity for the coenzyme. The spectrum of free PLP shows two main peaks 300nm and 390nm (figure 4.19).

Addition of 100mM glycine to the enzyme-PLP mixture resulted in the increase of the internal aldimine peak at 425nm to A=0.12 in the native and T388S mutant with a slight shift to the left (425nm). On addition of glycine the 330nm peak of T388S disappeared. The R452H mutant also exhibited an increase of the internal aldimine peak (A=0.10) with a slight shift to the right (425nm) and also a decrease of the 330nm peak. This kind of spectral change can be attributed to the formation of an external aldimine linkage between glycine and the enzyme-bound PLP.

The reaction of succinyl-CoA with the PLP-glycine-enzyme complex resulted in a pre-steady-state burst of quininoid intermediate formation (Hunter and Ferreira, 1999 b). Addition of 100μM succinyl-CoA led to a decrease in the external aldimine peak for the native enzyme and also for the T388S mutant. In the R452H mutant, the same concentration of succinyl-CoA (100μM) resulted in the appearance of a second absorbance maximum (at 510nm) with no change in the absorption spectrum of the external aldimine peak. The reduction in the external aldimine peak can only be seen after addition of 500μM succinyl-CoA to the R452H mutant and may indicate the ability of this mutant to condense succinyl-CoA with the deprotonated glycine that then accumulates at the active site (figure 4.20 A, B and C and 4.21).

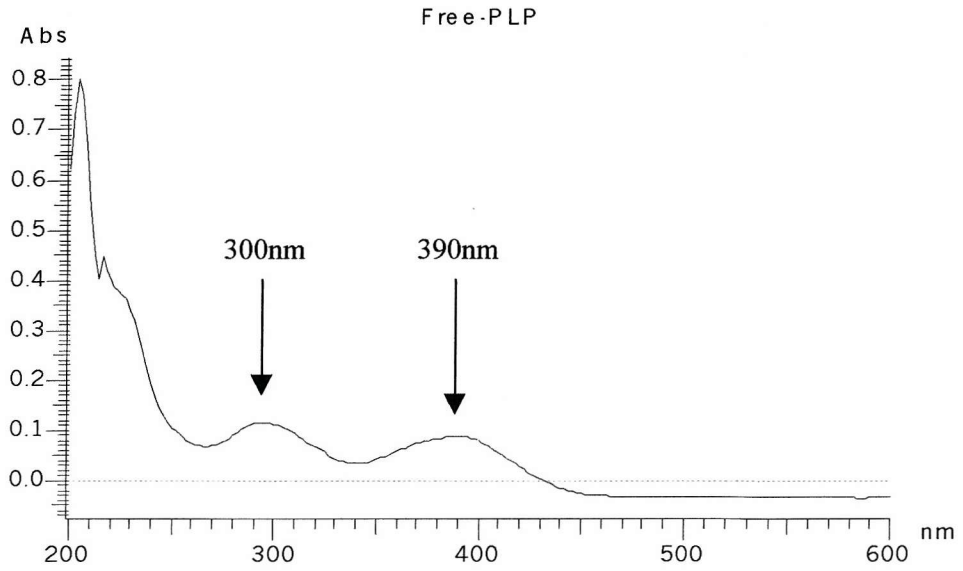

Figure 4.19 Spectrum of the free PLP (20μM) in 50mM phosphate buffer, pH 7.5 and it shows the 300nm and 390nm peak.

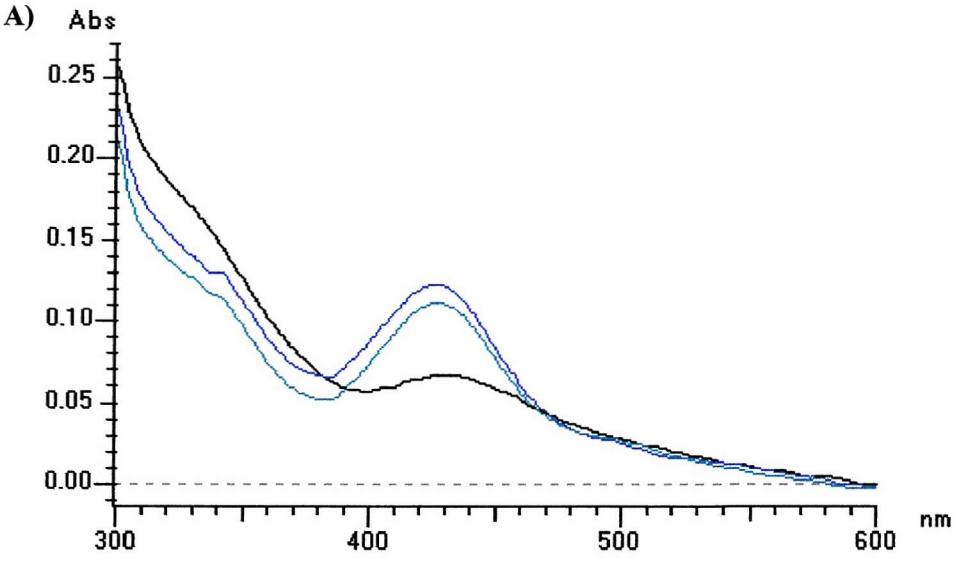

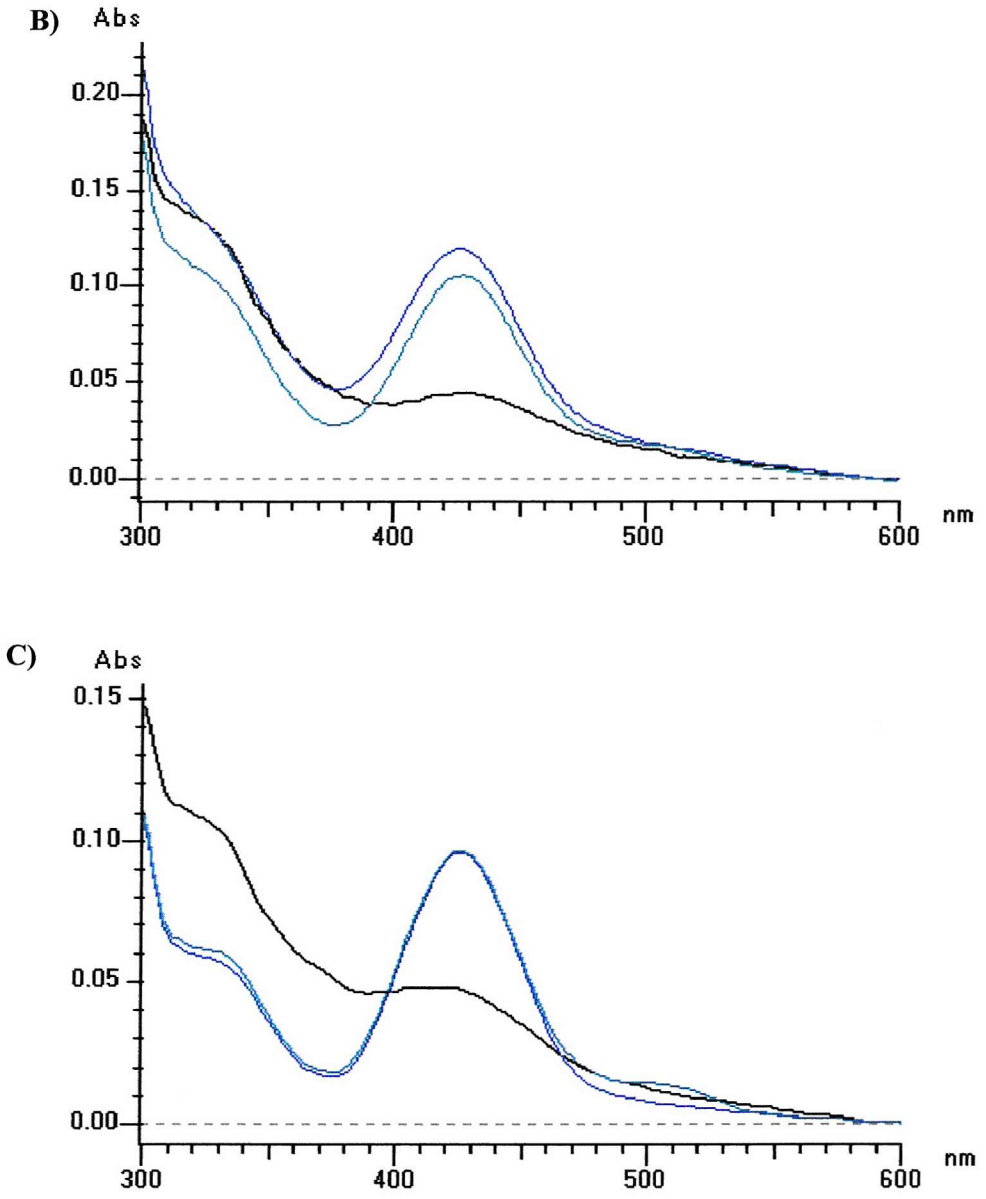

Figure 4.20 UV-visible absorption spectra of recombinant human ALAS2 enzymes. The absorption spectra to show the effect of adding pyridoxal 5'-phosphate to the apo-enzymes, followed by addition of glycine to form the external aldimine. The effect of succinyl-CoA on the PLP-glycine enzyme complex is also followed. UV visible absorption spectra were recorded in 20 mM phosphate buffer, pH 7.5. Figure A) native ALAS2. Figure B) T388S ALAS2. Figure C) R452H ALAS2. Black curve: absorption spectra of PLP bound to ALAS using 20μM PLP; blue curve: absorption spectra of glycine bound to the PLP-ALAS complex (the final concentration of glycine was 100mM); green curve: the effect of addition of 100μM succinyl-CoA.

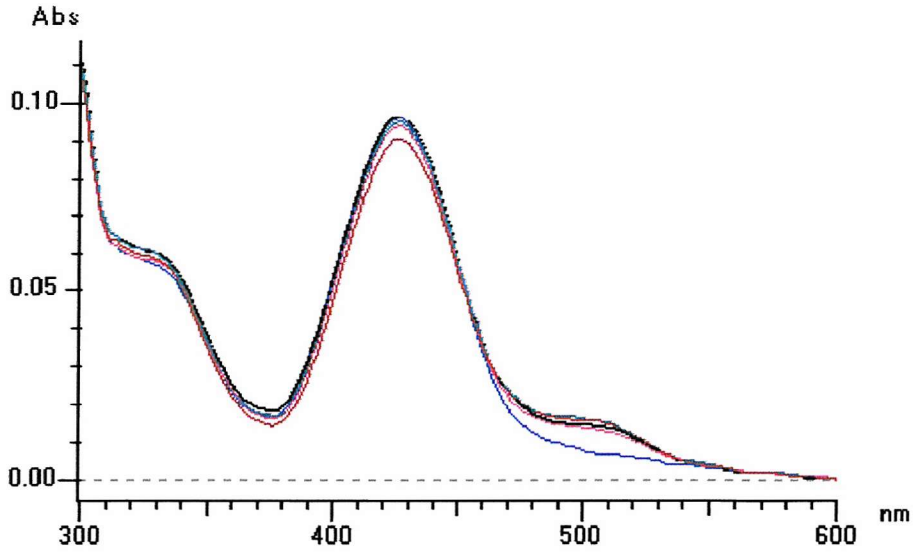

Figure 4.21 UV-visible absorption spectra of R452H with varying the concentrations of succinyl-CoA starting from 100μM up to 500μM. UV visible absorption spectra were recorded in 20 mM phosphate buffer, pH 7.5. UV absorption spectra recorded a peak at 510 nm after addition 100μM succinyl-CoA but no change had been noticed in the external aldimine peak. Whereas, after addition of 500μM succinyl-CoA, reduction of the external aldimine peak can be seen (brown curve).

4.8 CD spectroscopic properties

To investigate whether any gross changes in secondary structure had been introduced in the R452H and T388S mutants, UV CD spectra for the native and mutant human ALAS2 enzymes were obtained using a Jasco J720 spectropolarimeter. CD spectra of the native and mutant holo-enzymes in the UV region (200-270) are illustrated in figure 4.22. Using the same enzyme concentration (0.5 mg/ml), the R452H and T388S mutants exhibited CD spectra similar to that of the native in shapes but were different in depth. CD spectra in the UV region were also recorded for the apo-enzymes (figure 4.23). All apo-enzymes exhibited similar CD spectra of the native and different in depth. The ellipticity of the native ALAS2, on addition of PLP, falling from -25 to –80 and in the R452H and T388S mutants falling from –15 to –65 and –60,

respectively, consistent with coenzyme binding. Of interest, there is different between the spectra of the holo-enzymes and apo-enzymes in shape.

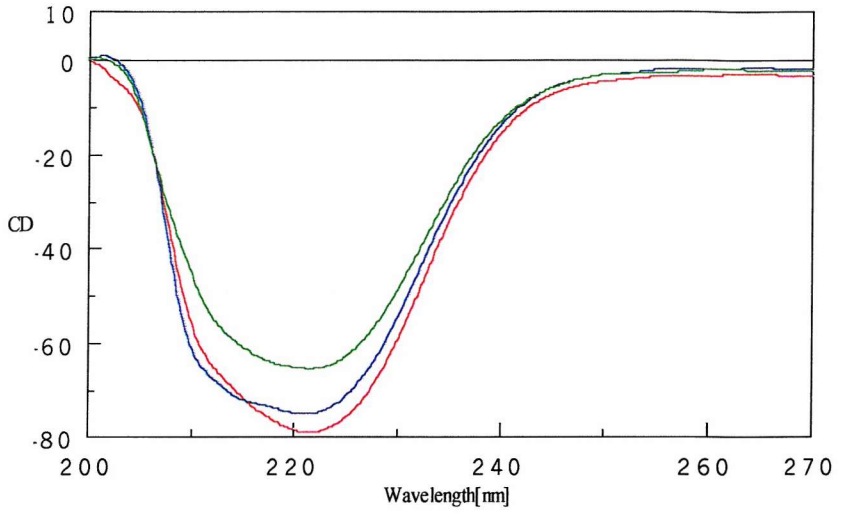

Figure 4.22 Far UV CD spectra of native human ALAS2 holo-enzyme compared to R452H and T388S mutant holo-enzymes. All spectra were recorded with 6μM ALAS2 protein in 50mM potassium phosphate buffer, pH 7.5, containing 20μM pyridoxal 5'-phosphate. The red spectrum shows the native ALAS2; the blue spectrum shows R452H mutant; the green spectrum shows the T388S mutant.

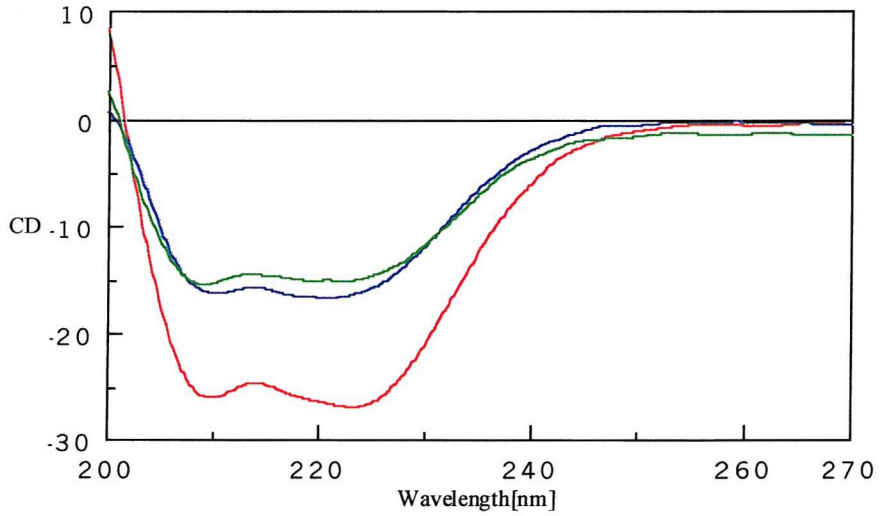

Figure 4.23 Far UV CD spectra of native human ALAS2 apo-enzyme compared to R452H and T388S mutant apo-enzymes. All spectra were recorded with 6μM ALAS2 protein in 50mM potassium phosphate buffer, pH 7.5. The red spectrum shows the native ALAS2; the blue spectrum shows the R452H mutant; the black spectrum shows the T388S mutant.

4.9 Discussion

The model of human ALAS2 highlights the position of important residues involved in the studies described. From the model, the R452 residue can be located on the surface of the enzyme in a patch where several positively charged residues are present together. This residue may thus contribute to stabilising a hydrogen bonding network. The other mutated residue, T388, is located in the vicinity of the coenzyme binding cleft. In the T388S mutant, a hydrogen bond between the hydroxyl group of threonine and the phosphate of the coenzyme may be displaced by the absence of the methyl group and allow solvent molecules to enter the cleft. In addition the threonine forms a network of hydrogen bonds that interacts with the adjoining subunit of the dimer (figure 4.3). Mutations involving R452 and T388 lead to X-linked sideroblastic anaemia that respond partially and completely to pyridoxine therapy, respectively.

Measuring the activity of the human ALAS2 mutant enzymes (R452H and T388S) showed about 60% decrease in the activity compared to the native enzyme. In the pedigree with hereditary sideroblastic anaemia caused by the R452H mutation, Edgar (1997) and his co-workers suggested that the proximity of the R452H mutation to lysine 391 alters the enzyme structure in the active site, thereby affecting the binding of pyridoxal 5'-phosphate and resulting in a deficient ALAS2 activity. From the model of human ALAS2 in chapter 3, R452H is located in a positively charged area far away from the active site (figure 4.5) and the mutation cannot exert its effect as proposed by Edgar *et al.*, 1997.

The reduced enzyme activity of the T388S may be due to a conformational change in the vicinity of the active site that reduces the affinity of the enzyme for its coenzyme (PLP) and, to lesser extent, the substrate (succinyl-CoA) as our study suggests. The activity of the native apo-enzyme, is 15% of that of the holo-form. In the R452H and T388S mutants, the activity

of the apo-form, is similarly, decreased to 14% and 13%, respectively, of the holo-form of the mutants.

The kinetic results show that the K_m for glycine was slightly changed, from 13.9 mM in the native enzyme to 10.55 mM and 10.37 mM for the R452H and T388S mutant, respectively. In reality there is no significant difference therefore in the affinity of the native and mutant enzymes toward glycine. There is also a negligible difference in the succinyl-CoA K_m between the native ALAS2, which is 0.8μM, and 0.58μM for R452H, whereas the K_m increases to 3.0μM in T388S mutant. Of particular interest with respect to pyridoxine therapy is the reduction in the affinity toward PLP found in the R452H and T388S mutants. This may be extrapolated to the *in vivo* situation when B_6 therapy is able largely to reverse the effects of the mutation. The mutation of threonine to serine is likely to affect the steric interaction of PLP at its binding site, where serine might form hydrogen bond to cysteine instead of PLP (figure 4.3 and 4.4). There is no significant difference in the turnover number of the PLP between the native ALAS2 and R452H and T388S mutants.

The holo-form of the native and R452H mutant exhibited similar thermostability, indicating that changing arginine to histidine does not affect the stability of the enzyme *in vitro*. The stability in T388S is actually improved for unknown reasons. In the apo-form, the native ALAS2 has a thermostability similar to R452H. The $T_{1/2}$ of all the apo-forms decrease two fold from that of holo-form.

Lysine 391 has been shown to form a Schiff base linkage with PLP and this residue has also been shown to have an important catalytic role in the protonation/deprotonation of glycine and 5-aminolaevulinic acid in the enzyme mechanism (Ferreira *et al.*, 1995). Ferreira and her co-workers established that mutagenesis of the equivalent lysine 313 in murine ALAS2 yields inactive ALAS enzymes that bind non-covalently to the coenzyme. Formation of the external aldimine occurs directly by reaction of the glycine amino group with the aldehyde of PLP. Our results showed that the UV-visible absorption for internal aldimine formation were similar for the native and mutant ALAS

enzymes, with the exception in the 330nm region. A peak at 330nm was observed for both mutants, but not for the native enzyme, suggesting that the PLP coenzyme in the R452H and T388S mutants is bound to the enzyme, but not fully covalently, as in the native enzyme.

Addition of glycine to the native ALAS2, caused an increase in the 430nm peak, reflecting the formation of the external aldimine. In the T388S mutant, the 330nm absorption maximum is shifted to 430nm, corresponding to the formation of an external aldimine. Similar external aldimine peak is seen at 430nm in the R452H mutant. These observations suggest that the catalytic lysine is less able to form Schiff base with PLP in the two mutants, possibly because of disruption to the PLP binding site caused by the mutation. The active site is not affected to the extent that the mutant enzymes cannot bind the glycine-PLP complex.

When succinyl-CoA was added to the native ALAS2-glycine-PLP complex, a decrease in the external aldimine peak was observed. A similar observation was made in the T388S mutant. In the R452H mutant, a high concentration of succinyl-CoA (500μM) was needed to reduce the external aldimine peak. Also, an additional absorbance maximum at 510nm with 100μM succinyl-CoA was noticed only with R452H. This might be related to the lower k_{cat} for R452H (0.0005 m^{-1}), compared to that of the native ALAS2 (6 m^{-1}) and also may indicate the inability of the R452H mutant to catalyse the condensation of succinyl-CoA with the deprotonated form of glycine. The quininoid form this accumulation and is seen as a small peak at 510nnm.

CD studies show that the structure of the enzyme is affected in the apo-enzyme form but that coenzyme binding restores much of the structural integrity. Similarly, the CD spectrum of mutant R452H, which responds partially to pyridoxine therapy, indicates that the binding of coenzyme generates a spectrum close to that of native ALAS2.

Chapter 5

Role of arginine 517 in substrate binding in recombinant human erythroid 5-aminolaevulinic acid synthase

5.1 Introduction

Examination of the amino acid sequences in a range of pyridoxal 5'-phosphate-dependent enzymes reveals a number of invariant residues. Several of these are involved in coenzyme and substrate binding, including an invariant aspartate that provides the counter-ion to the positively charged pyridinium nitrogen of the coenzyme and an invariant lysine that forms the Schiff base in the internal aldimine. This lysine also acts as a catalytic base in the abstraction of the proton from the α-position of the amino acid substrate (Ferreira *et al.*, 1993). In many of the pyridoxal 5'-phosphate dependent enzymes that catalyse reactions involving amino acids, an invariant arginine is involved in the binding of the carboxyl group of the amino acid. In the well studied pig cytosolic aspartate aminotransferase, it is Arg386 that plays this role, binding both aspartate and oxaloacetate and determining the orientation of the substrate moiety relative to the plane of the coenzyme-substrate imine. In mutational studies, Arg386 has been replaced by lysine, tyrosine and phenylalanine giving mutants that show dramatically reduced enzyme activity (Inoue *et al.*, 1989; Danishefsky *et al.*, 1991).

The residue analogous to Arg386 in aspartate aminotransferase is Arg517 in human erythroid ALAS. This residue is conserved residue in all ALASs (figure 5.1) and is thought to be essential for recognising and binding the carboxyl group of glycine, the amino acid substrate. Arg517 is mutated in one of the refractory X-linked sideroblastic anaemias in the form of Arg517Cys (May and Bishop, 1998). Such a mutation, if the residue was essential for the binding of glycine, would not be expected to respond to pyridoxine therapy. Indeed, the anaemia in patients suffering this mutation is refractory, as predicted, to pyridoxine therapy.

TVPRGEELLRLAP	Human ALAS2
TVPRGEELLRLAP	Mouse ALAS2
TVPRGEEILRLAP	Rat ALAS2
TVPRGQELLRIAP	Chicken ALAS2
TVPRGEELLRIAP	Chicken ALAS1
TVPRGEELLRIAP	Human ALAS1
TVPRGEELLRIAP	Rat ALAS1
TVARGQERFRLTP	*Rhodobacter sphaeroides hem T*
TVPRGTERLRFTP	*Rhodobacter sphaeroides hem A*
TVPRGTERLRFTP	*Rhodobacter capsulatus*

Figure 5.1 An alignment of amino acid sequences in the region of the R 517 residue of human ALAS2 in comparison to other ALASs. The R517 residue is in red (Tan *et al.*, 1998).

To investigate the role of Arg517 in the action of human ALAS2 and whether this residue plays a similar role to Arg386 in aspartate aminotransferase, investigations are described in this thesis that have been carried out on the purified Arg517Cys mutant to determine its ability to bind the coenzyme, pyridoxal 5'-phosphate, and its substrate glycine. In addition preliminary studies have been made to determine whether the mutation has any effects on the structure of the enzyme. To investigate further the importance of the Arg 517, additional mutants were constructed; one containing leucine that, like arginine, has a large branched side chain and another, containing lysine, an amino acid with an unbranched side chain but one containing a positively charged side chain like arginine. The catalytic and substrate binding properties of the three mutants (R517C, R517L and R517K) were compared to those of the native enzyme. Figure 5.2 shows the structures of the residue used in this study.

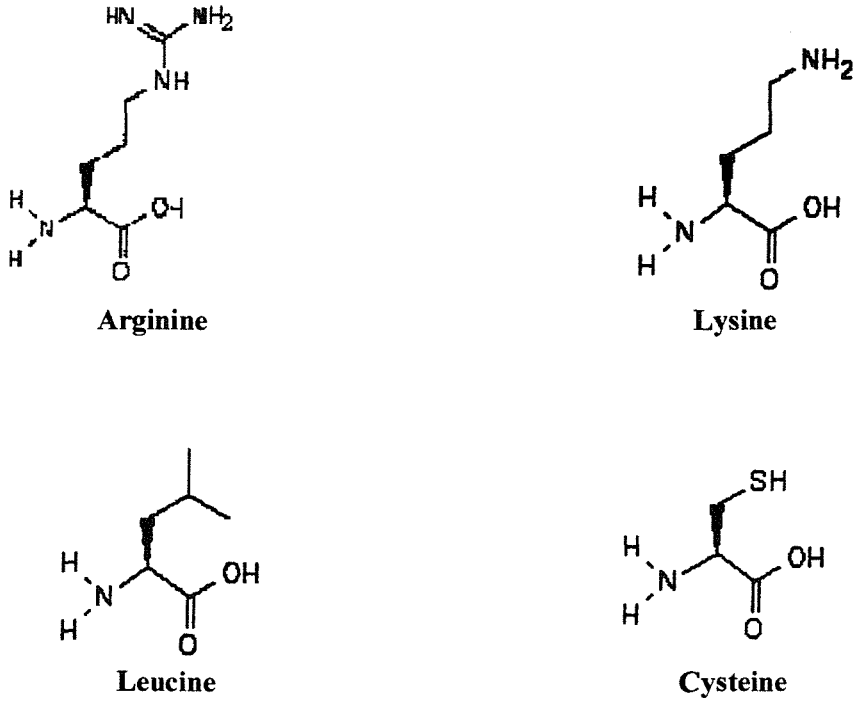

Figure 5.2 The structure of the amino acids involved in R517C, R517L and R517K mutants

5.2 Mutagenesis, expression and purification of human ALAS2 R517 mutants

Site-directed mutagenesis was performed using mutagenic oligonucleotides (27mers) to generate R517C, R517K and R517L as described in the Materials and Methods chapter, section 2.3.3.5. This was achieved by carrying out an initial PCR (PCR 1) as shown in figures 5.3 and 5.4. The main band from these gels were excised and subjected to a second PCR (PCR 2) as shown in figure 5.5.

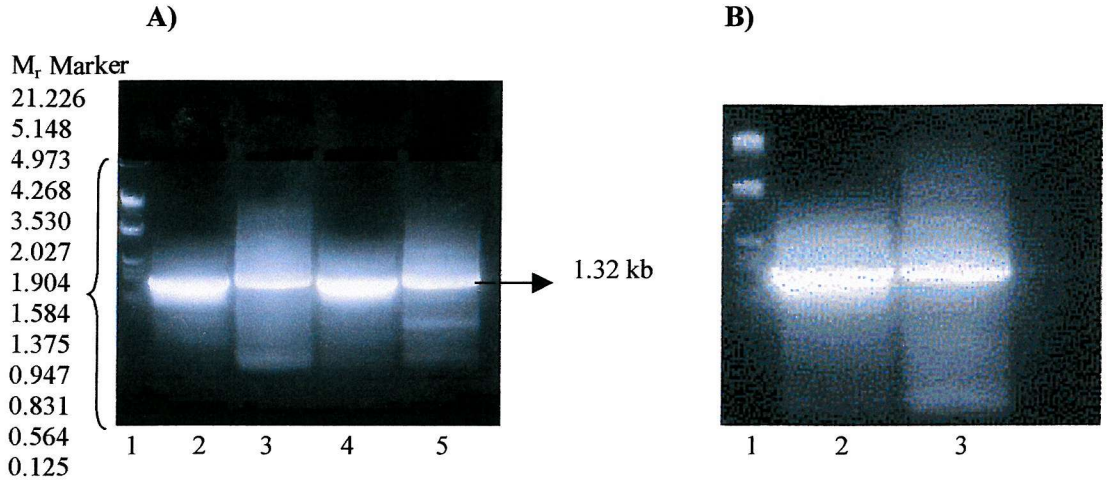

Figure 5.3 Formation of the PCR1 product of human ALAS2 cDNA to generate R517 mutants using native DNA as a template using coding primers containing the *Bam*HI site. A) The 1.3 kb PCR1 product for R517C and R517L. Lane 1, λDNA markers; lanes 2 and 3, PCR1 product for R517C; lanes 4 and 5, PCR1 product for R517L. B) The 1.3 kb PCR1 product for R517K. Lane 1, λDNA markers; lanes 2 and 3, PCR1 product of R517K.

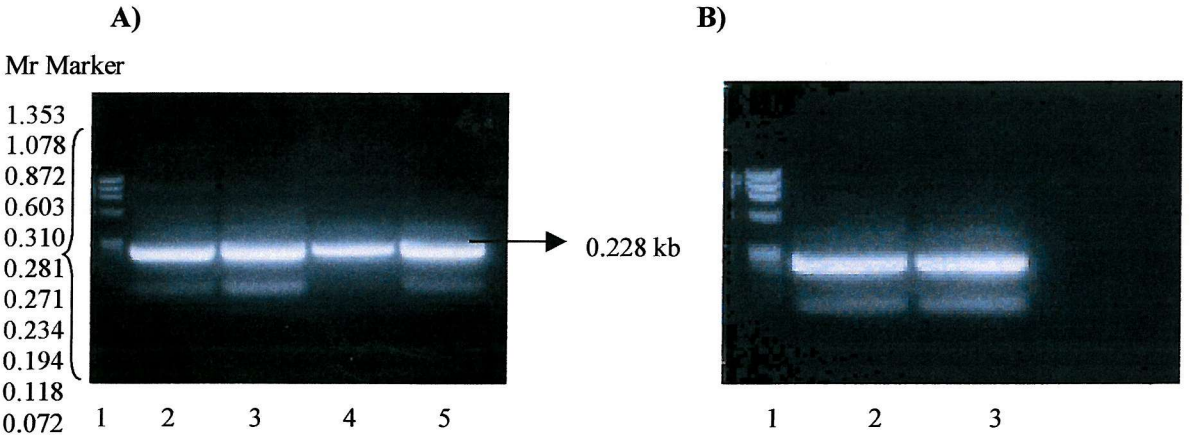

Figure 5.4 Formation of the PCR1 product of human ALAS2 cDNA to generate R517 mutants using native DNA as a template using non-coding primers containing the *Eco*RI site. A) The 0.22 kb PCR1 product for R517C and R517L. Lane 1, ϕXDNA markers; lanes 2 and 3, PCR1 product for R517C; lanes 4 and 5, PCR1 product for R517L. B) The 0.22 kb PCR1 product for R517K. Lane 1, ϕXDNA marker; lanes 2 and 3, PCR1 product of R517K.

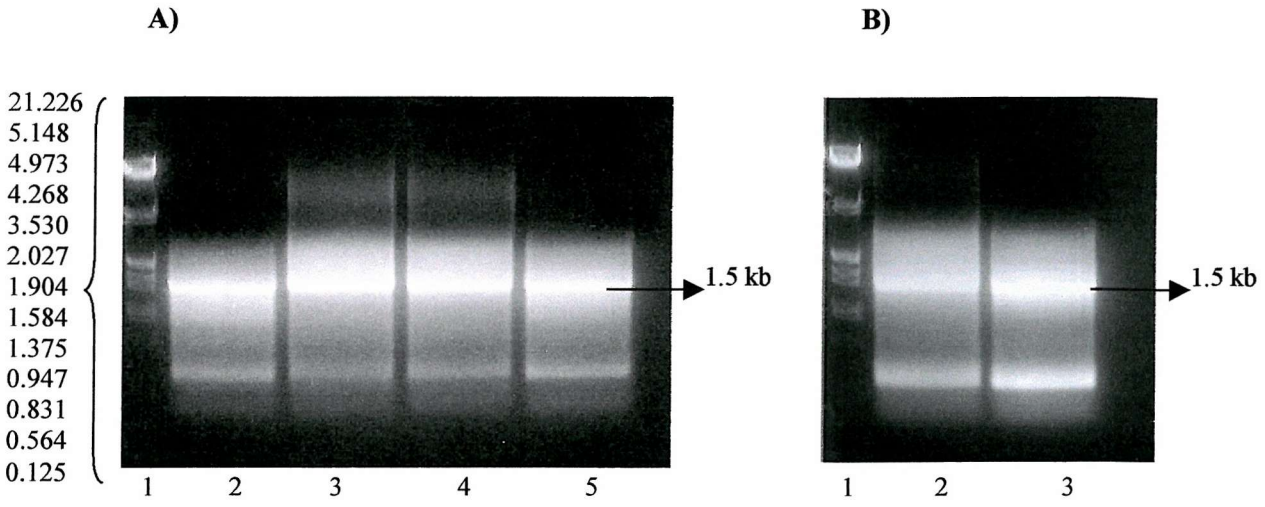

Figure 5.5 The product of PCR2 to generate R517 mutants, using the DNA produced from PCR1. A) PCR2 to generate R517C and R517L. Lane 1, λDNA markers; lanes 2 and 3 PCR2 product of R517C; lanes 4 and 5 PCR2 product of R517L. B) PCR2 of R517K mutant. Lane 1, λDNA markers; lanes 2 and 3 PCR2 product of R517K.

The PCR products were digested with *Bam*HI and *Eco*RI and purified by electrophoresis (figure 5.6). The purified fragments were cloned into the *Bam*HI and *Eco*RI sites of the pTrcHis B expression plamid to generate three plasmids containing the R517C, R517K and R517L mutant cDNAs.

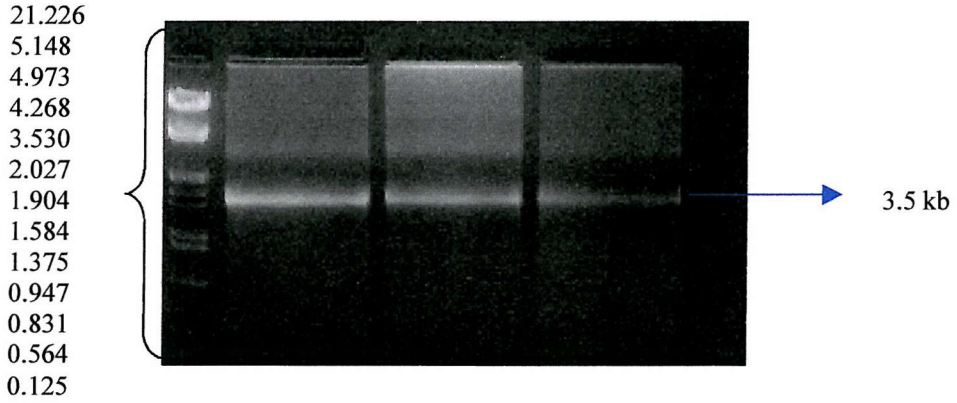

Figure 5.6 The products of the products of PCR2, specifying recombinant human ALAS2 mutants R517C, R517L and R517K, digested with *Bam*HI and *Eco*RI. The DNA was incubated at 37°C for 2hours with the restriction enzymes before purification by agarose gel electrophoresis. Lane 1, λDNA markers; lane 2, R517C; lane 3, R517L; lane 4, R517K.

The mutant human ALAS2 proteins were overproduced in the *E.coli* host strain, DH5α, harbouring these plasmids and purified to homogeneity using TALON "chalet" agarose resin chromatography, as previously described for the native enzyme in chapter 4. The mutant cDNAs were sequenced to check that no unwanted changes had occurred during the mutagenesis and cloning process (sequences determined by Oswel, Southampton).

5.3 Purification of recombinant human ALAS2 R517 mutant protein and activity determination

The purification method used for the isolation of the human ALAS2 R517 mutants was similar to that employed for the isolation of the native human ALAS2. The R517C, R517L and R517K mutant proteins were absorbed onto TALON resin and that was washed initially with buffer containing 5mM and 15mM imidazole followed by elution of the protein in seven 10mM steps from 20mM imidazole up to 80mM imidazole (See chapter 2 for details).

By running SDS/PAGE (12%) gels, as described by Laemmli (1970), the M_r for R517 ALAS2 mutants were determined and found to be similar to that recorded for the native ALAS2 (figure 5.7).

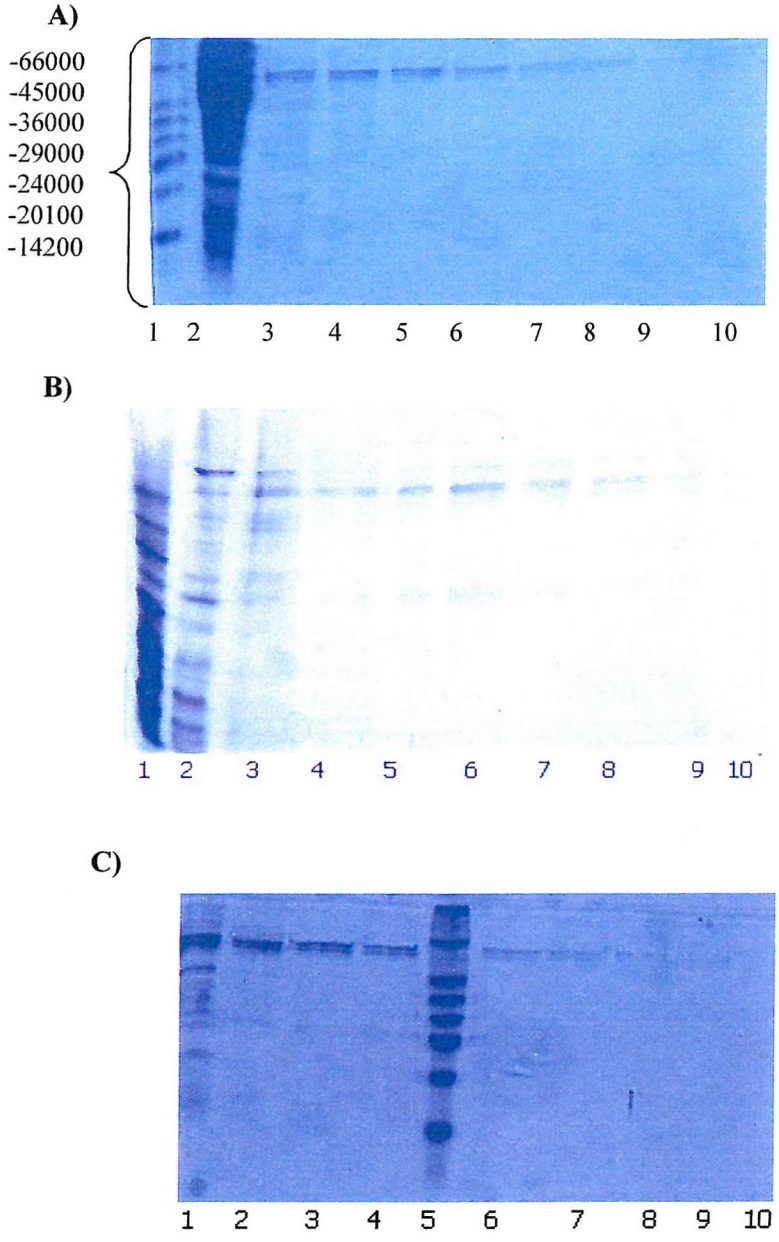

Figure 5.7 Purification of recombinant R517 human ALAS2 mutants protein using TALON resin. The mutants were analysed by SDS/PAGE as follows: **A)** R517C. Lane 1, Mr markers; lane 2, crude extract; lane 3, elution with 15mM imidazole; lane 4, elution with 20mM imidazole; lane 5, elution with 30mM imidazole; lane 6, elution with 40mM imidazole; lane 7, elution with 50mM; lane 8, elution with 60mM imidazole; lane 9, elution with 70mM imidazole; lane 10, elution with 80mM imidazole. **B)** R517L (Same order of lanes as A). **C)** R517K. Lane 1, crude extract; lane 2, elution with 15mM imidazole; lane 3, elution with 20mM imidazole; lane 4, elution with 30mM imidazole; lane 5, Mr markers; lane 6 elution with 40mM imidazole; lane 7, elution with 50mM imidazole; lane 8, elution with 60mM imidazole; lane 9, elution with 70mM imidazole; lane 10, elution with 80mM imidazole.

The amount of enzyme isolated from 1L of over-producing bacterial cells was usually about 0.48 mg. Protein concentrations were measured by using BioRad reagent kit. The activity of the recombinant human ALAS2 R517 mutants were determined by the method of Mauzerall and Granick (1956) in which the assay is terminated by the addition of trichloroacetic acid. After reaction with acetylacetone in 1M acetate buffer, ALA formation can then be measured quantitatively as "ALA" pyrrole, by reaction with modified Ehrlich's reagent to give a purple chromophore at 553 nm. Enzyme assays were performed in a final volume of 1ml. Only the R517K mutant shows any enzyme activity, giving 5% of the activity compared to the native human ALAS2 (table 5.1), whereas R517C and R517L gave no measurable activity. Table 5.2 shows a comparison of the activity obtained for R517 mutants and native ALAS2.

Table 5.1 Purification table for human ALAS2 mutant R517K mutant holoenzyme. Assays were carried out to determine the activity of the human ALAS2 R517K mutant. The assays were carried out using 50mM potassium phosphate buffer, pH 7.5, containing 250mM glycine, 2.5mM succinyl-CoA, 250μM PLP and 7μM ALAS. The specific activity of the R517K mutant was 0.97 μmol/hr/mg.

Stage	Volume (ml)	Protein (mg/ml)	Total protein (mg)	Specific activity (μmol/hr/mg)	Total activity (μmol/hr)	% Yield
Crude extract	50	8.67	433.5	0.011	4.76	100
Pure ALAS	3.5	0.59	2.06	0.97	1.99	4.1

Table 5.2 Comparison between the activity of native human ALAS2 with R517 mutants

Enzyme	Activity
Native ALAS2	100%
R517C	Not detectable
R517L	Not detectable
R517K	5%

5.4 Kinetic studies of ALAS R517K mutants

Values for the apparent K_m for the human ALAS2 R517K mutant was determined for the substrates glycine and succinyl-CoA and pyridoxal 5'-phosphate (PLP) from the line equation derived from the Eadie-Hofstee plot (Cornish-Bowden and Wharton, 1988). Assays were carried out by varying the concentration of substrate or PLP and keeping the concentrations of other components constant. Using a range of concentrations of glycine (1-100mM), succinyl-CoA (0.02-40μM) and the coenzyme, pyridoxal 5'-phosphate (0.2-30μM) the values were calculated from the graphs shown in figures 5.8 A), B) and C, respectively. Compared to the native human ALAS, the K_m for the glycine changed from 13.9mM to 64.1mM and that for PLP from 0.05μM to 0.30μM, while the K_m for succinyl-CoA decreased from 0.8μM to 0.2μM (table 5.3). As expected, R517K had a significantly lower affinity for glycine compared to the native ALAS2. In contrast, the affinity of the R517K mutant for succinyl-CoA was increased. The affinity of the mutant enzyme for the coenzyme, pyridoxal 5'-phosphate, was reduced compared to native ALAS2.

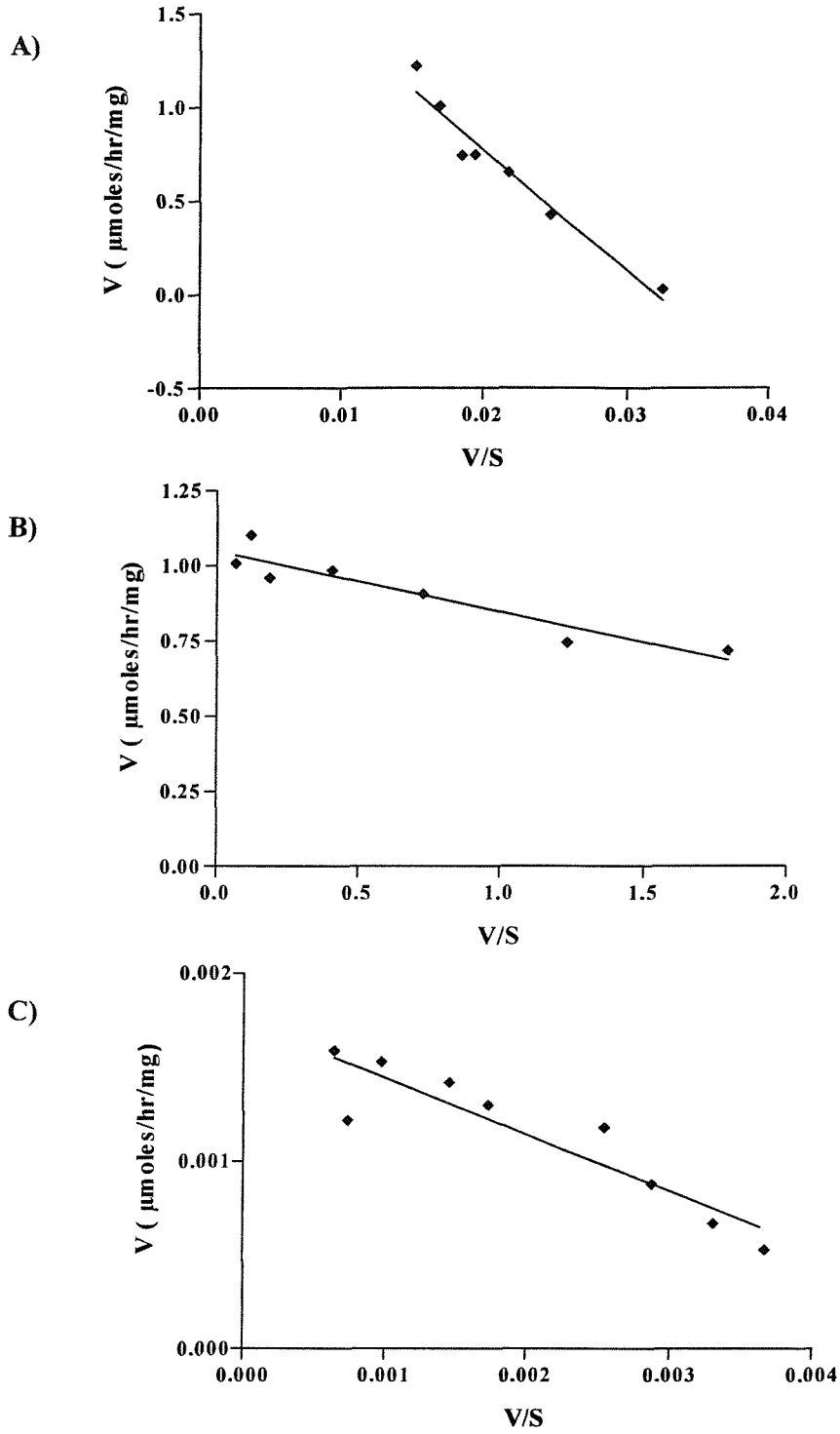

Figure 5.8 Eadie-Hofstee plots for glycine, succinyl-CoA and pyridoxal 5'-phosphate for the human ALAS2 R517K mutant. The K_m values for the substrates and the coenzyme were calculated from the slope derived from these plots. A) Glycine (1-100mM) at 2.5mM succinyl-CoA and 250µM pyridoxal 5'-phosphate; B) Succinyl-CoA (0.02µM-40M) at 250mM glycine and 250µM pyridoxal 5'-phosphate; C) Pyridoxal 5'-phosphate (0.2µM-30µM) at 250mM glycine and 2.5mM succinyl-CoA.

Table 5.3 Summary of the data from figure 5.8 to compare the kinetic parameters for native human ALAS2 and the R517K mutant.

Enzyme	K_m Glycine (mM)	K_m Succinyl-CoA (μM)	K_m PLP (μM)
Native ALAS2	13.90mM	0.80μM	0.05 μM
R517K	64.11mM	0.20μM	0.30 μM

The k_{cat} calculated for glycine, succinyl-CoA and the coenzyme pyridoxal 5'-phosphate, for the R517K mutant, is lower than that for native human ALAS2 (table 5.4).

Table 5.4 The k_{cat} of the ALAS2 enzymes for the substrate and the coenzyme. The k_{cat} obtained from the following equation: $k_{cat} = V_{max}/[E_t]$.

Enzyme	k_{cat} (m^{-1}) Glycine	k_{cat} (m^{-1}) SCoA	k_{cat} (m^{-1}) PLP
Native ALAS2	5	6	23.5
R517K	1.99	1.03	0.002

5.5 Investigations of human ALAS2 activity with different substrate analogues

ALASs are reported to be highly specific for glycine, with no other amino acids being accepted as substrate, however the enzyme can accept other acyl-CoA substrates in place of succinyl-CoA (Jordan *et al.*, 1997). In attempt to see if other compounds could act as substrates or inhibitors, the following were incubated with the enzyme, succinyl-CoA and pyridoxal 5'-phosphate in the absence, or presence, of glycine: methylamine, ethylamine, propylamine, 5-amino-1-pentanol and glycylglycine (see figure 5.9 for structures). None of the compounds acted as a

substrate instead of glycine and none, except, glycyl-glycine acted as a poor inhibitor.

Methylamine	CH_3NH_2
Ethylamine	$CH_3CH_2NH_2$
Propylamine	$CH_3CH_2CH_2NH_2$
5-Amino-1-pentanol	$HO(CH_2)_5NH_2$
Glycylglycine	$CO_2HCH_2NHCOCH_2NH_2$

Figure 5.9 The structure of compounds tested as a possible alternative substrate to glycine for human ALAS2

5.6 Determination of the thermostability of R517K

Point mutations in human genes may cause loss of activity of an enzyme due to a variety of reasons. For instance, substitution of an amino acid acting as a catalytic residue or substrate binding group invariably leads to a total loss of enzyme activity, although the enzyme may be folded normally. Other mutations can have a destabilising effect on the structure of the enzyme with a resulting reduction in $T_{1/2}$ or can even prevent the protein from folding correctly in the first place. It was hardly surprising therefore that the R517C mutation that involves the glycine substrate binding group, is catalytically inactive. This lack of catalytic activity meant that a study of the thermostability of R517C was not possible, therefore, an investigation was made using the R517K mutant enzyme. This was carried out by incubating the R517K ALAS sample at a protein concentration of 7μM at different temperatures for 5 min., starting from 0°C and rising to 100°C. After cooling the sample to 0°C, activity assays were performed on the treated sample at 37°C. The enzymatic activity from the sample treated at 0°C was set as 100%. The thermo-

transition temperature, $T_{1/2}$, is defined as the temperature needed for 50% loss of activity. Interestingly, when the values for $T_{1/2}$ for the R517K mutant holo-enzyme were compared with that of the native human ALAS2 holo-enzyme, the value for the R517K mutant was found to be 49°C, whereas the value for the native enzyme was 45°C (figure 5.10). The values for the apo-enzyme were also determined with $T_{1/2}$ being 54°C for the R517K mutant enzyme and 37.5°C for the native ALAS (figure 5.11).

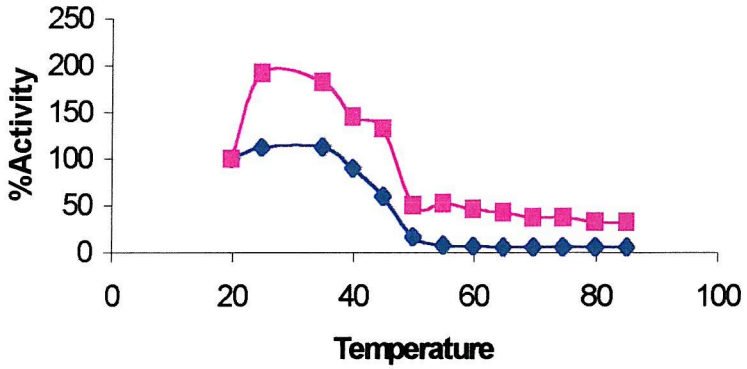

Figure 5.10 Thermostability of native human ALAS2 holo-enzyme compared with the R517K ALAS2 mutant. Thermostability was measured for the holo-enzymes to determine the stability of the enzymes. Samples were incubated at a given temperature for 5 min, then cooled to 0°C, and activity assays were performed. The enzymatic activity from the sample treated at 0°C was set as 100%. Blue curve, represent the native ALAS2; purple curve, the R517K mutant.

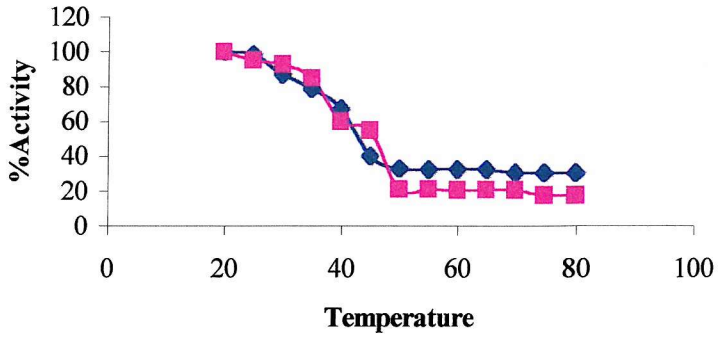

Figure 5.11 Thermostability of native human ALAS2 apo-enzyme compared with the R517K ALAS2 mutant. Thermostability was measured for the apo-enzymes to determine the stability of the enzymes. Samples were incubated at a given temperature for 5 min, then cooled to 0°C, and activity assays were performed. The enzymatic activity from the sample treated at 0°C was set as 100%. Blue curve, represent the native ALAS2; purple curve, the R517K mutant.

5.7 UV-Visible spectroscopic properties of ALAS R517 mutants

Several of the human ALAS2 mutants that lead to X-linked sideroblastic anaemia have been expressed in recombinant form and their properties investigated (Bottomley, personal communication). In some cases, the recombinant enzymes isolated show low specific activity but *in vivo* the patient is completely responsive to pyridoxine therapy, suggesting that the enzyme may behave differently *in vivo* and *in vitro* or that relatively low levels of enzyme are sufficient for normal haem synthesis. These studies however did not address the direct effects of pyridoxal 5'-phosphate and the substrates on the spectroscopic properties of the enzyme. In this section, investigation have been carried out using a Hitachi 3010U spectrophotometer to follow the formation of internal and external aldimines with the R517C, R517L and R517K mutants by their characteristic absorption between 410nm-430nm, as mentioned in chapter 4. The free pyridoxal 5'-phosphate has a maximum spectrum at 300nm and 390nm (figure 5.12).

All the purified R517 human ALAS2 mutants formed an internal aldimine when the apo-enzymes were treated with 20μM pyridoxal 5'-phosphate. However, the R517C and R517K mutants showed absorption maxima slightly higher than that of the R517L mutant. Thus, the R517C and R517K mutants (figure 5.13 and 5.14) had absorption maxima at 430nm (A=0.02) and (A=0.025), respectively, whereas the R517L mutant exhibited an absorption maximum at 410 nm (A=0.045) (figure 5.15). The lower maximum of the R517L mutant at 410nm suggests an internal aldimine in a slightly different environment. The maximum absorbance of all the R517 mutants, although lower than that recorded for native ALAS2 (A=0.07) (figure 5.16), still indicates there is substantial formation of the internal aldimine linkage between the aldehyde group of the coenzyme and the active site lysine of the protein. Of interest was the observation that the formation of the internal aldimine in the R517K mutant reached a maximum after 2 min (figure 5.17) whereas the other mutants and native enzyme appeared to form the internal aldimine with no delay.

Addition of 100mM glycine to the native enzyme-pyridoxal 5'-phosphate holo-enzyme resulted in an increase in absorption from A = 0.07 to A = 0.13 at 430nm due to the formation of the external aldimine, as described in chapter 4. In contrast, when glycine was added to the R517C and R517L human ALAS2 mutants holo-enzymes there was no external aldimine peak was observed. However, in the case of the R517K mutant, addition of glycine to the holo-enzyme resulted in the formation of an external aldimine peak at 426nm, but with a lower maximum (A = 0.103) than that recorded for the wild type.

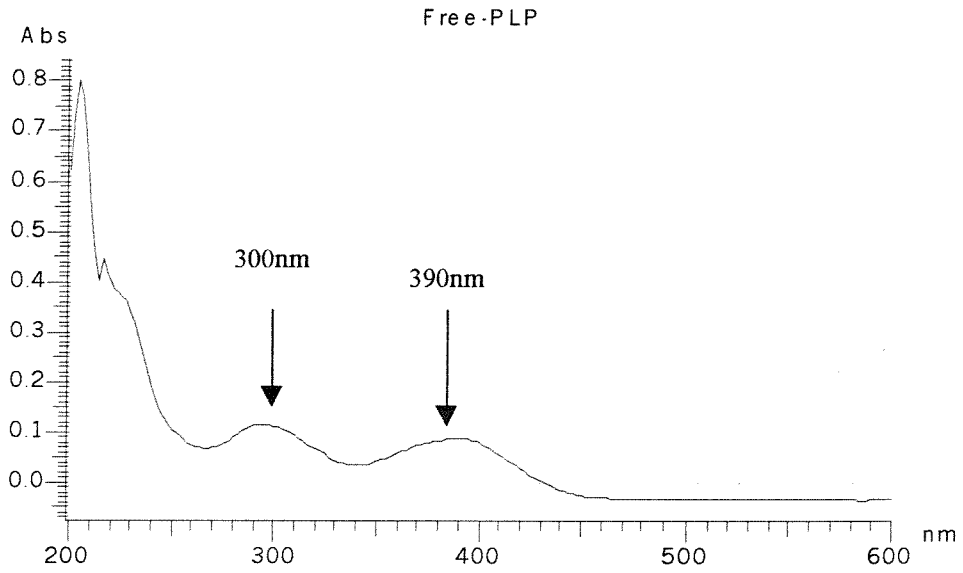

Figure 5.12 Spectrum of the free PLP (20μM) in 50mM phosphate buffer, pH 7.5 and it shows the 300nm and 390nm peak.

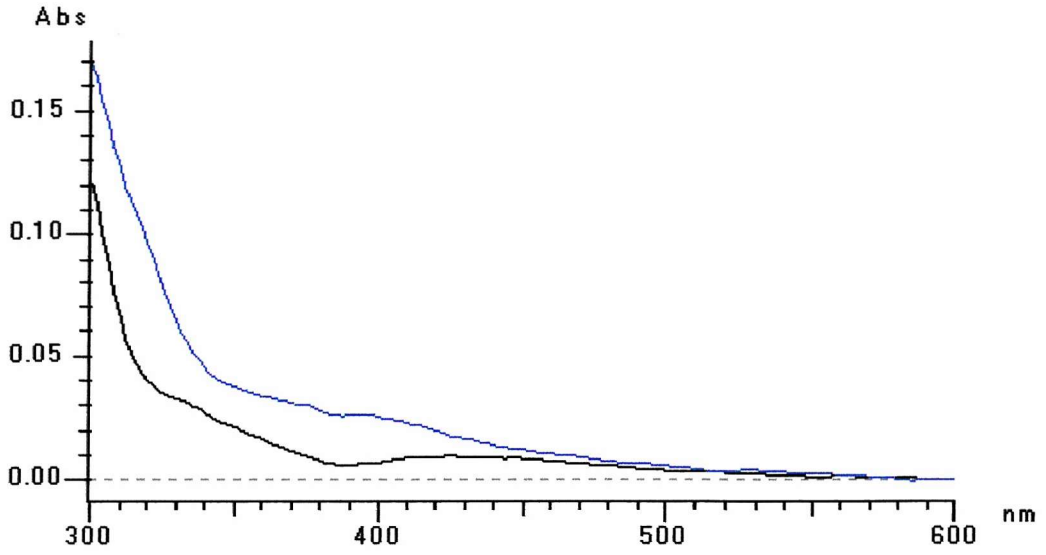

Figure 5.13 UV-visible absorption spectra of the human ALAS2 R517C mutant holo-enzyme before and after addition of glycine. UV visible absorption spectra were recorded in 20mM phosphate buffer, pH 7.5. The black curve represents the absorption spectrum of the R517C mutant holo-enzyme. The blue curve represents the absorption spectrum of glycine (100mM) bound to the holo-enzyme.

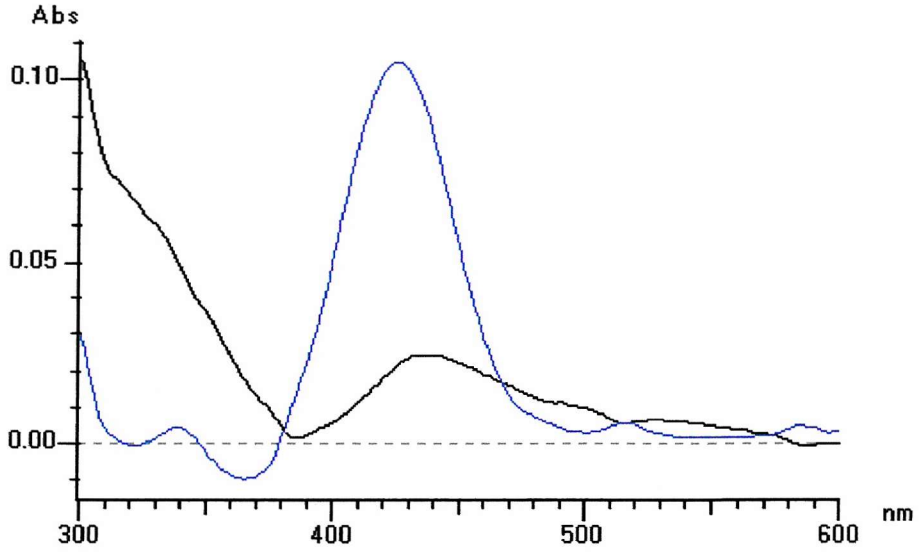

Figure 5.14 UV-visible absorption spectra of the human ALAS2 R517K mutant holo-enzyme before and after addition of glycine. UV visible absorption spectra were recorded in 20mM phosphate buffer, pH 7.5. The black curve represents the absorption spectrum of the R517K mutant holo-enzyme. The blue curve represents the absorption spectrum of glycine (100mM) bound to the holo-enzyme.

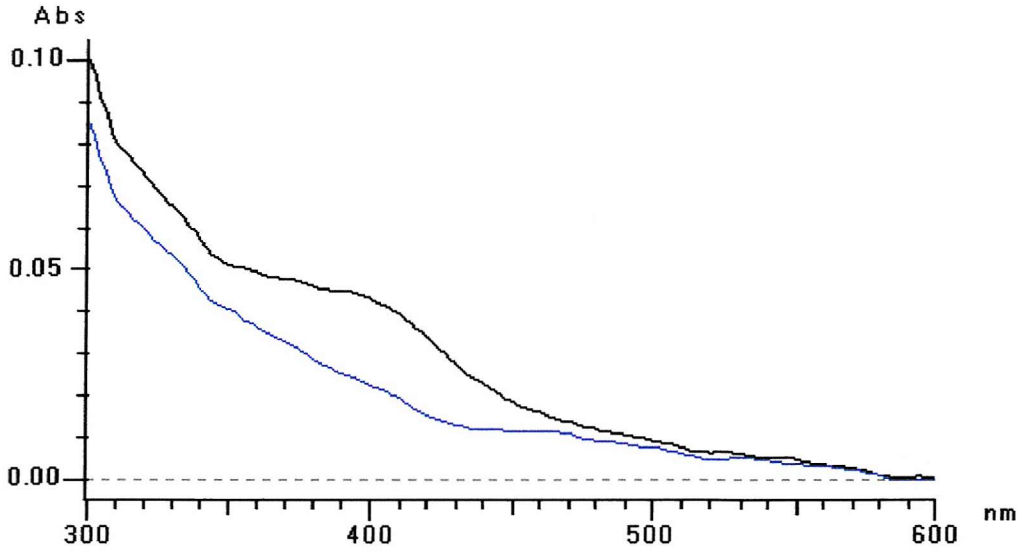

Figure 5.15 UV-visible absorption spectra of the human ALAS2 R517L mutant holo-enzyme before and after addition of glycine. UV visible absorption spectra were recorded in 20mM phosphate buffer, pH 7.5. The black curve represents the absorption spectrum of the R517L mutant holo-enzyme. The blue curve represents the absorption spectrum of glycine (100mM) bound to the holo-enzyme.

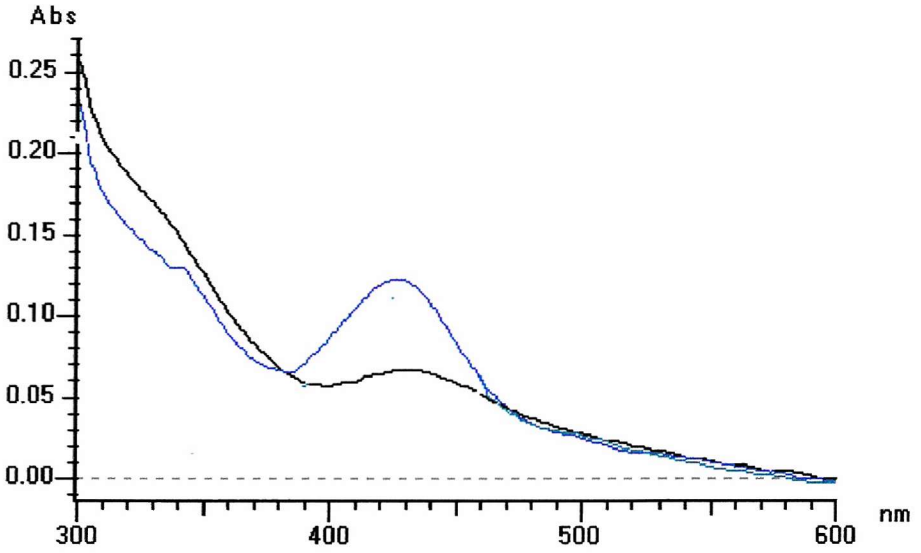

Figure 5.16 UV-visible absorption spectra of the native human ALAS2 holo-enzyme before and after addition of glycine. UV visible absorption spectra were recorded in 20mM phosphate buffer, pH 7.5. The black curve represents the absorption spectrum of the native ALAS2 holo-enzyme. The blue curve represents the absorption spectrum of glycine (100mM) bound to the holo-enzyme.

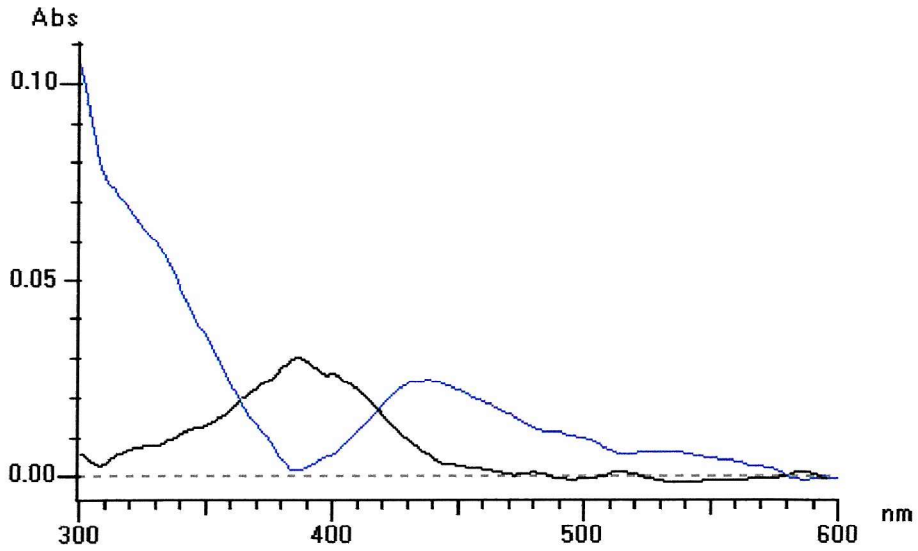

Figure 5.17 UV-visible absorption spectra of human ALAS2 R517K mutant immediately after the addition of pyridoxal 5'-phosphate and after two minutes incubation. Visible absorption spectra were recorded in 20mM phosphate buffer, pH 7.5. The black spectrum represents the absorption spectra of the R517K mutant enzyme immediately after addition of pyridoxal 5'-phosphate (20μM). The blue spectrum represents the R517K mutant after two minutes.

5.8 CD spectroscopic studies

Changes in protein secondary structure that may arise when a mutation is introduced can often be detected by the use of circular dichroism.

UV CD spectra were recorded for all three R517 human ALAS2 mutants and compared to the spectrum obtained for the native enzyme using a Jasco J720 spectropolarimeter. CD spectra of the R517C, R517L and R517K mutants in their holo-enzyme forms were recorded in the UV region (200-270nm) as illustrated in figure 5.18. Spectra for the three R517 mutants in their apo-enzyme form are shown in figure 5.19. At the same enzyme concentration (0.5mg/ml), the R517 holo-enzyme mutants exhibited CD spectra similar to that of the apo-form in shape, although the intensity of the trough observed was different. The spectrum of the holo-form for the R517 mutants is different from that observed for the native in the holo-form, so the presence of the PLP will not cause any changes in the secondary structure.

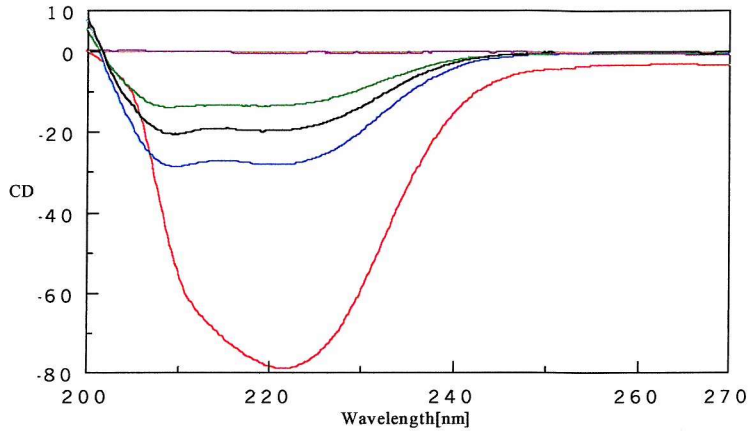

Figure 5.18 Far UV CD spectra of native human ALAS2 holo-enzyme compared to R517C, R517L and R517K mutant holo-enzymes. All spectra were recorded with 6μM ALAS2 protein in 50mM potassium phosphate buffer, pH 7.5, containing 20μM pyridoxal 5'-phosphate. The red spectrum shows the native ALAS2, the blue spectrum shows R517K mutant; the black spectrum shows the R517L mutant; the green spectrum shows R517C and the violet line near the grid line represent the 20μM PLP in phosphate buffer, pH 7.5.

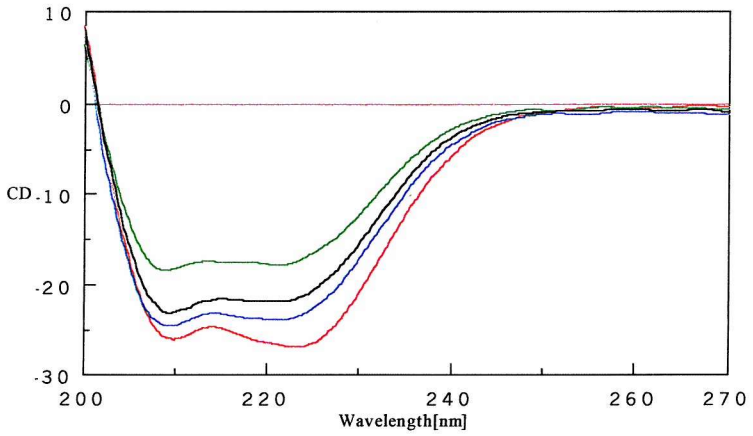

Figure 5.19 Far UV CD spectra of native human ALAS2 apo-enzyme compared to R517C, R517L and R517K mutant apo-enzymes. All spectra were recorded with 6μM ALAS2 protein in 50mM potassium phosphate buffer, pH 7.5. The red spectrum shows the native ALAS2; the blue spectrum shows the R517K mutant; the black spectrum shows the R517L mutant; the green spectrum shows the R517C mutant.

5.9 Discussion

The studies described in this chapter highlight the importance of arginine 517 for the function of ALAS. This amino acid residue, as shown by the model of ALAS2 described in chapter 3, is located close to pyridoxal 5'-phosphate in the vicinity of the proposed substrate binding site with the positively charged guanidino group providing the potential for binding the negatively charged glycine substrate carboxyl group as shown in figure 5.20. The guanidine group can also make hydrogen bonds with several nearby invariant residues including the main chain carbonyl groups of Ser322 and Met323 as well as the side chains of Asn197 and Tyr199. The hydroxyl group of the latter residue is hydrogen bonded to His360 that is, in turn, hydrogen bonded to the hydroxyl group of the coenzyme. Arg517 is also close to the catalytic lysine 391 and is potentially able to influence internal aldimine formation. Thus Arg517 forms an important part of an active site hydrogen bonding network as well as providing a potential binding group for the glycine carboxyl group.

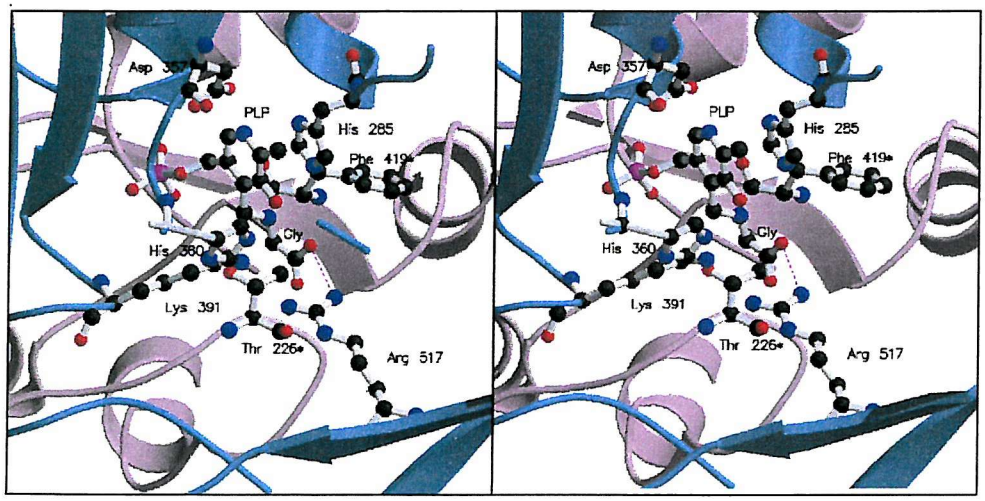

Figure 5.20 The location of R517 at the active site of human ALAS2 showing the interaction with the carboxyl group of the substrate glycine in the external aldimine.

The studies carried out on the human ALAS R517C mutant indicate that the loss of this important positively charged group has a disastrous effect (figure 5.21), resulting in an enzyme with no detectable activity. The reasons for this are probably two-fold. Firstly, the interaction of the apoenzyme with pyridoxal 5'-phosphate is substantially compromised. This is confirmed by the spectroscopic evidence that suggest the R517C mutant cannot form the internal aldimine as efficiently as the native enzyme. Thus the λ_{max} is little more than 10% of the value for the native enzyme at 430nm. Furthermore, on addition of glycine there is no obvious formation of any external aldimine as judged by the failure to observe any increase in the intensity at 430nm. In fact an anomalous rise in absorption around 400nm occurs.

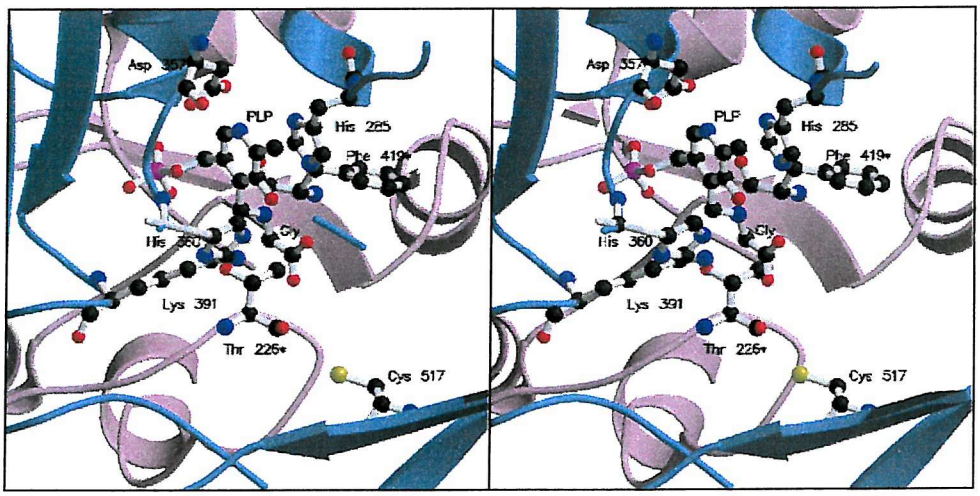

Figure 5.21 The replacement of R517 with the shorter uncharged amino acid, cysteine.

The data from CD spectroscopy also indicates the inability of the R517C mutant to bind the PLP normally. The far UV spectra of the R517C apoenzyme shows only a small difference compared to the native apo-ALAS2 (figure 5.19). However, on addition of PLP, a dramatic difference is seen, with the ellipticity of the native ALAS2 falling from -25 to -80 consistent with coenzyme binding. In contrast, in the R517C mutant the ellipticity rises from -18 to –10, suggesting that coenzyme binding is adversely affected. The failure of patients to respond to pyridoxine therapy is therefore explained not only by the fact that arginine 517 is the

potential glycine substrate binding group but, more importantly, that the loss of the positively charged group has major affects on PLP binding and on the formation of the holo-enzyme.

To determine whether the above observations were also due, in part, to the loss of the hydrophobic methylene chain of arginine, an artificial mutation was generated in which the side chain of arginine 517 was substituted by the branched hydrophobic chain of leucine (figure 5.22). UV visible spectroscopy also indicated little evidence for internal aldimine formation in the R517L mutant, with an anomalous peak around 400nm, suggesting of non-covalently enzyme-bound PLP. Addition of glycine caused a fall in the intensity with almost undetectable maxima appearing at 395 and 465nm. Thus in the R517L mutation, like that of R517C, both PLP and substrate binding was severely compromised. The findings with the R517L mutant using CD spectroscopy were broadly similar to those found above with the R517C mutant, indicating that leucine cannot substitute for arginine in this sensitive part of the active site.

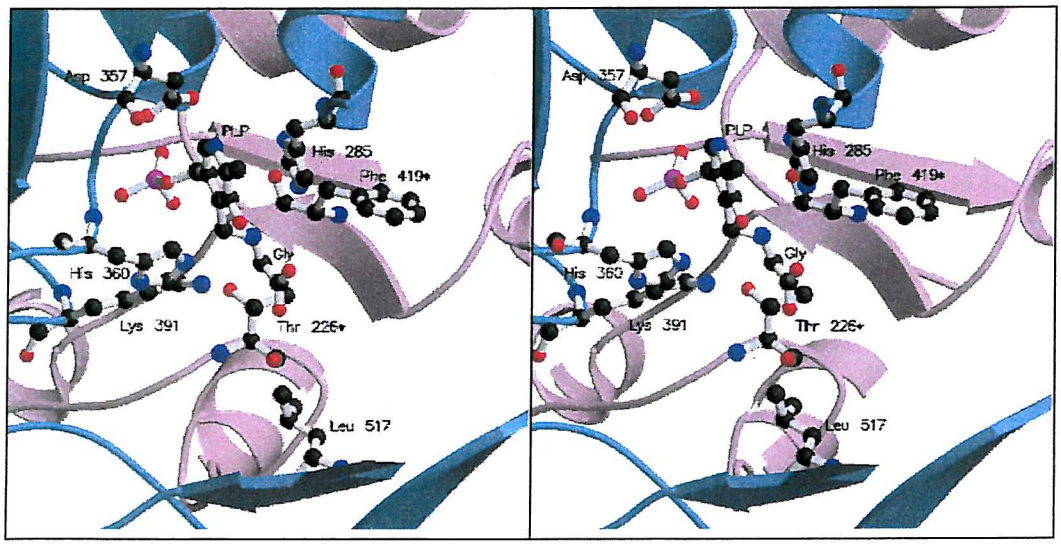

Figure 5.22 The replacement of R517 with the shorter amino acid, leucine.

Although lysine is very different from arginine, having a longer non-polar methylene chain, it does possess a positively charged amino group with a pKa of 10.8, quite close to that of arginine, 12.5. Lysine, however, is less suited to binding

carboxyl groups because the point charge is less dispersed than that of arginine (figure 5.23). Furthermore, the hydrogen bonding network seen in the wild type cannot be formed so extensively with lysine because of the single nitrogen atom. Interestingly, the R517K mutant had 5% of the activity of the native enzyme, a remarkably high value in view of its prominent location at the active site. Investigations with UV visible spectroscopy provided an explanation for the loss in activity, in that the absorption of the internal aldimine, although at 430nm, this was less than half of that of the native enzyme. However, on addition of the substrate a substantial rise in the peak at 430nm indicated that the holoenzyme that had been formed was capable of forming the external aldimine efficiently. Thus the major effect of the R517K mutation appears to be in the initial binding of the coenzyme by the apo-enzyme. This initial suspicion was confirmed by far UV CD spectroscopy in which the spectrum of the holoenzyme indicates a reduced binding of pyridoxal 5'-phosphate compared to the native enzyme.

Kinetic studies with the R517K mutant demonstrated that the affinity for the coenzyme was significantly reduced, the K_m rising from 0.05μM to 0.30μM. As expected, the K_m for glycine was similarly affected rising from 13.9mM to 64.11mM. It is of interest that there is a small decrease in the K_m for succinyl-CoA, but the significance of this is not known.

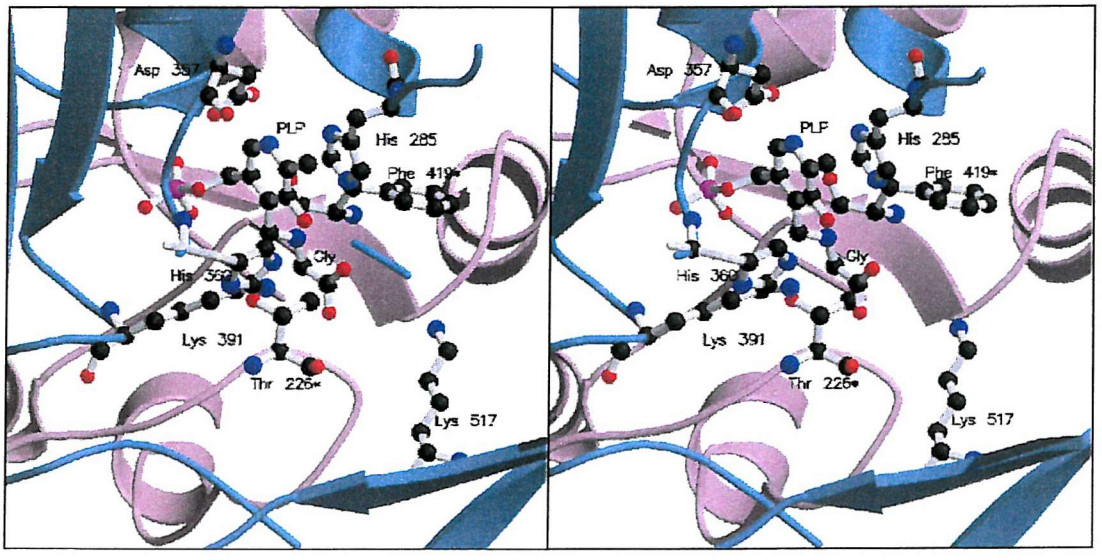

Figure 5.23 The replacement of R517 with the positively charged amino acid, lysine.

Related studies on the equivalent residue in mouse ALAS2 have also shown the R517K mutant to be catalytically active, indeed, this mutant had 77% activity compared to only 5% activity in the human ALAS2. The mouse R438K mutant also showed a 9-fold increase in K_m for glycine and a 5-fold decrease in external aldimine formation.

Arginine 386 of aspartate aminotransferase (AAT), which is equivalent to human ALAS2 R517, has also been mutated to lysine giving a protein that is incapable of interacting with the substrate within the active site. The conclusions from this work are that both size and shape of the positive charge are critical for efficient catalysis by AAT (Inoue *et al.*, 1989). Replacement of this residue with tyrosine or phenylalanine results in a 105-fold decrease in the catalytic function of AAT, highlighting the importance of this residue for substrate binding.

The studies presented in this chapter on human ALAS2 are consistent with R517 having a dual role: firstly, in binding the carboxyl group of the amino acid substrate, glycine, but more significantly in being involved with the formation of the internal aldimine. The R517K mutant was the only R517 mutant that showed only significant enzyme activity since the positively charged lysine could clearly substitute for arginine. More unexpected and interesting was the observation that the R517K mutant was much slower than the native ALAS2 to form the internal aldimine.

References

Akhtar M. and Jordan P. M. (1968) *J Chem Soc Chem Comm* 1691-1692.
The mechanism of action of 5-aminlaevulinate synthase and the synthesis of stereo specifically tritiated glycine.

Abboud M. M., Jordan P. M. and Akhtar M. (1974) *J Chem Soc Chem Comm* 643-644.
Biosynthesis of 5-aminolevulinic acid: involvement of a retention inversion mechanism.

Alexander W., Sandmeier E., Mehta P. K. and Christen P. (1993) *Eur J Biochem* **219,** 953-960.
Evolutionary relationships among pyridoxal 5'-phosphate dependent enzymes.

Alexeev D., Alexeeva M., Baxter R. L., Campopiano D. J., Webster S. P. and Sawyer L. (1998), *JMB* **284,** 401-419.
The crystal structure of 8-amino-7-oxononanoate synthase: A bacterial PLP-dependent, acyl-CoA- condensing enzyme.

Arnstein H. R. V. (1954) *Adv Prot Chem* **9,** 2-81.
The metabolism of glycine.

Bolt E. L., Kryszak L., Zeilstra-Ryalls J., Shoolingin-Jordan P. M., Warren M. J. (1999) *Eur J Biochem* **265,** 1-11.
Characterization of the *R. sphaeroides* 5-aminolevulinic acid synthase isozymes, HemA and HemT, isolated from recombinant *Escherichia coli.*

Bottomley S. S., May B. K., Cox T. C., Cotter P. D. and Bishop D. F. (1995) J *Bioenerg Biomem* **27,** 161-168.
Molecular defects of erythroid 5-aminolevulinate synthase in X-linked sideroblastic anaemia.

Cornish-Bowden A. and Wharton C.W. (1988) In enzyme kinetics (Rickwood, D., ed.), pp.5-14IRL Press. Oxford.

Cotter P. D., Baumann M. and Bishop D. F. (1992) *Proc Natl Acad Sci* **89**, 4028-4032.
'X-linked' sideroblastic anaemia: molecular evidence for erythroid delta-aminolevulinate synthase deficiency.

Cotter P. D., May A., Fitzsimons E. J., Al-sabah A. I., Wang L. and Bishop D. F. (1995) *J Clin Invest* **96,** 2090.
Late onset X-linked sideroblastic anemia: Missense mutations in the erythroid 5-aminolevulinate synthase (ALAS2) gene in two pyridoxine-responsive patients initially diagnosed with acquired refractory sideroblastic anemia and ringed sideroblasts.

Cotter P. D., May A., Liping L., Al-sabah A. I., Fitzsimons E. J., Cazzola M. and Bishop D. F. (1999) *Blood* **93,** 1757-1769.
Four new mutations in the erythroid-specific 5-aminolevulinate synthase (ALAS2) gene causing X-linked sideroblastic anemia: Increased pyridoxine responsiveness after removal of iron overload by phlebotomy and coinheritance of hereditary hemochromatosis.

Cotter P. D., Rucknagel D. L. and Bishop D. F. (1994) *Blood* **84,** 3915-3924.
X-linked sideroblastic anaemia: Identification of the mutation in the erythroid specific 5-aminolevulinic acid synthase gene (ALAS2) in the family originally described by Cooley.

Cox T. C., (1997) *J Inher Metab* **20,** 258-269
Erythropoietic protoporphyria.

Cox T. C., Bawden M. J., Abraham N. G., Bottomley S. S., May B. K., Baker E., Chen L. Z., and Sutherland G. R. (1990) *Am J hum Gen* **46,** 107-111.
Erythroid 5-aminolevulinate synthase is located on the X chromosome.

Cox T. C., Bottomley S. S., Wiley J. S., Bawden M. J., Mathews C. S. and May B. K. (1994) *N Engl J Med* 330 675.
X-Linked sideroblastic anemia due to a THR388-to-SER substitution in erythroid 5-aminolevulinate synthase.

Danishefsky A. T., Onnufer J. J., Petsko G. A. and Ringe D. (1991) *Biochemistry* **30**, 1980-1985.
Activity and structure of the active site mutants R386Y and R386F of *Escherichia coli* aspartate aminotransferase

Edgar, A. J., Losowsky, M. S., Noble, J. S. and Wickramasinghe, S. N. (1997), *Eur J Haematol* **58**, 1-4.
Identification of an arginine 452 to histidine substitution in the erythroid 5-aminolaevulinate synthase gene in a large pedigree with X-linked hereditary sideroblastic anaemia.

Edgar, A. J., Vidyatilake, H. M. S. and Wickramasinghe, S. N. (1998), *Eur J Haematol* **61**, 55-58.
X-linked sideroblastic anaemia due to a mutation in the erythroid 5-aminolaevulinate synthase gene leading to an arginine 170 to leucine substitution.

Elder H. E., Hift R. J. and Meissner P. N. (1997) *Lancet* **349,** 1613-1617.
The acute porphyria.

Elder H. E. (1998) *Photodermatol Photoimmunol Photomed* **14**, 66-69.
Update on enzyme and molecular defects in porphyria.

Erskine P. T., Norton E. D., Cooper J. B., Lambert R., Coker A., Lewis G., Spencer P., Sarwar M., Wood S. P., Warren M. J. and Shoolingin-Jordan P. M. (1999) *Biochemistry* **38,** 4266-4276.
X-Ray structure of 5-aminolaevulinic acid dehydratase from *Escherichia coli* complex with the inhibitor levulinic acid at 2.0 Å resolution.

Ferreira G. C., Neame P.J. and Daily H. A. (1993) *Protein Science* **2,** 1959-1965.
Heme biosynthesis in mammalian systems: evidence of a Schiff base linkage between the pyridoxal 5'-phosphate cofactor and a lysine residue in –aminolevulinate synthase.

Ferreira G. C. and Daily H. A. (1993) *J. Biol Chem* **268,** 584- 590.
Expression of mammalian 5-aminolevulinic acid synthase in *Escherichia coli.*

Ferreira G. C. and Gong J. (1995) *J Bioenerg and Biomemb* **27,** 151-158.
5-Aminolevulinic acid synthase and the first step of heme biosynthesis.

Ferreira G. C., Vajapey U., Hafez O., Hunter G. A. and Barber M. J. (1995) *Protein Science* **4,** 1001-1006.
5-Aminolevulinate synthase: Lysine 313 is not essential for binding the pyridoxal phosphate cofactor but is essential for catalysis.

Fiyaz M. (2001) PhD thesis, University of Southampton.

Furuyama K., Fujita H, Nagai T, Yomogida K, Munakata H, Kondo M, Kimura A, Kuramoto A, Hayashi N and Yamamoto M. (1997) *Blood* **90,** 822-830.
Pyridoxine refractory X-linked sideroblastic anemia caused by a point mutation in the erythroid 5-aminolevulinate synthase gene.

Furuyama K. and Sassa S. (2000) *J Clin Inves* **105,** 757-764.
Interaction between succinyl CoA synthetase and the heme-biosynthetic enzyme ALAS-E is disrupted in sideroblastic anemia.

Gong J. and Ferreira G. C. (1995) *Biochemistry* **34,** 1678-1685.
5-aminolevulinic acid synthase: functionally important residues at a glycine loop, a putative pyridoxal phosphate cofactor-binding site.

Grandchamp B. (1998) *Seminars in liver disease* **18**, 17-24.
Acute intermittent porphyria.

Hellman U., Wernstedt C., Gonez J. and Heldin C. (1995) *Analyt Biochem* **224**, 451-455.
Improvement of an "In-Gel" digestion procedure for the micropreparation of internal protein fragments for amino acids sequencing.

Hunter G. A. and Ferreira G. C. (1995) *Analytical Biochemistry* **226**, 221-224.
A continuous spectrophotometric assay for 5-aminolaevulinate synthase that utilizes substrate cycling.

Hunter G. A. and Ferreira G. C. (1998) *Biochemistry* **37,** 3509-3517.
Aspartate-279 in aminolevulinate synthase affects enzyme catalysis through enhancing the function of the pyridoxal 5'-phosphate cofactor.

Hunter G. A. and Ferreira G. C. (1999a) *Biochemistry* **38,** 3711-3718.
Lysine-313 of 5-aminolevulinate synthase acts as a general base during formation of the quininoid reaction intermediates.

Hunter G. A. and Ferreira G. C. (1999b) *J Biol Chem* **274,** 12222-12228.
Pre-steady-state reaction of 5-aminolevulinate synthase.
Evidence for a rate-determining production release.

Inoue Y., Kuramistu S., Inoue K., Kagamiyama H., Hiromi K., Tanase S. and Morino Y. (1989) *J Biol Chem* **246**, 9673-9681.
Substitution of a lysyl residue for arginine 386 of *Escherichia coli* aspartate aminotransferase.

Jackson A. A. (1990) *Proc Nutr Soc* **46**, 6A.
The urinary excretion of 5-oxoproline in healthy term infants.

Jackson A. A., Badaloo A. V., Forrester T., Hibbert J. M. and Persaud C. (1987) *Br J Nutr* **58**, 207-214.
Urinary excretion of 5-oxoproline (pyroglutamic aciduria) as an index of glycine insufficiency in norrnal man.

John R. A. (1995) *Biochimica et Biophysica Acta* **1248**, 81-96.
Pyridoxal phosphate-dependent enzymes.

Laemmli U. K. (1970) *Nature* **227,** 2304-2313.
Cleavage of structural proteins during the assembly of the head of bacteriophage T_4.

Mathew H. R., Freedland R. A. and Miesfeld R. L. (1997) Wiley-Liss, INC-USA.
Biochemistry a short course.

May A. & Bishop, D.F. (1998) *Haematologica* **83,** 56-70
The molecular biology and pyridoxine responsiveness of X-linked sideroblastic anaemia.

Mauzerall D. and Granick S. (1956) *J Biol Chem* **219,** 435-446
The occurrence and determination of δ-aminolevulinic acid and porphobilinogen in urine.

Meister A. and Anderson M. E. (1983) *Ann Rev Biochem* **52,** 711-760.
Glutathione.

Mills-Davies N. (2000) PhD thesis, University of southampton.

Neidle E. L. and Kaplan S. (1993) *J Bacteriol* **175,** 2292-2303.
Expression of the *Rhodobacter sphaeroides hemA* and *hemT* genes, encoding two 5-aminolevulinic acid synthase isozymes.

Nicholls A., Bharadwaj R. and Honig B. (1993) *Biophs J* **64,** 166-170.
GRASP: graphical representation and analysis of surface properties.

Prades E., Chambon C., Dailey T. A., Dailey H. A., Briere J. and Grandchamp B. (1995) *Hum Genet* **95,** 424.
New mutation of the ALAS2 gene in a large family with X-linked sideroblastic anemia.

Reed P. J. (1988) In *Comparative nutrition,* eds Blaxter K & MacDonald I, pp 55-72. London: John Libbey.
Nitrogen metabolism and protein requirements.

Sali A. and Blundell T. L. (1993) *J Mol Biol* **234**, 779-815.
Comparative protein modelling by satisfaction of spatial restraints.

Sassa S. and Kappas A. (2000*) Journal of Internal Medicine* **247**, 169-178.
Molecular aspects of the inherited porphyrias.

Scrutton N. S., Berry A. and Perham R. N. (1990) *Nature* **343,** 38-43.
Redesign the coenzyme specificity of a dehydrogenase by protein engineering.

Shoolingin-Jordan P. M. (1991) *In Biosynthesis of tetrapyrroles*, (Jordan,P.M., ED),pp.1-66, published by Elsiever.

Shoolingin-Jordan P. M and Cheung K. M. (1999) *Comprehensive Natural Products Chemistry* **4**, 62- 104.
Biosynthesis of heme.

Shoolingin-Jordan P. M., Lelean J. E. and Lloyd A. J. (1997) *Method in Enzymology* **281**, 309-316.
Continuous coupled assay for 5-aminolevulinate synthase.

Srivastava G., Borthwick I. A., Brookes J. D., Wallace J. C., May B. K. and Elliott W. H. (1983) *Biochem Biophys Res Commun* **117**, 344-349.
Hemin inhibits transfer of pre-5-aminolevulinate synthase into chick embryo liver mitochondria.

Sutherland G. R, Baker E., Hyland V. J., Callen D. F., May B. K., Bawden M. J. and Healy H. M. (1988) *Am J Hum Genet* **43**, 331-335.
5-Aminolevulinate synthase is at 3p21 and thus not the primary defect in X-linked sideroblastic anemia.

Tabor S. (1990) In Current Protocols in Molecular Biology, 16.2.1-16.2.11.
Expression using T7 RNA polymerase/promoter system.

Tan D., Barber M. J. and Ferreira G. C. (1998) *Protein Science* **7**, 1208-1213.
The role of tyrosine 121 in cofactor binding of 5-aminolevulinate synthase.

Tan D. and Ferreira G. C. (1996) *Biochemistry* **35**, 8934-8941.
Active site of 5-aminolevulinate synthase residues at the subunit interface. Evidence from *in vivo* heterodimer formation.

Thadani H., Deacon A. and Peters T. (2000) *BMJ* **320**, 1647-1651.
Diagnosis and management of porphyria.

Warren M. J., Cooper J. B., Wood S. P. and Shoolingin-Jordan P. M. (1998) Elsevier Science Ltd 217-221.
Lead poisoning, haem synthesis and 5-aminoleavulinic acid dehydratase.

Warnick G.R. and Burnham B. F. (1971) *J Biol Chem* **246,** 6880-6885.
Regulation of porphyrin biosynthesis. Purification and characterization of the 5-aminolevulinic acid synthase.

Whitby F. G., Phillips J. D., Kushner J. P. and Hill C. P. (1998) *EMBO J* **17**, 2463-2471.
Crystal structure of human uroporphyrinogen decarboxylase.